INFORMATION TO USERS

This manuscript has been reproduced from the microfilm master. UMI films the text directly from the original or copy submitted. Thus, some thesis and dissertation copies are in typewriter face, while others may be from any type of computer printer.

The quality of this reproduction is dependent upon the quality of the copy submitted. Broken or indistinct print, colored or poor quality illustrations and photographs, print bleedthrough, substandard margins, and improper alignment can adversely affect reproduction.

In the unlikely event that the author did not send UMI a complete manuscript and there are missing pages, these will be noted. Also, if unauthorized copyright material had to be removed, a note will indicate the deletion.

Oversize materials (e.g., maps, drawings, charts) are reproduced by sectioning the original, beginning at the upper left-hand corner and continuing from left to right in equal sections with small overlaps.

Photographs included in the original manuscript have been reproduced xerographically in this copy. Higher quality 6" x 9" black and white photographic prints are available for any photographs or illustrations appearing in this copy for an additional charge. Contact UMI directly to order.

ProQuest Information and Learning
300 North Zeeb Road, Ann Arbor, MI 48106-1346 USA
800-521-0600

UMI®

LINKING TIME-EQUIVALENT PALEOSOLS AND LACUSTRINE ROCKS TO RECONSTRUCT PALEOCLIMATE IN THE ISCHIGUALASTO BASIN, NW ARGENTINA

by

Tara Meegan Curtin

A dissertation submitted to the Faculty of the

DEPARTMENT OF GEOSCIENCES

In Partial Fulfillment of the Requirements

For the Degree of

DOCTOR OF PHILOSOPHY

in the Graduate College

THE UNIVERSITY OF ARIZONA

2001

THE UNIVERSITY OF ARIZONA ®
GRADUATE COLLEGE

As members of the Final Examination Committee, we certify that we have read the dissertation prepared by Tara M. Curtin

entitled Linking Time-Equivalent Paleosols and Lacustrine Rocks to Reconstruct Paleoclimate in the Ischigualasto Basin, NW Argentina

and recommend that it be accepted as fulfilling the dissertation requirement for the Degree of Doctor of Philosophy

Judith D. Parrish	7/3/01
Dr. Judith Parrish	Date
Jay Quade	7/3/01
Dr. Jay Quade	Date
David Dettman	3 July 01
Dr. David Dettman	Date
Dr. Clement Chase	Date
C G Chase	3 July 2001
	Date

Final approval and acceptance of this dissertation is contingent upon the candidate's submission of the final copy of the dissertation to the Graduate College.

I hereby certify that I have read this dissertation prepared under my direction and recommend that it be accepted as fulfilling the dissertation requirement.

Judith D. Parrish	
Dissertation Director	Date

STATEMENT BY AUTHOR

This dissertation has been submitted in partial fulfillment of requirements for an advanced degree at The University of Arizona and is deposited in the University Library to be made available to borrowers under rules of the Library.

Brief quotations from this dissertation are allowable without special permission, provided that accurate acknowledgment of source is made. Requests for permission for extended quotation from or reproduction of this manuscript in whole or in part may be granted by the copyright holder.

SIGNED: Dawn M. Curtin

ACKNOWLEDGEMENTS

I am grateful to the many individuals who provided expertise and support of this project. I thank the members of my committee, Drs. Judith T. Parrish, Clem Chase, Andrew Cohen, David Dettman, and Jay Quade for helpful discussions and analytical advice along the way. I thank J.T. Parrish for introducing me to paleoclimatology and the Ischigualasto Basin during my first year. I am especially grateful to Dr. Milana, from the Universidad Nacional de San Juan, and Dr. Martínez, from the Museó de Ciéncias Naturales in San Juan, Argentina, who introduced me to the Triassic stratigraphy of the Ischigualasto Basin and logistical support. I would also like to thank Dr. Stephen Altaner for allowing me to use his laboratory at the University of Illinois to prepare and analyze samples for XRD analyses; Drs. Lisa Pratt and Erika Elswick for access to their Biogeochemcial Laboratory facilities at Indiana University for organic analyses; and Joost VanVaren at Columbia University's Biosphere 2 Center for access to the analytical laboratory for CHN analyses. Thanks to David Finkelstein, Oscar Gonzalez, Lorena Previley, and Carina Colombi for able field assistance in adverse weather conditions. Special thanks to David Finkelstein, Aviva Sussman, Erin Rosenberg, Sarah Tindall, Steve and Lois Sorenson, Mike Neilsen, Melanie Lenart, Tom Moore, Dani Montague-Judd, Catherine O'Reilly, D Robinson, and all of my hiking buddies for all their help, moral support, and friendship during the last four years. Without the support of David Finkelstein; my sisters, Caitlin and Ciàra Curtin; my parents; and Aviva Sussman, all of this effort would not have been possible.

Financial support for fieldwork was provided by numerous student research grants from the Department of Geosciences, Institute for the Study of Planet Earth, and Graduate College of the University of Arizona, ARCO, and the Society of Sedimentary Geology. The Clay Mineral Society, the American Association of Petroleum Geologists, Geochron Laboratories, and the Geological Society of America funded laboratory research.

TABLE OF CONTENTS

TABLE OF CONTENTS - *Continued*

LIST OF ILLUSTRATIONS

LIST OF TABLES

ABSTRACT

Field relationships between the coeval Ischichuca and Chañares Formations in the southern part of the Ischigualasto rift basin, northwestern Argentina, combined with mineralogical, geochemical, and petrographic analyses demonstrates that the climate was semi-arid to semi-humid during the Middle Triassic. Although climate changes (sediment and water supply) controlled the types of sediment that accumulated in the basin, facies distribution is controlled by differential subsidence in the rift basin. Asymmetrical subsidence is inferred from the change in thickness of the rocks perpendicular to the western basin-bounding Valle Fértil fault. Braidplain and fluvially-dominated lacustrine deltaic deposition occurred closest to the Valle Fértil fault. The rivers drained the surrounding highlands composed of Precambrian metamorphic rocks and Paleozoic plutons. Fluvial systems tended towards the topographic minimum, in this case, the lake, which is 10 km from the Valle Fértil fault. The lack of Gilbert-style deltas suggests that the fluvial systems entering the lake were not on a steep gradient and the lake was not very deep. The widespread lateral extent and thin palustrine deposits and B horizons of moderately well-developed Vertisols along the southern and eastern margins illustrates slow aggradation of material. Vertic features in paleosols, pedogenic mud chips in fluvial and lacustrine deposits, and clastic-organic and carbonate-organic couplets in lacustrine facies indicate seasonality of precipitation. The C_{org}/S_{total} ratios, presence of *Unionids*, charophytes, and detrital clay minerals, and lack of desiccation features or saline and saline alkaline minerals indicate the lake was fresh. Significant coal swamp deposition occurred along the lake margins. The combination of Vertisols,

coals, and lack of pedogenic carbonate in the paleosols suggests the mean annual precipitation in the Ischigualasto Basin was between 120-250 cm. The carbon isotopic composition of terrestrial organic matter in fluvial and lacustrine deposits and Vertisols documents that plants were subjected to significant water stress.

CHAPTER 1: INTRODUCTION

Statement of the Problem

The purpose of this study is to identify the relative roles of tectonics and climate on sedimentation processes in the Ischigualasto rift basin (San Juan and La Rioja provinces, NW Argentina) in order to discern specific climatic information about temperature, precipitation, and seasonality of precipitation from the rock record. Interpreting the relative effects of climate and tectonics on sedimentation in a rift basin is especially difficult because of the complex tectonic evolution of rift systems (Bosworth, 1985; Lambiase, 1990; Leeder and Gawthorpe, 1987). In rift basins, the basin-fill sequence patterns are controlled by the balance between the amount of accommodation space, driven by tectonics, and the sediment and water supply, driven by climate (Talbot and Allen, 1996; Carroll and Bohacs, 1997a, 1997b, 1999). Work done in other ancient continental rift systems such as the Permo-Triassic Mombasa Basin (Africa), Precambrian Mid-Continent Rift (USA), Triassic Newark Basin (USA), and Cretaceous Sudan Basin (Africa) shows a tripartite sequence of depositional environments, starting with a fluvial or alluvial basal sequence followed by a sharp contact with overlying deep lacustrine facies and capped by a shallow lacustrine or fluvial deposition (Bosworth, 1985; Lambiase, 1990; Olsen, 1990). This tripartite depositional sequence may be repeated if the basin undergoes multiple rift stages (Lambiase, 1990). The basin–fill model developed by Lambiase (1990) accounts for sedimentation in rifts as a function of slow versus fast subsidence, topographic evolution, and depositional style. He suggests structural constraints have a more important control on large lake development than

climate, but the amount of water available does impact the topographic evolution and therefore depositional environments in the basin (Lambiase, 1990). Others suggest that a positive water balance is crucial for lakes to exist, even briefly, in geologic time (Barron, 1990).

Two tripartite depositional sequences (Table 1) are observed in the Triassic Ischigualasto Basin. The basal formations, the Lower Triassic Talampaya and Tarjados Formations (Fms) reflect alluvial and braidplain deposition and represent the basal alluvial to fluvial deposition of the tripartite sequence; the Middle Triassic Chañares, Ischichuca, and Los Rastros Fms reflect fluvio-lacustrine and palustrine environments and corresponds to the middle and upper part of the tripartite sequence; the Late Triassic Ischigualasto Formation (Fm) is characterized by fluvial deposition and paleosol development and reflects the beginning of another tripartite depositional sequence; and the Los Colorados Fm is interpreted to represent playa lakes, ephemeral stream deposits, and eolian environments of the second and third part of the tripartite sequence (Stipanicic and Bonaparte, 1979, López-Gamundi et al., 1989; Milana and Alcober, 1994).

The focus of this dissertation is on the coeval Middle Triassic Ischichuca and Chañares Fms. These formations were chosen for study for three reasons: 1) the Middle Triassic in Australia, at a similar latitude as the Ischigualasto Basin, and in Antarctica (at ~70°S) has been interpreted to be wetter than other time periods in the Triassic (Retallack, 1977; Tucker and Benton, 1982; Fawcett et al., 1994; Parrish et al., 1996; Retallack and Alonso-Zarza, 1998), and may represent a different expression of the Pangean megamonsoon than what was observed on the Colorado Plateau during the Late

Triassic (Dubiel et al., 1991); 2) a detailed investigation of climate in the southwestern region of Pangea has not been accomplished, except a preliminary compilation of South American climate through the Phanerozoic by Volkheimer (1967), Stipanicic and Bonaprte (1979), and Alcober (1996) and this needs to be done to complete a global picture over time; and 3) comparison of synchronous events across the Ischigualasto Basin is possible using coeval fluvio-lacustrine deposition and paleosol development. This latter reason is the underlying motivation for studying these deposits. Coeval paleosol formation and lacustrine deposition provide complimentary datasets for climate studies because paleosols reflect direct information about the overall local climate during active soil formation whereas laminated lacustrine sediments provide an "instantaneous," indirect, and episodic record of climate. Paleosols are in direct contact with the atmosphere (e.g., temperature and precipitation fluctuations), but lake sediments, through higher resolution, accumulate through a "filter;" the water column modulates sedimentation processes affected by climate parameters. Comparison of these two paleoclimate indicators reveals whether the Middle Triassic in SW Pangea reflects an overall wetter climate or is a function of increased accommodation space.

Goals of the Dissertation

This dissertation project has five main goals: 1) to describe the sedimentology and interpret the depositional environments of the coeval Middle Triassic Ischichuca and Chañares Fms; 2) to identify and interpret the climate indicators preserved in these two formations; 3) to investigate how climate affects organic matter preservation in coeval lacustrine rocks and paleosols; 4) to evaluate the carbon isotopic composition of the

organic matter in the lacustrine rocks as a function of climate and environmental factors; and 5) to describe the role of provenance, transport, climate, and diagenesis on sandstone composition and clay mineral assemblages of the Ischichuca and Chañares Fms in order to discern additional climatic information. This dissertation provides evidence that climate influence on sedimentation can be distinguished from tectonic controls on development of accommodation space. Observations and data from the Ischigualasto Basin are compared with regional climate data on Gondwana.

Triassic Climate of Pangea

The Triassic is a unique episode in Earth history because it is characterized by the most arid climate of the Phanerozoic (Crowley and North, 1991). Evidence of the unusual distribution of lithologic climate indicators on Pangea was first described on the basis of the locations of evaporites, red beds, and coals (Robinson, 1973). These climate indicators do not reflect latitudinal zonation patterns observed on continents today. Robinson's (1973) study was the first to recognize the possibility of a monsoonal climate on Pangea. The evolution of the Pangean "megamonsoon," a term coined by Kutzbach and Gallimore (1989), has since been described in numerous papers (Parrish et al., 1982, 1986; Parrish and Peterson, 1988; Dubiel et al., 1991; Parrish, 1993; Francis, 1994; Parrish et al., 1996). Monsoonal circulation is defined as the reversal of wind direction by almost 180° between seasons (Webster, 1987). Wind reversals are a function of differential heating of adjacent landmasses and oceans, Coriolis force, and latent heat storage (Webster, 1987). The degree of differential heating is accentuated in regions with high plateaus (e.g., Tibetan Plateau). Numerical models of Pangean paleoclimate support

the interpretation of a monsoonal circulation system (Crowley et al., 1989; Kutzbach and Gallimore, 1989; Wilson et al., 1994; Hay and Wold, 1998). In general, conditions invoked to explain widespread aridity often include the size of the landmass, the presence of high-elevation plateaus, cool global temperatures, the small size of warm tropical oceans, and the relative lack of vegetation (Hay and Wold, 1998). During the Triassic, none of these conditions was significantly different from those observed during the Permian or Jurassic. Recently, Wold and Hay (1998) suggested that uplifts along the eastern and western margins of Pangea could explain the widespread extent of aridity and the absence of an equatorial rain belt.

Triassic Climate of South America

In general, the Triassic climate of Argentina has been described as warm to hot and humid to arid (Volkheimer, 1967). Interpretation of the climate of South America is based on the presence of eolian sandstone in Argentina and Brazil (Bigarella, 1973; Milana, 1993), which reflect arid and hot conditions; red beds and gypsum in west-central Argentina (Volkheimer, 1967), which suggest wet and dry conditions respectively; coal beds from Argentina to Brazil (Volkheimer, 1967), which indicate a high water table; and the association of *Dicroidium* fossil plants in Argentina (Volkheimer, 1967; Retallack, 1977) with the widespread distribution and association of tetrapods including primitive dinosaurs, archosaurs, cynodonts, dicynodonts, rhynchosaurs, and amphibians (Rogers et al., 1993; Bonaparte, 1997), which suggest food for these fauna was plentiful across a widespread area. Numerous authors showed that alluvial and lacustrine sedimentation occurred in Triassic rift basins along the western

margin of South America. These studies concluded that the presence of lakes is a function of a humid climate (Stipanicic and Bonaparte, 1979; Tucker and Benton, 1982). The contradiction in the climate interpretation (arid vs. humid and warm vs. hot) for the Triassic of Argentina is hypothesized to reflect the alternation in climate on a seasonal basis as a result of monsoonal circulation on Pangea, similar to that initially interpreted for the Colorado Plateau (Demko, 1995). Volkheimer (1967) suggested there was a precipitation gradient from Patagonia to west-central Argentina on the basis of the distribution and types of plants found in coal and presence of well-defined growth rings in petrified wood. Precipitation may have been more evenly distributed throughout the course of a year in the southern part of South America and more seasonal in central western Argentina (Volkheimer, 1967).

Previous Work

The research presented in this dissertation builds on decades of research in the Ischigualasto Basin that focused mostly on the paleontology of the Chañares and Ischigualasto Fms (Bonaparte, 1997, and references therein). The sedimentology, paleontology, and depositional environments of the Ischichuca and Chañares Fms have already been described in a tectonstratigraphic framework by Milana and Alcober (1994), Bonaparte (1997), and Milana (1998). The Tarjados Fm is overlain by the Chañares Fm across the basin (López -Gamundi et al. 1989; this study). The Ischichuca and Los Rastros Fms appear to be part of the same sequence of lacustrine deposition that reflects a complex interaction between accommodation space and sediment infilling (López - Gamundi et al., 1989; Milana and Alcober, 1994; Milana, 1998). The Ischichuca and

Chañares Fms are interpreted to be coeval and interfinger with each other, and the Los Rastros Fm is thought to reflect final infilling of a widespread, shallow lake (López-Gamundi et al. 1989). Previously identified climate indicators in the Ischigualasto Basin of Middle Triassic formations include large reptiles, which are inferred to reflect warm climates (Volkheimer, 1967), thin coal beds, interpreted to reflect warm, most conditions.

Explanation of the Dissertation Format

Three manuscripts contained in following appendices represent the body of this dissertation. The common theme shared by these papers is the recognition of the influence of climate on depositional environments, basin-scale sedimentation patterns, organic matter preservation, sandstone composition, and clay mineral assemblages during Triassic rifting. Each paper is written for publication in different journals, so some overlap in basic introductory material is necessary. The following paragraphs describe the most important conclusions presented in each of the following chapters.

The first paper, *Distinguishing Climate from Tectonic Signals in Coeval Middle Triassic Lacustrine Deposits and Lake Marginal Paleosols in the Ischigualasto Basin, NW Argentina*, presents sedimentologic and stratigraphic evidence used to infer climate and tectonic signals in the rock record. Low-gradient basin margins are inferred with a fluvially dominated lacustrine deltaic margin on the western side of the basin and extensive palustrine deposits to the south and east. Key sedimentological features indicative of a wet or seasonally wet climate are: 1) gleyed paleosols that formed in fluctuating water tables, 2) abundant coal formed in swamps and lacustrine environments, 3) braided stream deposits, 4) shell impressions of *Unionids* with growth bands, 5)

abundant mudchips in braided stream deposits, 6) laminated organic-clastic lacustrine deposits, and 7) presence of charophytes and ostracods in laminated lacustrine deposits. Tectonic activity controlled the amount of accommodation space available for sediment deposition and the lateral distribution of different lithofacies. A seasonally wet climate is inferred based on the types of sediment and sedimentary structures preserved. The climate indicators are further described in Appendix B and C.

The second manuscript entitled *Evaluation of Provenance, Climate, and Post-Depositional Controls on the Composition of Coeval Fluvio-lacustrine Deposits and Paleosols* concludes that the majority of sand was sourced from local Precambrian metamorphic rocks and Paleozoic plutons. The clay mineralogy of the bentonites documents the absence of typical illitization patterns associated with burial diagenesis. Lacustrine clay mineral assemblages reflect proximity to shoreline, burial depth, and pore fluid composition. Pore fluids from the fresh lake water that migrated through the lacustrine sediment during compaction are interpreted to have controlled the clay mineral composition of the altered volcanic ash deposits and authigenic cements in the prodeltaic sandstone and channel conglomerate close to the basin-bounding fault.

The third manuscript, *Preservation of a Seasonal Signature in Organic Matter of Middle Triassic Lacustrine Deposits, NW Argentina*, illustrates the use of carbon isotopic signals of terrestrial organic matter to decipher climate and environmental controls on organic matter production and preservation in the Ischigualasto Basin. A seasonally wet-dry climate is inferred based on the carbon isotopic values of organic matter preserved in lacustrine intervals. The scientific conclusions from this paper are similar to those

presented in Appendix C. This paper summarizes the climatic significance of the sedimentologic and geochemical data from the Ischigualasto Basin in context of the evolution of the Pangean megamonsoon. Most lithologic, geochemical, and paleontological evidence across southern Pangea suggest a warm to cool seasonally wet temperate climate.

In the final appendix, I include three tables of supplemental data from geochemical and mineralogical analyses of samples from the southern region of the Ischigualasto Basin. The first table lists the whole rock mineralogical data; the second table the clay mineralogical data; and the third table lists the organic geochemical data.

The research involved in this dissertation and described the in following appendices was done entirely by the author. However, co-authors on the first appendix (Judith Totman Parrish, Juan Pablo Milana, and Ricardo Martínez) provided invaluable information about potential field sites and help with field logistics. Dr. Parrish suggested that I conduct research in the Ischigualasto Basin and revised many versions of all of the included appendices. Dr. Milana, from the Universidad Nacional de San Juan, and Dr. Martínez, from the Muséo de Ciéncias Naturales in San Juan, Argentina, introduced me to the Triassic stratigraphy of the Ischigualasto Basin. Dr. Milana was especially helpful in identification of key stratigraphic localities to describe in order to answer my research questions.

TABLE 1- 1. Stratigraphy and depositional environments of the Triassic Ischigualasto Basin, NW Argentina. Interpretations of the depositional environment are based on Lopez-Gamundi (1989), Milana and Alcober (1994), Alcober (1996), and this study.

Age	Formation	Depositional Environment
Upper Triassic	Los Colorados	eolian sand sheets; playa lakes
Upper Triassic	Ischigualasto	fluvial channels; paleosols
Middle Triassic	Los Rastros	fluvio-lacustrine
Middle Triassic	Ischichuca/Chañares	fluvio-lacustrine; paleosols
Lower Triassic	Tarjados	alluvial to braidplain
Lower Triassic	Talampaya	alluvial to braidplain

CHAPTER 2: PRESENT STUDY

The methods, results, and conclusions of this study are presented in the three papers appended to this dissertation. The following is a summary of the most important findings in this paper.

The relative roles of tectonics and climate on sedimentation processes in the Ischigualasto rift basin (San Juan and La Rioja provinces, NW Argentina) were examined in order to discern specific climatic information preserved in coeval lacustrine and paleosols deposits. Tectonic activity controlled the amount of accommodation space available for sediment deposition and the lateral distribution of different lithofacies in the Ischigualasto Basin, NW Argentina during the Middle Triassic. Stratigraphic, geochemical, and mineralogical evidence all support the interpretation that the climate was seasonal with respect to rainfall. Sedimentologic evidence for seasonality of precipitation is indicated by gleyed paleosols, vertic features observed along the distal regions of the hanging wall of the asymmetric rift basin, pedogenic mud aggregates in the fluvial and lacustrine lithofacies, abundant coal that formed in swamps and lacustrine environments, shell impressions of *Unionids* with growth bands, and the dominance of clastic laminae in the lake sequences. In the lacustrine deposits of the Ischichuca Formation, the $\delta^{13}C_{org}$ of the land plants ranges from –22.1 to –24.9‰. The relatively high $\delta^{13}C_{org}$ values of the land plants suggest that water stress was a significant environmental condition in the Ischigualasto Basin. The combination of Vertisols, coals, and lack of pedogenic carbonate in the paleosols suggests that the mean annual precipitation was between 120-250 cm/year.

WORKS CITED

Alcober, O., 1996, Revision de los Crurotarsis, estratgrafia y tafonomia de la formacion Ischigualasto, Thesis docoral, Universidad Nacional de San Juan Facultad de Ciencias Exactas Fisicas y Naturals. 254p.

Barron, E.J., 1990, Climate and lacustrine petroleum source prediction, in B.J. Katz, Lacustrine Basin Exploration: Case Studies and Modern Analogs, AAPG Memoir 50, 1-18.

Bigarella, J.J., 1973, Paleocurrents and the problem of continental drift, Geologisches Rundschau, 62, 447-477.

Bonaparte, J.F., 1997, El Triasico de San Juan-La Rioja Argentina y sus Dinosaurios, Museo Argentino de Ciencias Naturales, Buenos Aires, Argentina, 196p.

Bosworth, W.P., 1985, Geometry of propagating continental rifts: Nature, v. 316, p. 625-627.

Carroll, A.R. and Bohacs, K.M., 1997a, Lacustrine source quality and distribution; lake type controls on hydrocarbon generation, Annual Meeting Abstracts- American Association of Petroleum Geologists and Society of Economic Paleontologists and Mineralogists, v. 6, p. 18.

Carroll, A.R. and Bohacs, K.M., 1997b, Stratigraphic and biogeochemical cycles in ancient lake deposits: Annual Meeting Abstracts- American Association of Petroleum Geologists and Society of Economic Paleontologists and Mineralogists, v. 6, p. 18.

Carroll, A.R. and Bohacs, K.M., 1999, Stratigraphic classification of ancient lakes: balancing tectonic and climatic controls, Geology, v. 27, 99-102.

Crowley, T.J., Hyde, W.T., and Short, D.A., 1989, Seasonal cycle variations on the supercontinent Pangea, Geology, 17, 457-460.

Crowley, T.J. and North, G.R., 1991, Paleoclimatology, Oxford UP, NY, 339p.

Dubiel, R.F., Parrish, J.T., Parrish, J.M., and Good, S.C., 1991, The Pangean megamonsoon- evidence from the Upper Triassic Chinle Formation, Colorado Plateau, Palaios, v. 6., p. 347-370.

Fawcett, P.J., Barron, E.J., Robison, V.D., and Katz, B.J, 1994, The climatic evolution of India and Australia from the late Permian to mid-Jurassic: a comparison of climate model results with the geologic record, *in* Klein, G.D. (ed.), Pangea:

Paleoclimate, Tectonics, and Sedimentation During Accretion, Zenith, and Breakup of a Supercontinent: Boulder, Colorado, Geological Society of America Special Paper 288, 139-157.

Francis, J.E., 1994, Paleoclimates of Pangea- Geological Evidence, *in* A.F. Embry, B. Beauchamp, and D.J. Glass (eds.) Pangea: Global Environments and Resources, Canadian Soc. of Petroleum Geologists Memoir 17, 265-274.

Hay, W.W. and Wold, C.N., 1998, The role of mountains and plateaus in a Triassic climate model, *in* Crowley, T.J., and Burke, K.C., eds., Tectonic Boundary Conditions for Climate Reconstructions: Oxford University Press and American Geophysical Union, 116-243.

Kutzbach, J.E. and Gallimore, R.G., 1989, Pangean climates: megamonsoons of the megacontinent, J. Geophys. Res., 94, 3341-3357.

Lambiase, J.J., 1990, A model for tectonic control of lacustrine stratigraphic sequences in continental rift basins *in* Katz, B.J., ed., Lacustrine basin exploration: case studies and modern analogs, AAPG Memoir 50, 265-276.

Leeder, M. R. and Gawthorpe, R.L., 1987, Sedimentary models for extensional tilt-block/ half-graben basins. *in*: Continental extensional tectonics. Coward, M.P., Dewey, J.F., Hancock, P.L. (eds.) Geological Society Special Publications. 28; Pages 139-152.

Lopez-Galamundi, O.R., Alvarrez, L., Andreis, R.R., Bossi, G.E., spejo, I., Seveso, F.F., Legarreta, L., Kokogian, D., Limarino, C.O., and Sessarego, H., 1989, Cuencas intermontanas, Cuencas Sedimentarias Argentinas 1989, p. 123-167.

Milana, J.P. and Alcober, O., 1994, Modelo tectosedimentario de la cuenca triásica de Ischigualasto (San Juan, Argentina), Revista de la Asociación Geológica Aregntina, 49 (3-4), 217-235.

Milana, J.P., 1998, Anatomía de parasecuencias en un lago de rift y su relación con la generación de hidrocarburos, Cuenca Triasica de Ischigualasto, San Juan. Revista Asociación Geológica Argentina, v. 53.

Olsen, 1990 *in* Katz, B.J., ed., Lacustrine basin exploration: case studies and modern analogs, AAPG Memoir 50

Parrish, J.T. and Curtis, R.L., 1982, Atmospheric circulation, upwelling and organic-rich rocks in the Mesozoic and Cenozoic eras, Palaeo. Palaeo. Palaeo., v. 40, p. 31-66.

Parrish, J.T., Ziegler, A.M., and Scotese, C.R., 1982, Rainfall patterns and the distributions of coals and evaporites in the Mesozoic and Cenozoic, Palaeogeography, Palaeoclimatology, Palaeoecology, 40, 67-101.

Parrish, J.T., and Peterson, F., 1988, Wind directions predicted from global circulation models and wind directions determined from eolian sandstones of the western United States- a comparison, Sedimentary Geology, 56, 261-282.

Parrish, J.T., 1993, Climate of the supercontinent Pangea, J. Geol., 101, 215-233.

Parrish, J.T., Bradshaw, M.T., Brakel, A.T., Mulholland, S.M., Totterdell, J.M, and Yeates, A.N., 1996, Paleoclimatology of Australia during the Pangean interval: Palaeoclimates- Data and Modelling, 1, 23-57.

Retallack, G.J., 1977, Two new approaches for reconstructing fossil vegetation; with examples from the Triassic of eastern Australia. Journal of Paleontology. 51; 2, Suppl., Part III, 22.

Retallack, G.J. and Alonso-Zarza, A.M., 1996, Middle Triassic paleosols and paleoclimate of Antarctica, Journal of Sedimentary Research, 68, 169-184.

Robinson, P.L., 1973, Paleoclimatology and continental drift, in Tarling, D.H. and Runcorn, S.K. (eds.), Implications of Continental Drift to the Earth Sciences, 1: London, Academic Press, 449-476.

Stipanicic, P.N. and Bonaparte, J.F., 1979, Cuenca triásica de Ischigualasto-Villa Union (Provincias de La Rioja y San Juan), in Turner, J.C., ed., Segundo Simmposio de Geología Regional Argentina: 1, Córdoba, Academia Nacional de Ciencias, 253-575.

Talbot, M.R. and Allen, P.A., 1996, Lakes in H.G. Reading, Sedimentary Environments: Processes, Facies and Stratigraphy, Blackwell Science, Oxford, p. 83-124.

Tucker, M.E. and Benton, M.J., 1982, Triassic environments, climates and reptile evolution, Palaeogeography, Palaeoclimatology, Palaecology, 40, 361-179.

Volkheimer, W., 1967, Paleoclimatic evolution in Argentina and relations with other regions of Gondwana, Gondwana stratigraphy, IUGS Symposium, Buenos Aires, p. 551–574.

Webster, P.J., 1987, The elementary monsoon, *in* Fein JS and Stevens, PL (eds.), Monsoons, John Wiley, New York), 3-32.

Wilson, K., Pollard, D., Hay, W.W., Thompson, S.L., and Wold, C.N., 1994, General circulation model simulations of Triassic climates: preliminary results, in Klein, G.D. (ed.), Pangea: Paleoclimate, Tectonics, and Sedimentation During Accretion, Zenith, and Breakup of a Supercontinent: Boulder, Colorado, Geological Society of America Special Paper 288, 91-116.

APPENDIX A: DISTINGUISHING CLIMATE FROM TECTONIC SIGNALS IN COEVAL MIDDLE TRIASSIC LACUSTRINE DEPOSITS AND LAKE MARGINAL PALEOSOLS IN THE ISCHIGUALASTO BASIN, NW ARGENTINA

Abstract

Vertical and lateral lithofacies analysis of Middle Triassic rocks from the southern region of the Ischigualasto Basin in northwestern Argentina illustrates how continental sedimentation responds to both climate changes and rifting. Coeval alluvial and fluvio-lacustrine depositional systems evolved in response to subsidence in the rift basin and changes in water and sediment supply to the basin. The following criteria were used to differentiate climatic from tectonic signals in the stratigraphic record: 1) the lateral and vertical distribution of lithofacies across the basin, 2) lacustrine couplets and stacking patterns, 3) deltaic style, 4) pedogenic mud aggregates, and 5) Vertisols. Lacustrine intervals, although not the dominant component of the basin fill, are temporally and spatially linked to distal alluvial fan and marginal lacustrine deposits. The lateral and vertical facies associations, deltaic style, position of lake margin deposition, and lateral extent of palustrine deposits were used to infer basin geometry. Basin subsidence is thought to have kept pace with sedimentation because lake-margin benches are not observed along either basin margin. A shallow lake is bounded by low energy ramp-type on all margins. This interpretation is based on deltaic styles, lithofacies associations, and position of marginal deposits relative to the border fault. Clastic-organic laminated lacustrine deposits indicate high sedimentation rates. Gradual deepening and shallowing

events occurred in three lake phases. High aggradation and sedimentation rates in the basin were also inferred based on a low ratio of fluvial channel to overbank deposits and the abundance of climbing ripples in channel deposits. Stacked sequences of Bt horizons of Vertisols in the eastern part of the basin also indicate significant vertical aggradation and subaerial exposure. Seasonality of precipitation is indicated by vertic features observed along the distal regions of the hanging wall, pedogenic mud aggregates in the fluvial and lacustrine lithofacies, and the dominance of clastic laminae in the lake sequences. Tectonic and climatic activity likely remained fairly constant during the Middle Triassic, but climatic conditions played a major role on the presence of the lake in the Ischigualasto Basin. The climate is inferred to have been semi-arid to semi-humid.

1. Introduction and Objectives of the Study

Differentiating tectonic and climatic information stored in continental sedimentary rocks is crucial for interpreting climate change because changes in either climate or tectonic activity may produce the same effect in the geologic record (Hay, 1996). Interpreting the relative effects of climate and tectonics on sedimentation in a rift basin is especially difficult because of the complex tectonic evolution of the rift system (Bosworth, 1985; Lambiase, 1990; Leeder and Gawthorpe, 1987). In rift basins, the basin-fill sequence patterns are controlled by the balance between the amount of accommodation space, driven by tectonics, and the sediment and water supply, driven by climate (Talbot and Allen, 1996; Carroll and Bohacs, 1997a, 1997b, 1999). Middle Triassic lake deposits and lake-marginal paleosols provide an outstanding opportunity to examine the relative controls of climate and tectonics on sedimentation in the southern

part of the Ischigualasto Basin in northwestern Argentina. The combination of these two climate indicators, paleosols and laminated lacustrine rocks, offers the greatest amount of information about long-term and short-term changes in climate because they formed over very different time scales. Paleosols preserve an integrated response to direct changes in atmospheric conditions, especially the hydrologic budget and temperature. Thick, mature soils record long-term, time-averaged information about local climate because chemical weathering reactions occur over thousands of years (Retallack, 1990; Mack and James, 1992; Birkeland, 1999; Kraus, 1999). In contrast, laminated lacustrine rocks are important archives of rapid changes in climatic conditions because lakes respond quickly to climate perturbations (Talbot and Kelts, 1990; Glenn and Kelts, 1991; Talbot and Allen, 1996).

Previous studies of Triassic climate recorded in continental rocks as well as general circulation and conceptual climate models suggest there was a strong, megamonsoon during the Mesozoic (Parrish and Curtis, 1982; Kutzbach and Gallimore, 1989; Parrish, 1993; Francis, 1994). During the Triassic, the land area of Pangea was equally distributed across the equator, permitting seasonal cross-equatorial wind reversals to develop as a result of strong seasonal changes in insolation (Parrish, 1993). In the midlatitudes, the climate likely was arid with a strong seasonality of rainfall (Kutzbach and Gallimore, 1989; Francis, 1994). The geologic expression of the megamonsoon is expected to reflect an annually fluctuating water table in the Ischigualasto Basin.

This paper examines the sedimentology and facies distribution patterns of Middle Triassic fluvio-lacustrine and paleosol deposits of the rift-fill sequence in order to

evaluate relative climate and tectonic controls on sedimentation in a chronostratigraphic framework. Although the initial interpretation of a humid climate during the Middle Triassic in the Ischigualasto Basin is based on the presence of a lake and its fossil content (Volkheimer, 1967; Stipanicic and Bonaparte, 1979; Alcober, 1996), the available accommodation space in the rift basin may have played a more important role in determining the presence of a lake system than the amount of water available (Lambiase, 1990). How the Triassic megamonsoon is expressed in the Ischigualasto Basin will be assessed using this tectono-stratigraphic model.

2. Geologic Setting

The Ischigualasto Basin is a large (~50 km wide and ~130 km long) half graben located along the suture zone between Paleozoic accreted terranes and Precambrian and Paleozoic basement rocks of the eastern Sierras Pampeanas (Fig. 1a). The basin lies in the San Juan and La Rioja provinces, ~150 km northeast of the city of San Juan. The Ischigualasto Basin is part of a cluster of subparallel north-northwest trending Triassic rift basins located in western and southern South America. Extension occurred prior to the breakup of Pangea (Ramos and Kay, 1991). These basins are thought to have developed as a result of extensional reactivation of the pre-existing Paleozoic structural fabric (Uliana et al., 1989). Basement rocks exposed in the Sierras Pampeanas include metamorphosed Precambrian granite batholiths, gneiss, schist, and mylonite (Jordan and Allmendinger, 1986). Paleozoic marine limestone, shale, and sandstone are also exposed along numerous thrust faults in the Sierra Pampeanas (Jordan and Allmendinger, 1986).

The Ischigualasto Basin is interpreted to have been asymmetric on the basis of seismic data and systematic decrease in rift-fill thickness away from the main basin-bounding Valle Fértil fault (Fig. 2) (Jordan and Allmendinger, 1986; Milana and Alcober, 1994). Shortening along the Sierra de Valle Fértil thrust fault system may have began as early as 10 Ma, but recent studies suggest thrusting began ~2.6 Ma and is still active (Jordan and Allmendinger, 1986; Zapata and Allendinger, 1996; Jordan, 2000). A series of plunging, asymmetric folds parallel to the Valle Fértil fault system exhumed the Triassic-age rocks (Jordan and Allmendinger, 1986).

Triassic rift evolution of the Ischigualasto Basin is divided into four major phases: 1) an initial extensional period, which created the half graben system during the Early to Middle Triassic; 2) a post-rift phase of subsidence during the late Middle Triassic; 3) a second period of extension during the Late Triassic; followed by 4) another period of post-rift thermal subsidence in the Late Triassic (Milana and Alcober, 1994). This paper focuses on the reconstruction of the paleoenvironments of Middle Triassic rocks with an emphasis on the sedimentological response to tectonic and subsidence pulses and climatic changes.

3. Stratigraphic framework

The Ischigualasto Basin is filled with a maximum of ~4 km of Triassic nonmarine rocks (Stipanicic and Bonaparte, 1979; Milana and Alcober, 1994) (Fig. 2). Seven formations comprise the basin fill: the Talampaya, Tajardos, Chañares, Ischichuca, Los Rastros, Ischigualasto, and Los Colorados Formations (Fms).

The Early Triassic Talampaya Formation (Fm) lies unconformably over Pennsylvanian or Permian units (López Gamundi et al., 1989). Both the Talampaya and Tarjados Fms consist of red-colored interbedded sandstone and conglomerate that formed in an alluvial fan/braidplain environment and are up to 1100m thick (Milana and Alcober, 1994; Alcober, 1996). A prominent silcrete horizon occurs at the boundary of the Tarjados and the coeval Middle Triassic Ischichuca and Chañares Fms. Some workers think that the Chañares Fm corresponds to the base of the Ischichuca Fm (Bonaparte, 1997). The Chañares Fm is characterized by tuffaceous sediments that ranges in thickness form 20 to 70 m (Alcober, 1996; Bonaparte, 1997). Calcareous concretions are present in the Gualo-Chañares and Cañon de la Peña regions, and often contain tetrapod bones (Alcober, 1996; Bonaparte, 1997). The Ischichuca Fm includes conglomerate, sandstone, siltstone, and shale and the formation ranges in thickness from 200 to 4050 m (Bonaparte, 1997; May, 1998; Milana, 1999). The flora of the Ischichuca Fm corresponds to the *Dicoidium* flora (*Zuberia*, *Dicroidium*, *Sphenopteris*, *Cladophlebis*, *Johnstonia*, cycads, and conifers) (Bonaparte, 1997). The transition from the Ischichuca Fm to the overlying Los Rastros Fm is gradational. The Los Rastros Fm is between 470 and 1000 m thick (Alcober, 1996). The Los Rastros Fm consists of sandstone and shale and similar flora as the Ischichuca Fm, but the Los Rastros Fm also contains fish (*Myriolepis elongatus*) and insects (Bonaparte, 1997). Both the Ischichuca and Los Rastros Fms are thought to represent lacustrine deltas and shallow lacustrine environments (López Gamundi et al, 1989; May, 1998; Milana, 1999). A discontinuous conglomerate separates the Los Rastros and overlying Ischigualasto Fm. The Late

Triassic Ischigualasto Fm contains abundant tuffaceous siltstone, sandstone, conglomerate, abundant fossil wood, and calcareous concretions with tetrapods (Bonaparte 1997). This formation is interpreted to represent fluvial and overbank deposits and paleosols. The Ischigualasto Fm is between 175 and 500 m thick (Alcober, 1996). The transition from the Ischigualasto to the overlying Late Triassic Los Colorados Fm is gradational. The Los Colorados Fm is characterized by red sandstone, evaporite, and red siltstone, and may represent eolian and playa environments (Lopez Gamundi et al., 1989; Milana and Lopez, 1995; Bonaparte, 1997). The Los Colorados Fm ranges from 95-1000m in thickness (Alcober, 1996).

The ages of these formations are poorly constrained but are thought to represent the entire Triassic (Bonaparte, 1997). The chronology of these units is primarily based on vertebrate and floral biostratigraphy (Stipaniac and Bonaparte, 1979; Bonaparte, 1997; May, 1998). The ages of the Talamapaya and Tarjados Fms are unknown, but based on ages of vertebrate fauna from other Triassic rocks from the Sierras Pampeanas region, these formations are considered to be Early Triassic (Alcober, 1996). Fossil plants and vertebrates in the Chañares and Ischichuca Fms suggest a Middle Triassic age (Alcober, 1996; Bonaparte, 1997). Basalt flows found interbedded with the Los Rastros and Ischigualasto Fms formed at 229 $\pm$ 5 Ma (Carnian), but the stratigraphic level and location of the samples dated are unknown (Odin and Létolle, 1982). Based on its megaflora and reptile fauna, the Ischigualasto Fm is considered to be Carnian or Norian (Retallack, 1977; Anderson and Cruickshank, 1978). Ar-Ar age dates of sanidines from the Herr Toba (bentonite) places the base of the Ischigualasto Fm at 227.8 $\pm$ 0.78 Ma, in

the Carnian (Late Triassic) (Rogers et al., 1993). The average of several K/Ar ages of the alkaline basalts found in the southern part of the Ischigualasto Basin, close to the town of Los Balecitos, is 224 ± 5 Ma (late Carnian) (Valencio, Medía, and Vilas, 1975).

4. Methods

Four detailed stratigraphic columns were measured perpendicular to the strike of the rift basin to investigate spatial and temporal patterns of sedimentation in the southern region of the basin (Fig. 1b). Two hundred and fifty outcrop samples were collected. Correlation between the stratigraphic sections is based on a continuous basal silcrete that occurs at the contact between the Tarjados and the overlying coeval Ischichuca-Chañares Fms, which is traceable across the basin, and on bentonites (Fig. 3). Rock colors were recorded in dry conditions using Munsell soil color charts. Paleocurrent data were collected from ripples (Tucker, 1996) and trough cross-beds (DeCelles et al., 1983).

Petrographic studies of representative samples were conducted using an optical microscope. Standard thin sections were prepared from freshly cut rock samples to study the mineralogy, micromorphology, paragenesis, and diagenetic features. Sandstone composition and provenance of detrital framework grains were determined using the Gazzi-Dickinson method (Dickinson and Suczek, 1979; Dickinson, 1985).

Mineralogical analyses of bulk rock and size-fractionated samples were performed using a Phillips X-ray diffractometer (XRD) equipped with a Cu tube and a graphite monochromometer. Bulk-rock samples were ground with a mortar and pestle and micronized with a micronizing mill using agate grinding elements in isopropyl alcohol. Size-fractionated samples were prepared by centrifuging ground and sonified

sample dispersions. The filter transfer method of preparing clay films on glass slides was used (Drever, 1973; Moore and Reynolds, 1989). Clay-sized fractions were treated with ethylene gylocol for identification. XRD patterns of clay-sized samples were modeled with the computer programs NEWMOD® and MIXER® to determine the percent abundance of illite in mixed-layered illite-smectite and interlayer ordering and the percent abundance of each clay mineral in the sample (Reynolds, 1985). Relative mineral abundances were determined using selected peak areas and mineral intensity factors for each mineral (Bayliss, 1986). All mineral abundances are within $\pm$7% (Bayliss, 1986). Mineral intensity factors were experimentally determined using quartz as an internal standard after Bayliss (1986), and all total clay values were from Hoffman (1976), and clay minerals from Reynolds (1985). The Mg^{2+} content in calcite was estimated from the position of the [104] peak (Brindley and Brown, 1980).

5. Facies analysis and interpretations of the Chañares-Ischichuca paleosol-paleolake complex

Thirteen lithofacies were recognized in the Chañares-Ischichuca paleosol-paleolake complex based on the geometry of the deposit, lithology, sedimentary textures, color, mineralogy, and fossil content (Table 1). These facies were grouped together into three lithofacies associations: red and green-gray mudrock+silicified claystone+fine-grained sandstone (association 1); conglomerate+sandstone (association 2); and fine-grained, laminated sandstone and siltstone+laminated claystone+shale+limestone (association 3). These groupings are based on vertical stratigraphic and basin-wide lateral lithofacies relationships.

5.1 Facies association 1

Facies association 1 is dominated by massive mudrock (~82-98%) with subordinate sandstone (~0-6%), silicified claystone and bentonite (~1-12%), and carbonate (<1%). This facies association is observed in all measured sections (Fig 2). This is the only facies association observed at Rio Gualo and Cerro Morado, and occurs at the base of the Rio Marco and Cañon de la Peña sections (Fig. 3). At the base of each section, silicified wood fragments and root structures were observed. The massive mudrock displays color mottling, muddy aggregate structures, carbonate peloids, carbonate-filled vertical and horizontal root and burrow traces, minor amounts of disseminated organic matter, and rare gastropods (Table 1). Clay coats (cutans) are prominent on sand- and silt-sized quartz and feldspar grains, and mud aggregates. Vertical changes in size and shape of aggregates of muddy material are common. Shapes range from subrounded, blocky interlocking (5-65 cm in diameter) to granular (0.5-2 cm in diameter) and rarely, platy structures in the mudrock (Fig. 4 a, b). Pseudoslickensides are found on edges of muddy aggregates. The clay mineralogy is dominated by mixed-layered illite-smectite or smectite with minor kaolinite. The sand- and silt-sized component of the mudrock is dominated by quartz. Relict silt-sized, thin bubble-wall volcanic shards are preserved by quartz and clay minerals in some mudrock beds. Subrounded, yellow-green sand-sized mud aggregates occur in some mudrock beds.

One laterally continuous carbonate unit (~0.2 m thick) and subrounded nodules in the Cañon de la Peña section contains volcanic shards, gastropods, ostracods, and charophytes. A few tabular, pink-colored, well-sorted feldspathic arenite beds with

planar cross-stratification occur in the Cañon de la Peña and Rio Marco sections. Paleocurrent data indicates flow to the north-northeast. Pink to gray silicified, continuous and discontinuous, wavy-bedded claystone range in thickness from 1-20 cm and have wavy bounding surfaces. Bentonites are both laterally continuous and discontinuous and typically less than 1 cm thick.

Interpretation

Both the vertical and lateral arrangements of facies association 1 reflect transitions from palustrine (pedogenically modified) and paleosol environments. The mudrock units in facies association 1 generally lack primary sedimentary structures, but pedogenic features are common. The diagnostic evidence that these deposits are of palustrine or paleosol origin include 1) the lack of well-defined soil horizons (laminations), 2) vertical and horizontal calcified root traces, 3) clay coatings around detrital grains (argillans) and clay-lined peds (ped argillans), 4) rounded muddy aggregates, 5) abundance of expandable clay minerals (smectite), and 6) mottling (bioturbation) (Retallack, 1988; Smoot and Olsen, 1988; Mack and James, 1992; Mack et al., 1993). Macroscopic structures include a variety of subrounded shapes of aggregates of muddy material interpreted to be peds. The crumbly granular and blocky weathering textures and rare pseudoslickensides are interpreted to be paleovertisolic (stress argillans) brought about by shrinking and swelling in response to wet/dry oscillations in the muddy material (Mack and James, 1992). The massive mudrock is interpreted to be a series of stacked, compound Bt horizons of moderately well-developed Vertisols. Individual paleosols are recognized on the basis of changes in ped size and shape and clay content

upsection (Retallack, 1990; Mack and James, 1992). In almost all cases, only stacked Bt horizons were preserved. Thick Bt horizons with multiple gradational sets of small to large interlocking blocky peds and wedge-shaped peds (4-65 cm diameter) are common. The Bt horizons each range from 1-10 m in thickness. Similar crumb fabrics and root structures are found in massive mudrock units in the Newark Supergroup (Smoot and Olsen, 1988), but in the Ischigualasto Basin, the massive mudrock is not intensely brecciated or mudcracked.

Crumb fabrics are often associated with modern aggrading playa environments (Smoot and Olsen, 1988). The abundance of stacked, low chroma, smectitic Bt horizons suggests that new sediment was incorporated into the soil profile by illuviation as a result of aggradation (Kraus, 1999). Silt-sized quartz and feldspars may represent aeolian influx into the muddy material. Evidence of clay translocation down profile into the Bt horizons of the stacked paleosols includes clay coating around detrital grains (argillans) and clay-lined peds (ped argillans). Sedimentation rates were likely moderate to high because the Vertisols do not display well-developed horizonation (Kraus, 1999). Compound pedogenesis often occurs as a result of aggrading fluvial systems and creates thicker sequences of stacked Bt horizons than observed in most modern Vertisols (Fastovsky et al., 2000). Aggradation in a palustrine setting could also account for the stacked nature of the observed macrostructures in the mudrock. Subaerial exposure of fine-grained lacustrine rocks at low-lake stands commonly shows evidence of pedogenesis (Platt, 1989a, b). Tabular, platy peds in the mudrock units are calcareous, contain burrows and rhizocretions, and a few mudcracks filled in by calcite. Carbonate

nodules, mudcracks, roots, and color mottling are typical of palustrine muddy environments (Cohen, 1982; Mount and Cohen, 1984; Platt, 1989a,b; Platt and Wright, 1991; Alsonzo-Zarza and Calvo, 2000). Additional support for a periodic lake level rise includes the presence of gastropods and charophyte stem fragments in the carbonate bed and carbonate nodules. The mudrock units are floodplain or pedogenically modified shallow lacustrine deposits. The carbonate is interpreted to be part of a few shallow, freshwater lakes in a distal alluvial fan setting.

Tabular sandstone beds in the Rio Marco and Cañon de la Peña sections are separated by sequences of mudrock (Fig. 3). Sandstone beds are interpreted to be either part of a distal fan channel or sheet flood deposit on an alluvial fan based on the bed geometry, organization of the sandstones, and planar cross-bedding.

Silicified claystone beds observed in the Cerro Morado, Cañon de la Peña, and Rio Marco sections contain relict volcanic ash, possibly deposited by sheetfloods that filled in the pre-existing topography of the area. In the Cañon de la Peña and Rio Marco sections, the morphology of these altered ash deposits suggest a moderately flat terrain. In the Rio Gualo and Cerro Morado sections, these deposits are not laterally continuous because of bioturbation and pedogenesis.

5.2 Facies association 2

Facies association 2 contains abundant fine-grained massive sandstone (~70%) and subordinate pebble conglomerate (~30%) and bentonite (<1%). This facies association comprises most of the basin-fill sequence in the western part of the basin in the Cañon de la Peña and Rio Marco sections, and is absent in the Rio Gualo and Cerro

Morado sections (Figures 2 and 3). Conglomerate beds are 0.2-4 m thick and are separated by packages of 0.3 to 3 m thick beds of massive sandstone (Figure 3; Table 1). The conglomerate units are laterally continuous on outcrop scale. Occasional lenticular bodies are recognized, but channel geometries cannot be accurately measured because the lateral extent of the sandstone bodies exceeds the length or width of outcrop exposure on canyon walls (Fig 5a). The conglomerate beds have erosional bases (Fig. 5b) and commonly contain load structures. These units exhibit crude upward fining trends, and trough cross-beds, horizontal laminations, and climbing ripples (Fig. 5c). The coarse-grained sandstone to conglomerate composition is dominated by quartzose fragments (average: ~80%) and less amounts of feldspar (average: ~10%) and lithic fragments (average: ~10%). Rare carbonized plant debris occurs in the conglomerate beds. Green-gray mudchips range from sand-size to up to 8 cm in length (Fig 5d). They contain plant debris and are composed of kaolinite and illite.

The erosive bases of the pebble conglomerate beds are incised into underlying massive, tabular beds of red- and green, fine- to medium-grained sandstones (Table 1). The transitions between the conglomerate beds and overlying and underlying red and green fine-grained, micaeous sandstone and siltstone beds are abrupt (Fig 5b). Most of the sandstone beds lack evidence of primary sedimentary structures, except red or green mottling and rarely calcareous mudcracks and rhizocretions (Table 1). Plant debris is common in the massive sandstone.

Interpretation

Facies association 2 is interpreted to be braided stream, fluvially-dominated lacustrine deltas, and fluvial and lacustrine overbank deposits that are intercalated with lacustrine units. Braided river and braid deltas deposits are characterized by normal size grading from gravel conglomerates to sandstone caps, abundance of cross-stratification, lack of muddy matrix, sheet geometry, and high porosity and permeability (McPherson et al., 1987). Evidence for braided, bedload streamflow processes includes clast-supported, trough and planar cross-bedded conglomerate beds that form large-scale lenticular bodies with high width-to-depth ratios (Collinson, 1996; Miall, 1996). The scoured bases of the conglomerate beds, predominance of bedforms, and well-sorted, clast-supported fabric indicate deposition by subaqueous three-dimensional ripples in shallow waters (Heward, 1978; Hubert and Hyde, 1982; Allen, 1985). Each conglomerate bed exhibits deceleration of flow sedimentary structures along with an upward fining sequence, and terminates with low-angle climbing ripples and mudchips, characteristic of sudden deceleration of flow (Smoot, 1991).

Sand-sized and larger mud aggregates were transported as bedload, typical of modern semi-arid climates such as in the Lake Eyre Basin, Australia (Rust and Nanson, 1989; Collinson, 1996). The process of wetting and drying swelling clays (smectites) in floodplains is enough to form clay aggregates (Rust and Nanson, 1989). Mud curls form during dry conditions and these curls are incorporated into the next flood event (Rust and Nanson, 1989). Mudchips are not destroyed during transport (Smith, 1972). Pedogenic mud chips are recognized in other ancient fluvial and coeval paleosols such as in the Jurassic East Berlin Fm (Connecticut, USA), Triassic Hawkesbury Sandstone (NWS,

Australia), Carboniferous Maringown Fm (New Brunswick and Nova Scotia, Canada), and Lower Devonian Lower Red Sandstone (SW Wales) (Rust and Nanson, 1989; Ékes, 1993; Gierlowski-Kordesch and Rust, 1994; Gierlowski-Kordesch, 1998). The Triassic Hawkesbury Sandstone has the most in common with deposits from the Ischigualasto Basin. The Hawkesbury Sandstone is interpreted to have formed in semi-arid climates, but had higher rainfall and water tables than the other deposits listed above based on the gleyed colors, relative lack of desiccation cracks, scattered plant fragments, and local roots (Rust and Nanson, 1989), which is similar to the mudrock of facies association 1.

The channel-fill sequences alternate with sequences of massive sandstone beds (Sm) (Table 1). Braided streams likely avulsed and were abandoned on the floodplain between meters 25-60 in Rio Marco and between meters 30-175 in Cañon de la Peña or lake-margins were overtopped (Figure 3). Sand and silt likely accumulated from suspension in flood water that invaded the floodplain after spilling over the braided river channel banks or lacustrine overbanks as crevasse splay or levee deposits. These massive, micaeous sandstone beds may indicate low flow conditions because abundant platy particles often inhibit ripple formation (Collinson, 1996). Bioturbation could also explain the lack of primary stratification in the massive sandstone because roots and disseminated organic matter are common. The red and green colors of the sands are likely due to early diagenetic alteration of feldspars and micas to clay minerals or resulted from the removal of iron in ferrous iron-organic complexes in reducing waters (Dubiel and Smoot, 1994). Plant debris may have been the origin of the reducing conditions because oxygen would be depleted quickly in the presence of abundant organic matter

(Dubiel and Smoot, 1994). Similar stratigraphic relationships and sedimentologic features are observed in the fluvially-dominated lacustrine deposits of the Mississippi delta plain (Tye and Coleman, 1989). The absence of Gilbert-style deltas in Louisiana is attributed to a low gradient basin and high volume of sediment in the fluvial systems (Tye and Coleman, 1989).

High channel migration, avulsion, and aggradation rates are apparent by the stacked arrangement of isolated, wide channels and massive, tabular fine-grained overbank deposits and climbing ripples (Fig. 4 a) (Ashley et al., 1982; Bristow and Best, 1993; Miall, 1996). Avulsion frequency in braided systems is the result of high rates of sediment accumulation and increase in flooding or tectonic events (Bristow and Best, 1993). Deceleration of flow and fining upwards sequences within conglomerate bodies may indicate these beds were deposited as they intersected a shallow, standing body of water (Smoot, 1985; Smoot, 1991). Fining-upward trends like these are interpreted to be the result of broad, flat lacustrine delta fronts because of their association with lacustrine facies discussed in the next section. Periodically, at meters 175-255 in the Cañon de la Peña section and between meters 50-190 in the Rio Marco section, these braided streams were probably overtaken by a lake (Fig. 3). Braided stream and finely-laminated lacustrine deposits are intercalated with each other in those intervals. Similar vertical and lateral facies relationships are seen in the Late Triassic Stockton and Hammer Creek Formations of the Newark Supergroup (USA) (Smoot, 1991). Classic Gilbert-style deltas were likely absent during lake formation because lake depths may not have been great enough for large-scale clinoforms to develop, perhaps because of high sedimentation

rates (Smoot, 1985; Platt and Wright, 1991). Gilbert-type deltas are common in deep, freshwater lakes with steep gradient rivers flowing into the lake (Talbot and Allen, 1996).

5.3 Facies association 3

This association is characterized by a dominance of fine-grained laminated sandstone, siltstone, claystone, and carbonate; shale; and massive siltstone (Table 1). Most beds are tabular and have sharp, non-erosive bases (Figure 6a). Facies association 3 accumulated preferentially in the western part of the basin, in the Rio Marco and Cañon de la Peña sections (Figure 3). Rio Marco has the thickest sequences, and these facies dominate the section (~55%). At Cañon de la Peña, this facies association comprises a minor component of the section (~12%).

Three lamina types are present in facies association 3: clastic, organic, and carbonate. Sequences of clastic (0.5-2 mm thick) and organic (< 0.5-1 mm thick) couplets are much thicker and more abundant than carbonate/organic and organic/ clastic couplets. In general, siliciclastic laminae are not graded and clastic particles in individual laminae are moderately well sorted. Successive laminae are distinguished by compacted organic matter (Fig. 6b). The organic matter has a cellular structure or is amorphous. Sand-sized mud aggregates are common in the clastic laminae. Rarely, the sandstone beds are symmetrically rippled (Fig. 6c). Ripple indices range from 8 to 25. The sequences of carbonate (0.5-1 mm) and organic (< 0.1 mm) couplets contain low-Mg calcite cements, shell hash, ostracods, gastropods, and charophyte stem fragments. Organic matter associated with carbonate laminae does not show obvious woody

structures. Carbonate-organic laminae are commonly but not always rippled. Ripple indices range from 8-15.

Siltstone beds have traces of remnant lamination based on the abundant, scattered distribution of carbonized plant debris. Rarely, impressions of Unionid shells are scattered within the siltstone beds.

Interpretation

The predominance of laterally continuous millimeter-scale laminations and fine grain size suggest deposition occurred in a quiet lacustrine environment. Both littoral and profundal lacustrine environments are preserved in facies association 3. The abundant millimeter-scale clastic-organic laminae are interpreted to be prodeltaic deposits in littoral to profundal environments because these laminations may be traced laterally to fluvial conglomerate beds. In addition, all the laminated clastic-organic couplets have sand-sized mud aggregates, which likely were deposited from fluvial input into the lake because the conglomerate units of facies association 2 have the same mudchips. The laminated sandstone units often coarsen and thicken upwards, which is typical of delta progradation into a lake during lake level fall, a pattern especially evident in the Rio Marco section between meters 70-90 (Figure 3) (Smoot, 1993). Ripple indices of some laminated sandstone beds imply both current and wave reworking of sands in a shallow, nearshore environment. The lack of evidence for bioturbation, gas bubble escape from organic-rich intervals, pyrite, siderite, manganese oxides, or fossil kill accumulations from overturn events suggest the lake was a shallow, oxygenated freshwater lake with high sedimentation rates, similar to what is observed in Lake Turkana (Cerling, 1986).

The accumulation and preservation of finely laminated, regular alternations of clastics and organics requires at least one of the following favorable conditions: 1) absence of bioturbating organisms, 2) high sedimentation rates in oxic lake bottom conditions, 3) minimal bottom current activity, 4) a relatively extensive flat lake floor, and 5) minimal gas bubble generation from organic matter decay (Talbot and Allen, 1996). Lamination may be preserved in lakes if the sediment remains undisturbed after deposition (Anderson and Dean, 1988). Preservation of organic matter and laminations in lake sequences does not require a stratified water body or permanently anoxic conditions (Anderson and Dean, 1988; Talbot and Allen, 1996). The clastic-organic rhythmite formation in the Ischigualasto Basin may result from seasonal or episodic changes in sediment supply related to runoff events in the watershed.

The black shale units of the Ischigualasto Basin are interpreted to be lake-marginal swamp deposits based on their relationship with facies association 2 and the presence of coarse, sand-sized material and the abundance of organic matter with a cellular structure. Black shale is often thought to reflect deep lake waters conditions when in fact they are found in lakes as shallow as 4 m (Lorenz, 1988). Lake marginal peat deposits often are composed of almost pure plant remains (Talbot and Allen, 1996).

The laminated carbonate deposits reflect both low-energy profundal and littoral lacustrine deposition. The low-energy profundal facies is represented by silt-sized calcite crystals in the laminated micrite, probably formed by inorganic precipitation, but may have been aided by algal blooms. The lamination in this lithofacies is highlighted by amorphous organic films. The littoral facies is represented by reworked, episodic sand-

and gravel-sized allochems of mainly charophyte stems and a few gastropods and ostracods in ripple-laminated carbonate. The preservation of charophyte stem fragments and other bioclastic material in rippled laminae suggest these particles were deposited above wave base and relatively close to shore. The charophytes indicate shallow water because most charophytes meadows occur within <20 m depth, in the littoral zone (Anadón et al., 2000). Ostracods, gastropods, and charophytes are all common in freshwater carbonate lake environments (Kelts and Hsü, 1978).

The massive siltstone beds owe their sedimentary fabric to bioturbation because burrowing often completely homogenizes beds and disrupts sedimentary structures. These beds were likely deposited in oxic conditions in shallow water along the lake margin in the littoral zone. Impressions of Unionid shells in the siltstone indicate freshwater water conditions in a shallow lake environment.

6. Summary and Paleoenvironmental Reconstruction of the Ischichuca-Chañares Paleolake-Paleosol Complex

The thickness of the Ischichuca-Chañares paleosol-paleolake complex varies across the basin, depending on the proximity to the border fault (Fig. 2). In the eastern region of the basin, the total thickness is between 30 and 60 meters. Closer to the border fault, the thickness ranges between 180 and 250 meters.

Facies associations in the Ischigualasto Basin are dominated by fluvial and fluvio-deltaic deposits of facies association 2 along the western margin of the basin, and palustrine deposits and paleosols of facies association 1 in the southern and eastern regions of the basin (Figure 3). Mudrock deposits of facies association 1 are also located

along the base of the western basin margin at the base of the measured sections. Channelized conglomerates and coarse-grained sandstones of facies association 2 are separated by sequences of finer-grained massive beds of sandstone. These deposits interfinger with laminated lacustrine units of facies association 3. Three major phases of lake development are recognized in the western region of the basin, closest to the border fault (Figure 3). Several lateral and vertical trends are clear in the western region of the basin: 1) a rapid transition from distal alluvial fan facies to braided stream facies near the base of the sections, 2) a vertical increase in the abundance of laminated lacustrine units, 3) abrupt lateral and vertical facies changes in the western region of the basin, and 3) lack of evidence for desiccation. In the southern and eastern part of the basin, no significant change in grain size or facies was noted. Stacked sequences of compound Bt horizons of Vertisols dominant the stratigraphic sections. Lateral and vertical facies transitions across the southern end of the Ischigualasto Basin can be used to reconstruct paleoenvironmental change during the Middle Triassic.

Two temporal paleogeographic reconstructions of the southern region of the Ischigualasto Basin can be made using lateral and vertical facies relationships and paleocurrent and provenance data. The reconstructions reflect temporally distinct sedimentary depositional phases (Figure 7). Distal alluvial fan depositional environments prevailed across the basin during the initial depositional phase across the basin (Fig. 7a). The abundance of pedogenic features and the rare occurrence of lacustrine flora or fauna suggests the mudrock deposits are modified marginal lacustrine mudrock or, in the more distal parts of the basin, Vertisols. The occurrence of rounded mud aggregates, similar to

those seen in the laminated lacustrine and fluvio-deltaic deposits, indicates either these are wind-blown mud pellets or they are from reworked lacustrine material during shoreline oscillations. Preserved volcanic shard textures in some mudrock units indicates a volcanic source of silt-sized ash.

During the second time interval (Figure 7b), stream-dominated braidplains prograded from the west-southwest basin margin onto the floodplain and graded into lacustrine environments to the north-northeast. Several fluvio-deltaic depocenters existed during this time interval. Paleocurrent indicators and the predominance of Precambrian granitoid and schistose rocks and hematite-stained sand-sized quartz grains from the Lower Triassic Tarjados and Talampaya Fms suggest north-northeast paleoflow. Initiation of braided streams and associated overbank deposits near the border fault reflects a change in conditions in the basin, either due to increased erosion because of a wetter climate, or basin subsidence, or both. Marginal lacustrine deposits are found in the southern and western parts of the basin at Cerro Morado and Rio Gualo. Oscillations of the lake shoreline likely exposed marginal lacustrine facies. Pedogenic modification during emergence resulted in mottling, rhizocretions, and rare charophyte fragments as recorded in the palustrine and moderately developed Vertisols. During this interval, the lake expanded, likely covering at least a 40 km^2 aerial extent based on lateral facies relationships.

7. Separating Climate and Tectonic Effects on Rift Sedimentation

Both tectonics and climate exert a strong control on the basin fill and sedimentological architecture in rift systems (Lambiase, 1990; Platt and Wright, 1991;

Anadón et al, 1991). In the following sections, the relative contribution of tectonic activity and climate on facies distribution is discussed.

7.1 Tectonic Influence

Large-scale architectural features and trends of the basin-fill sediment reflect the tectonic influence on rift sedimentation (Table 2). Both rapid motions along the border fault during active rifting and slower post-rift subsidence play an important role in the position and amount of accommodation space available for sediment to accumulate (Leeder and Gawthorpe, 1987; Lambiase, 1990; Platt and Wright, 1991). The thickness of the Ischichuca and Chañares Fms is greatest closer to the Valle Fertil border fault (180-250 m) along the western edge of the Ischigualasto Basin than at the eastern zone (20-30 m) of the rift system (Milana and Alcober, 1994; Bonaparte, 1997), suggesting that higher rates of subsidence and sedimentation occurred along the western margin (Figure 2).

The distribution of sedimentary sequences that develop during active rifting and post-rift subsidence are unique and can be distinguished in the stratigraphic record (Leeder and Gawthorpe, 1987; Lambiase, 1990). In active rifts, the deep lakes develop directly over the deepest region of the basin (Lambiase, 1990; Platt and Wright, 1991). Lake marginal deposition of the Ischichuca-Chañares complex occurred ~10 km from the border fault. Deposition of lake marginal facies adjacent to steep rift lake margins typically occurs within ~2 km of the border fault in the modern East African Rift lakes (Lakes Tanganyika and Turkana) and is inferred to be less than ~2 km in ancient systems such as the Newark Supergroup and Camp Rice and Palamo Formations of the Rio

Grande Rift (Lorenz, 1985; Cohen, 1990; Olsen, 1990; Mack and Seager, 1990). The position of lacustrine sedimentation in the Ischigualasto Basin suggests the hanging wall gradient was gentle near the footwall scarp (Fig. 7b).

Lake depth and morphology of the western region of the Ischigualasto Basin was controlled by a complex interplay between basin subsidence and sediment influx. Braidplain and fluvial-dominated lacustrine deltaic sedimentation are common in basins with low-gradient slopes (Tye and Coleman, 1989). During the Middle Triassic, a low-energy ramp (gentle slope) is indicated by the lack of evidence for slumps or large-scale, high-angle foresets dipping lakeward (clinoforms; Gilbert-style deltas) along lake margins. There are two competing, but not mutually exclusive, hypotheses that could explain the lack of clinoform development: 1) inhibition of clinoform development during rapid transgressions in a broad, shallow lake (Smoot, 1985) or 2) sedimentation rates kept pace with subsidence rates (Platt and Wright, 1991). Modern examples of small drainage basins with either small or large lakes often do not have Gilbert deltas (Smoot, 1985). In those cases, river mouths are drowned out by the rising lake levels, inhibiting topset and foreset formation (Smoot, 1985). If sedimentation kept pace with subsidence in the Ischigualasto Basin, there should be a gradual transition between shallow and deep lacustrine sedimentation, which would cause lake depths to remain shallow. The observed stacked symmetric sequence of transgression-regression facies suggests that climatic conditions had more control on the presence of the lake. If tectonics had a major control over the presence of the lake, then an asymmetric lithofacies assemblage (deep water to shallow water facies) would accumulate in the

basin and a coarsening upwards trend would be recorded in the rock record (Gore, 1989; Lambiase, 1990). If climate had the major influence on sedimentation, then the lake basin would gradually deepen and be filled in by shoreline progradation (Gore, 1989; Gierlowski-Kordesch and Kelts, 1994). The sequence of deposition of lacustrine deposits during each of the three major lake phases is generally symmetric in the western margin of the Ischigualasto Basin (Fig. 8).

High sedimentation and aggradation rates in the Ischigualasto Basin are indicated by both fluvial and paleosol deposits. The fluvial systems in the western region of the Ischigualasto Basin indicate high aggradation rates based on high overbank:channel ratios. Sediment originating from the footwall uplands that progrades onto the hanging wall dip slope and will decrease the gradient between the highlands and the basin floor (Alexander and Leeder, 1987).

The hanging wall slope in the eastern and southern part of the Ischigualasto Basin is also interpreted to be gentle. The lateral extent and thickness of the moderately well-developed Vertisols, which experienced minor or no lacustrine influx, suggests there was a low-gradient basin floor in those regions (Fig. 7a,b). Minor fluctuations in lake level often expose extensive areas if the lake margin is flat (Platt and Wright, 1991). Minor lacustrine influx is inferred for the southern part of the basin based on accumulations of a few ostracods within the carbonate-rich peds. Cumulative packages of compound, stacked Bt horizons of Vertisols in the eastern region of the basin indicate significant aggradation and pedogenesis occurred. Multiple paleosol horizons are not preserved, suggesting that erosion or composite paleosols developed.

In summary, deposition of sediments occurred during slow, post-rift subsidence of the rift basin. The lake margins near the footwall scarp and the hanging wall dip slope are inferred to be gentle, low gradient ramps.

7.2 Climatic Influence

Several small-scale, diagnostic sedimentologic features in all paleovironments in the Ischichuca-Chañares Fms can be used to decipher past climatic conditions (Table 2). A number of these features indicate regionally high water tables and seasonally wet and dry conditions. The abundance of plant debris in fluvial, overbank, deltaic, and lacustrine deposits indicates that hydrologic conditions were optimal for organic matter preservation (Demko et al., 1998). Regionally high water tables are indicated because samples from many different paleoenvironments contain fossil plant remains. The presence of freshwater fauna and flora (bivalves, gastropods, ostracods, and charophytes) and detrital clay mineral assemblages, and lack of saline minerals and desiccation cracks in lacustrine sequences also suggest a perennial lake or at least an annual positive water balance (Kelts and Hsü, 1978; Chamley, 1989).

Several sedimentological features indicate seasonality of rainfall. Episodic changes in climate are inferred from the presence of vertic features in marginal paleosols and moderately developed Vertisols; abundant sand-sized mud aggregates in fluvial, prodelta, and profundal deposits; and repetitive millimeter-scale lacustrine laminations. Moderately developed Vertisols are distributed laterally and vertically throughout the rift-fill sequences, suggesting semi-humid to semi-arid conditions persisted throughout the Middle Triassic. Modern occurrences of Vertisols experience shrinkage and cracking

during the dry season and swelling and shearing in the wet season. As a result of these wet-dry oscillations, angular to subangular blocky peds (soil aggregates) bounded by stress cutans form.

Sand-sized mud aggregates in fluvial systems occur in semi-arid climates (Rust and Nanson 1989). In the Ischigualasto Basin, channel deposits, prodeltaic sediments, and lacustrine laminae also contain pedogenic mud aggregates. The process of wetting and drying swelling clays (e.g., smectite) in floodplains is enough to form mud aggregates (Rust and Nanson, 1989). Mud curls form during dry conditions in the soils, and these curls are incorporated into the next flood event (Rust and Nanson, 1989).

Lacustrine couplets are another indicator of episodic changes in environmental conditions, producing repetitive couplets in the littoral and profundal zones. Clastic-organic couplets dominate the lacustrine sequences, but carbonate-organic couplets also exist. Fluvial systems supplied abundant clastic material and terrestrial organic matter to the lake system. Lake levels are interpreted to have fluctuated as a result of sediment and water supply. Clastic dominated lacustrine sequences are often thought to reflect high rates of precipitation in the watershed (Glenn and Kelts, 1991).

Although climate changes (sediment and water supply) controlled the types of sediment that accumulated in the Ischigualasto Basin, facies distributions in the rift basin are controlled by differential subsidence (east vs. west) across the basin.

8. Conclusions

1. The basin fill of the Ischigualasto Basin provides a detailed record of climatic and tectonic conditions during rifting. Along the western edge of the basin, distal alluvial

paleosols grade upward into braided stream deposits followed by deltaic and lacustrine deposits. Palustrine and marginal paleosols are restricted to the eastern and southern edges of the basin.

2. There are two important environmental implications of this study. The lake system in the Ischigualasto Basin was a freshwater lake based on the presence of freshwater fauna, detrital clay mineral assemblages, lack of evaporite minerals, and absence of desiccation features. Despite evidence of lake-level fluctuations, there is no evidence of complete desiccation of the lake. Significant pedogenesis and pedogenic modification of palustrine deposits only occurs in the eastern and southern parts of the basin.

3. During deposition of the Ischichuca-Chañares Formations, braided streams flowed to the north-northeast from the western margin of the basin into a lake. Lacustrine deposition expanded during deposition of these formations to a maximum areal extent of ~40 km^2. The central region of the Ischigualasto Basin has subsequently been eroded or is buried by Quaternary sediments, so detailed evaluation of profundal lake deposition cannot be accomplished using outcrop data.

4. Basin hydrology is inferred from organic matter preservation and root systems in overbank deposits. Widespread fossil plant distribution in fluvial, overbank, deltaic, and lacustrine deposits indicate a high regional water table. Shallow root systems support this hypothesis. The western lake margin was likely heavily vegetated, based on the abundance of swamps, which contributed abundant organic matter to the lake.

5. Seasonality of climate is indicated by the development of vertic features in Vertisols and palustrine deposits along the hanging wall dip slope. Pedogenic mud aggregates found in both fluvial and lacustrine rocks also indicate seasonal wet and dry conditions. Successive clastic/organic lacustrine couplets may also imply episodic changes in water and clastic supply to produce repetitive laminae.

6. During the Middle Triassic, several lines of evidence show that the rift basin was slowly subsiding: basin fill patterns, lateral extent of palustine-paleosols in the distal region, location of lake shoreline deposits with respect to the basin bounding fault, and lacustrine deltaic architecture. The thickest deposits occur in the western part of the basin where maximum subsidence occurred. Marginal lacustrine facies accumulated ~10 km from the border fault. The lack of Gilbert-style delta formation and slumps indicates a low-relief lake margin. Palustrine deposits are extensive to the east and south resulting from the low-gradient ramp-type margin. High avulsion rates in the western art of the basin are likely due to high sedimentation rates. Compound Vertisols in the eastern margin of the basin also indicate significant aggradation. Sedimentation rates and basin subsidence likely kept pace with each other in order to produce the basin fill sequence during the Middle Triassic in the Ischigualasto Basin.

7. The climate indicators preserved in the Ischichuca-Chañares paleolake-paleosol point to strong seasonality in the Ischigualasto Basin during the Middle Triassic. The climate is inferred to reflect a semi-humid to semi-arid environment.

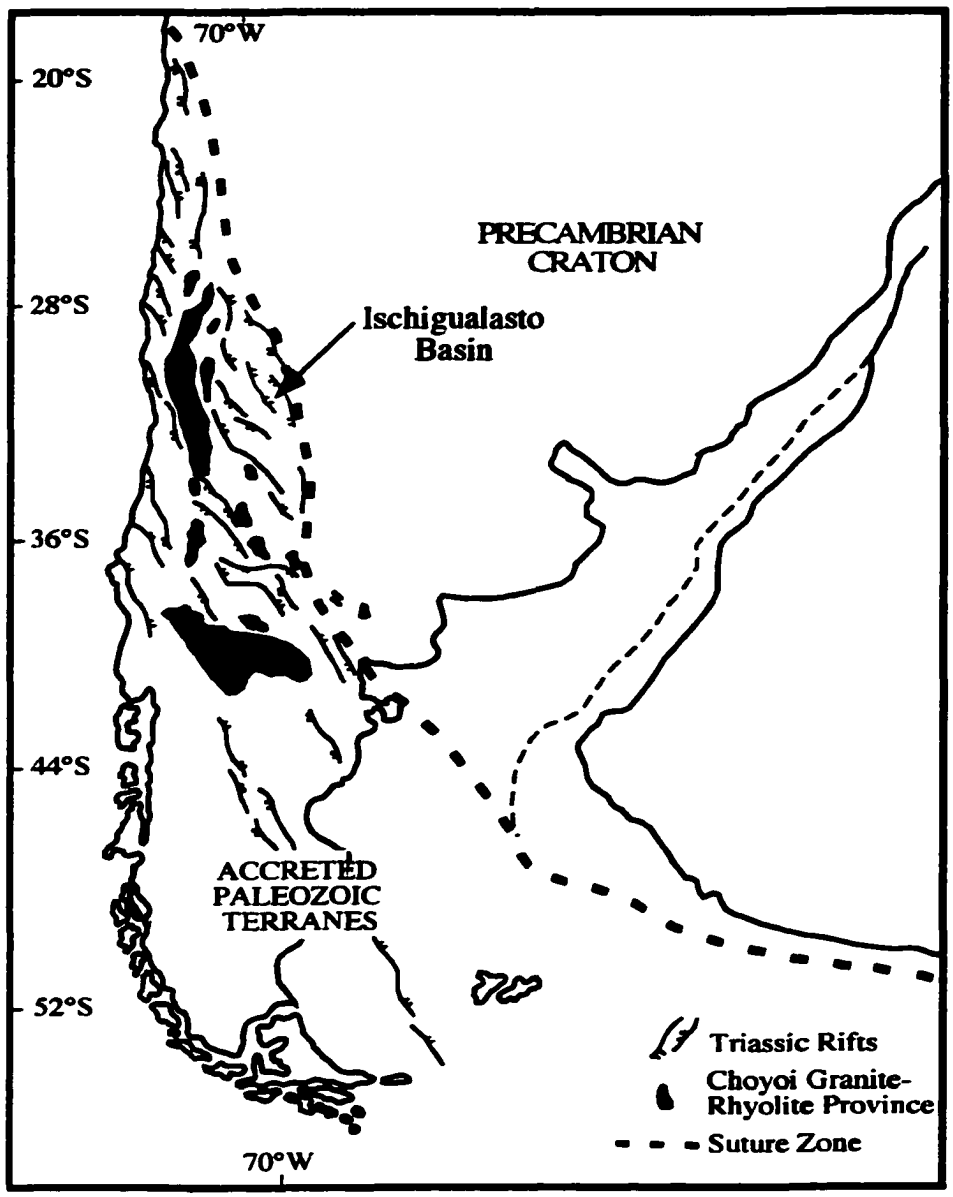

FIGURE A-1A. Geologic setting of the Ischigualasto Basin (labeled IB on map) in context of South American Triassic rift basins (modified from Ramos and Kay,1991).

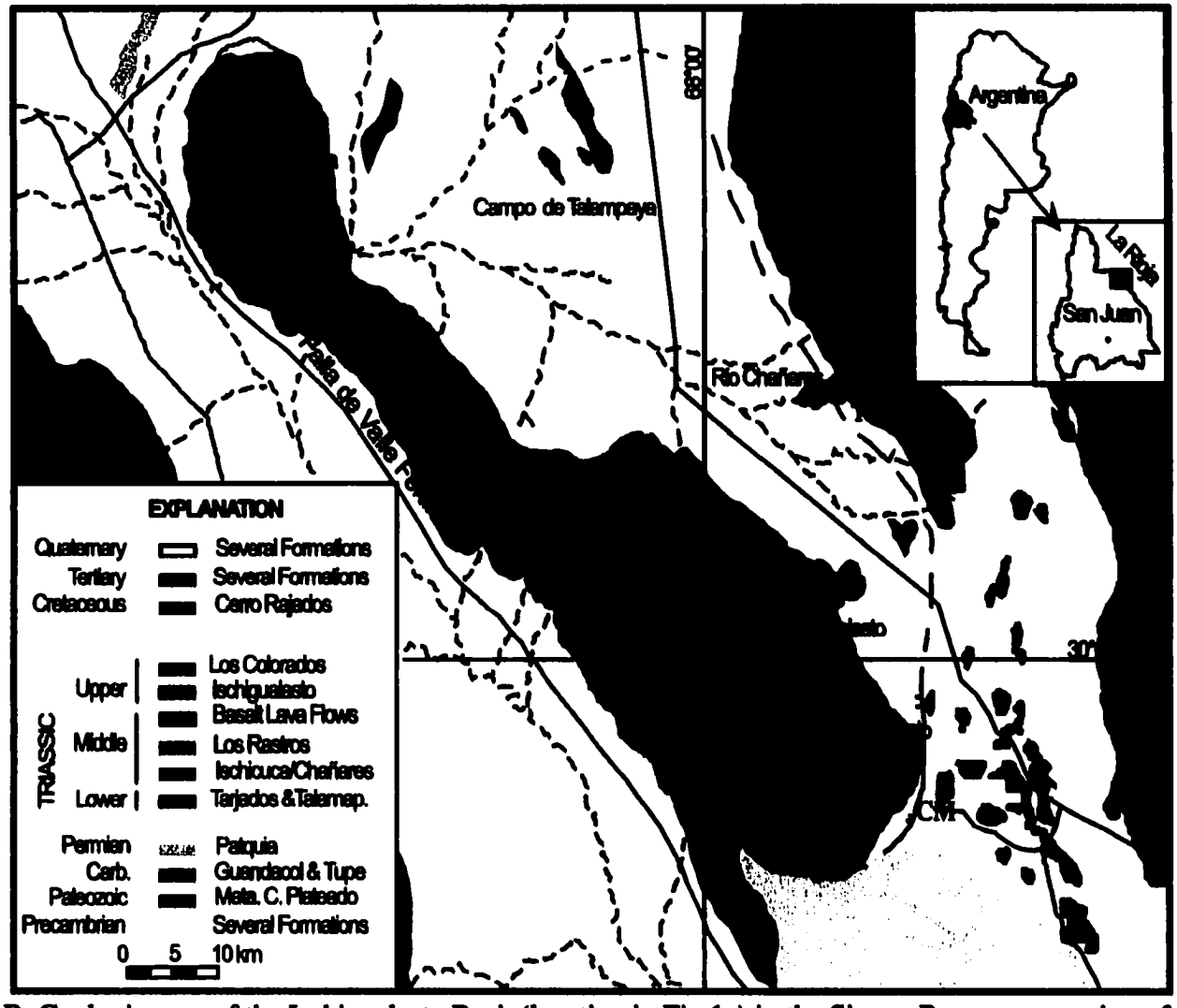

FIGURE A-1B. Geologic map of the Ischigualasto Basin(location in Fig 1a) in the Sierras Pampeanas region of NW Argentina (from Milana and Alcober, 1994). Measured sections are labeled on the map as follows: CP- Canon de la Pena, RM- Rio Marco, CM- Cerro Morado, and RG- Rio Gualo.

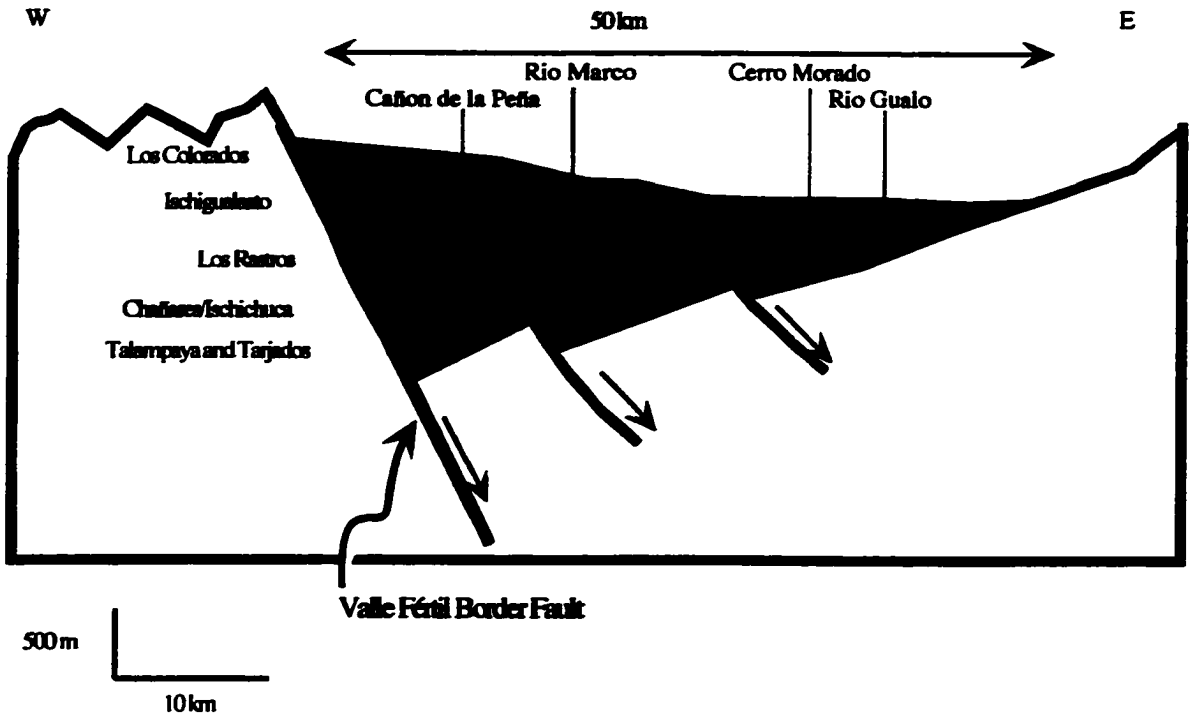

FIGURE A-2. Stratigraphy and generalized basin fill geometry of Triassic continental sediments of the Ischigualasto Basin based on lithostratigraphic log made perpendicular to the trace of the Valle Fertil border fault (based on information from Lopez-Gamundi et al. (1989), Milana and Alcober (1994), Alcober (1996), and this study).

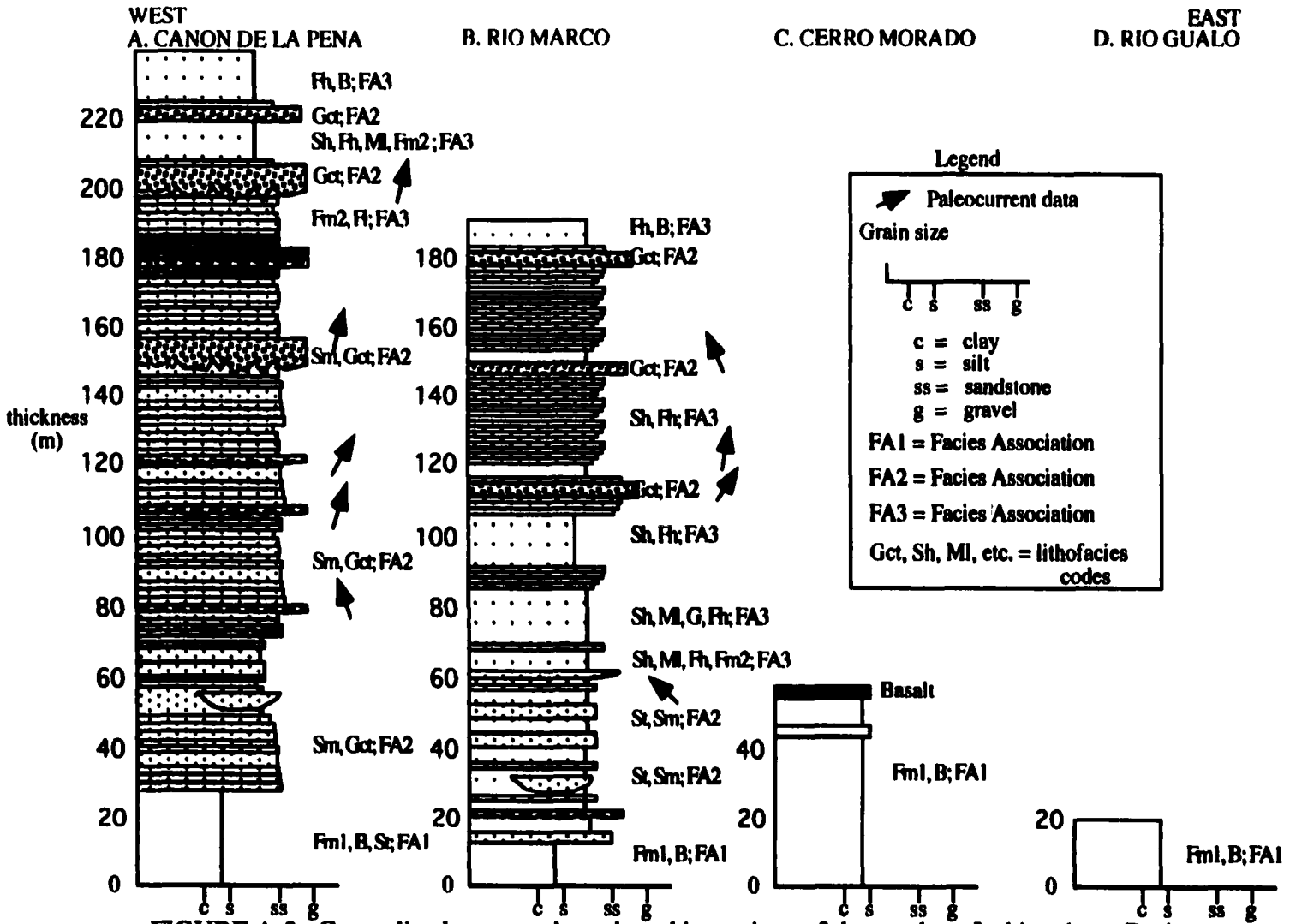

FIGURE A-3. Generalized measured stratigraphic sections of the southern Ischigualasto Basin showing the transition between lithofacies associations across the basin. See Figure 1b for section locations. See TABLE A-1 for lithofacies codes and descriptions. See text for discussion of facies associations.

FIGURE A-4 a) Large interlocking subrounded peds from the Rio Gualo section. Jacob staff is 1.5 m tall

FIGURE A-4 b) Platy ped texture from the Cañon de la Peña section. Note the mottled texture. Hammer for scale.

FIGURE A-5a) Stacked channelbodies from Cañon de la Peña. Note how channel widths exceed heights and pinch out. Channels are separated by red- and green-colored sandstone beds. Arrow points to pinchout.

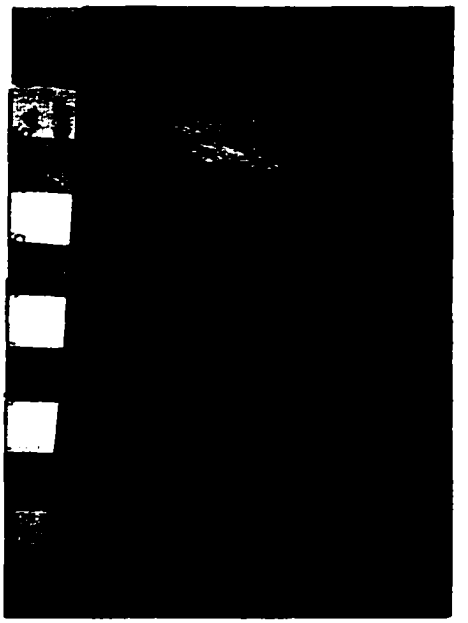

FIGURE A-5b) Channel incises into the red and green-colored sandstone. Note the mottling. Jacob staff increments are 10 cm. Arrow points to mottled region.

FIGURE A-5c) Trough cross-beds in pebble conglomerate from Cañon de la Peña. Arrow points to a basal trough scour surface.

FIGURE A-5d) Green-gray colored mudchips in sandstone bed in Rio Marco. Arrow points to mudchip. Hammer for scale.

FIGURE A-6a) Laterally continuous laminated mudrock from Canon de la Pena. Hammer for scale.

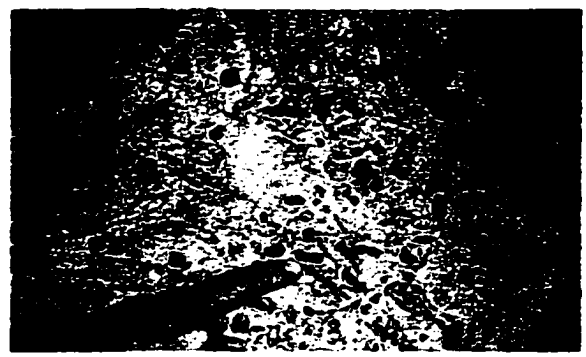

FIGURE A-6b) Laminated sandstone with terrestrial plant fragments.

FIGURE A-6c) Rippled sandstone from the Rio Marco section. Hammer for scale.

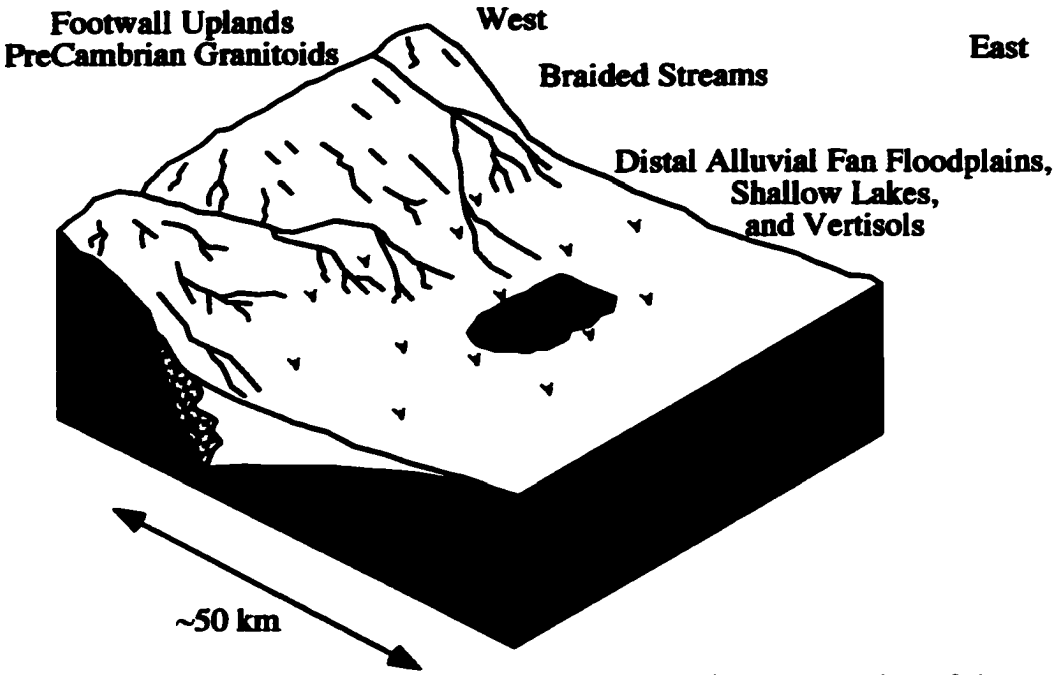

FIGURE A-7a) Time Interval 1:Paleoenvironmental reconstruction of the southern Ischigualasto Basin.Few braided streams drained the highlands and most of the basin was a floodplain. Pedogenesis was extensive.

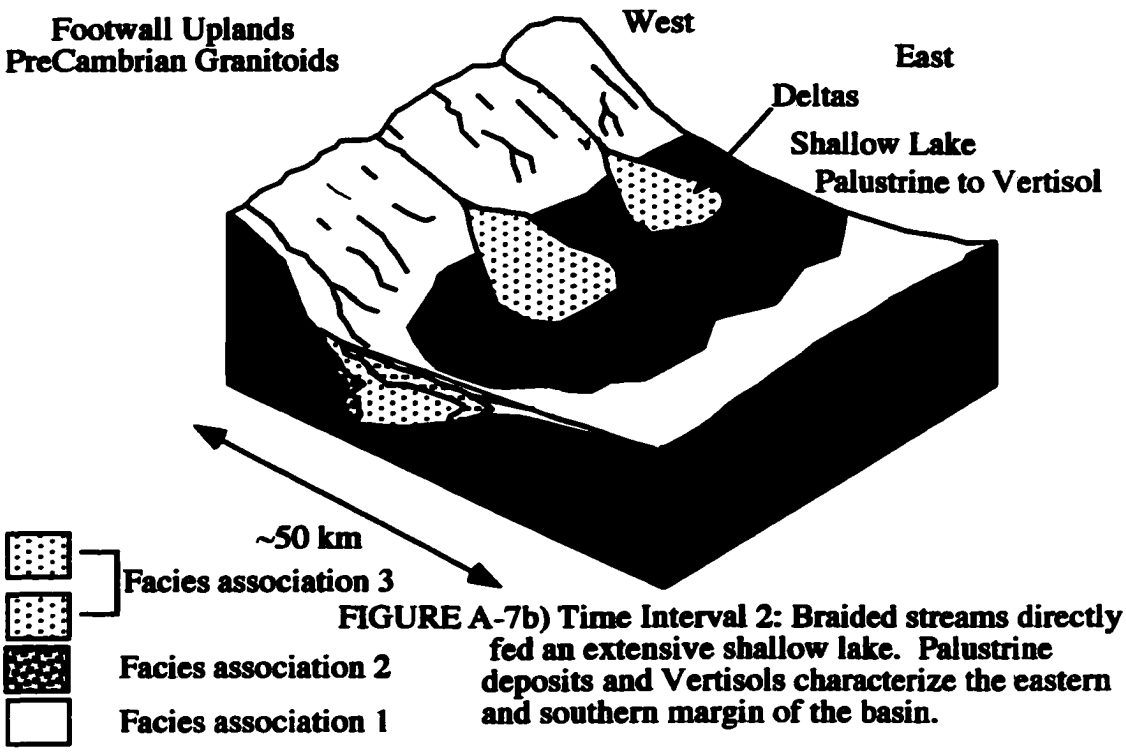

FIGURE A-7b) Time Interval 2: Braided streams directly fed an extensive shallow lake. Palustrine deposits and Vertisols characterize the eastern and southern margin of the basin.

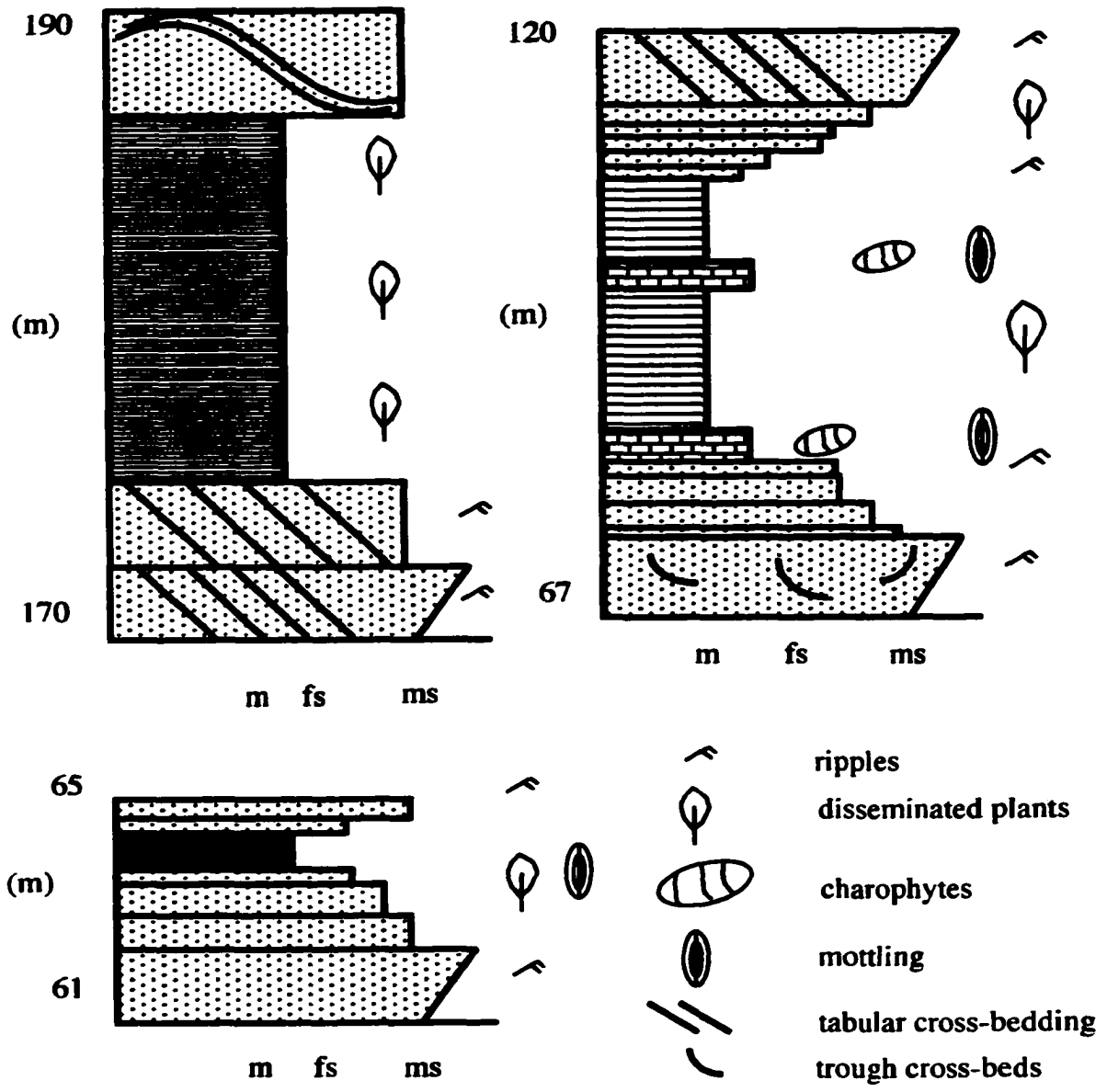

FIGURE A-8. Idealized lacustrine sections from Rio Marco. Straigraphic heights are the same as those in FIGURE A-3. Lakes #1, #2, and #3 indicate gradual deepening and filling of the rift lake.

TABLE A-1. Summary of dominant lithofacies and interpretations of the Ischichuca and Chañares Formations.

Lithofacies	Lithofacies Code(s)[a]	Description	Process Interpretation	Paleoenvironmental Interpretation
Massive mudrock	Fml	Red-brown to green-gray colored massive mudstones; subrounded, blocky interlocking peds (5-65 cm diameter); granular peds (0.5-2 cm diameter); clay cutans; rhizocretions; rare plant debris; gastropods; bioturbation; carbonate peloids; thin-walled volcanic shard textures	Pedogenesis and bioturbation	Pedogenic and palustrine (marginal lacustrine environments)
Massive Limestone	Lm	0.2 m thick tabular bed; ostracods and peloids	Bioturbation	Shallow lake on distal alluvial fan
Planar Cross-Bedded Sandstone	Sp	Pink-colored tabular, laterally continuous well-sorted sandstones; 0.3-1.2 m thick; planar cross-bedded; paleocurrents to NNE	3D ripple migration in stream flow	Distal stream- dominated alluvial fan
Silicified Claystone	C	Pink to gray-colored silicified claystones; wavy bounding surfaces; 1- 20 cm thick beds; laterally continuous to discontinuous	Sheetfloods of volcanic ash and water	Distal alluvial fan
Bentonites	B	White colored clay-rich beds; 0.25- 2 cm thick; laterally continuous to discontinuous	Silicic volcanic ash fallout	Paleosols, overbank, and lacustrine deposits
Massive Sandstone	Sm	red to green-colored, massive fine- to medium-grained, clast-supported sandstones; 0.3 to 0.8 meters thick; laterally continuous-10s of meters; planar upper and lower bounding surfaces; moderately well-sorted; mottled; a few rhizocretions; plant debris; 70-80% quartzose grains, 20-30% micas, 1-2% feldspars	Suspension fallout, pedogenesis, and bioturbation	Overbank deposits

Lithofacies	Lithofacies Code(s)[a]	Description	Process Interpretation	Paleoenvironmental Interpretation
Organized pebble conglomerate	Gct to Sr	White-colored, clast-supported, tabular to lenticular beds; 0.2-4 m thick beds; scoured bases and load casts; fining-upwards sequences from pebbles to coarse sand; rounded to subrounded clasts; clast composition - 80-85% quartzose grains, 10-20% schist and phyllite fragments, 1-5% albite, ~1% micrcocline; deceleration-of-flow sequences (trough cross-bedding to planar bedding to climbing ripple); 5-10 cm diameter outsized clasts; a mudchips; rare plant debris; paleocurrents to the NNE	3D ripple migration in streamflow; rapid deposition of sediment in decelerating streamflow conditions	Distal braided stream plain and intersection of braided stream with shallow lake
Laminated sandstones and siltstones	Sh, Sr, Fr	Gray-green colored, laterally continuous, non-graded, finely laminated sandstones; no bioturbation; lamination marked by marked disseminated leaves; rarely rippled; abundant sand-sized mud aggregates; rare cut and fill structures	Suspension settling or rarely turbidity flow	Littoral to produndal zone of lake
Black shales	Sh	Black, organic-rich shale; coarse sand-sized grains; sand-sized mud aggregates; discontinuous organic laminae; laminae defined by compressed organic matter	Suspension settling	Swamp to littoral zone of lake
Laminated claystones	Fl	Parallel, flat, continuous laminae of clay <1-2 mm thick; alternate with laterally continuous organic laminae (< 0.1mm thick; few clay peloids	suspension settling	profundal zone of lake

Lithofacies	Lithofacies Code(s)[a]	Description	Process Interpretation	Paleoenvironmental Interpretation
Massive siltstone	Fm2	Bioturbated black siltstone; ~0.5 m thick; disseminated plant fragments; shell impressions of Unionids	Bioturbation	Littoral zone of lake; oxic conditions
Laminated grainstone	Gcr	Laminated grainstones; calcified, sand-sized charophyte fragments; laminae are 1-2 mm thick; alternate with bands of wispy organic matter 0.1 mm thick; rare ostracods and gastropods; often rippled; silt-sized quartz and minor clay occur with the calcite	Transport of charophyte stems to deeper littoral zone	Shallow littoral zone; above wave base; poorly oxygenated
Laminated micrite	Ml	Alternating layers of (low-Mg calcite) micrite (1mm thick) and organic-rich clay (<1mm thick); rare ostracods	Suspension settling of calcite crystals or *in situ* precipitation	Deposition in profundal zone

[a] All lithofacies codes are from Miall (1978) except C = silicified claystone, B = bentonite, Lm = massive mudstone; Gcr = rippled, charophyte-rich grainstone; Ml = laminated micrite

TABLE A-2. Diagnostic criteria used to distinguish climate versus tectonic controls on sedimentation patterns.

Indicator	Inferred Paleoclimatic Significance	Inferred Tectonic Significance
stacked Bt horizons of Vertisols	seasonally wet and dry	slow basin subsidence; high aggradation rates
pedogenic sand-sized mud aggregates in fluvial sandstones and laminated lacustrine deposits	seasonally wet and dry	none available
allochthonous plant debris in lake, deltaic, overbank, and fluvial deposits	regionally high water table	rapid sedimentation to preserve leaves may be related to basin subsidence and/or erosion
lack of clinoforms	none available	ramp-type lake margin near border fault ; slow subsidence in rift basin
distance from lake margin to border fault is ~9 km	none available	shallow gradient basin in proximal zone
extensive, exposed area of stacked, gleyed Vertisols in eastern and southern	small lake-level fluctuations	shallow basin gradient in distal basin region
laminated clastic-organic lacustrine deposits	episodic clastic material and water to lake basin	related to basin subsidence and/or erosion
Unionids, charophytes, ostracods	freshwater; shallow lake; positive water balance	none available
abundance of quartzose grains relative to feldspars and lithic fragments in sandstone and conglomerate	humid	source of detritus constant

Works Cited

Alcober, O., 1996, Revision de los Crurotarsis, estratgrafia y tafonomia de la formacion ischigualasto, Thesis docoral, Universidad Nacional de San Juan Facultad de Ciencias Exactas Fisicas y Naturals. 254p.

Alexander, J. and Leeder, M.R., 1987, Active tectonic control on alluvial architecture, in F.G. Ethridge, R.M. Flores, and M.D. Harvey (eds), Recent Developments in Fluvial Sedimentology, SEPM Spec Pub No 39, 243-252.

Allen, J.R.L., 1985, Principles of Physical Sedimentology, George Allen and Unwin Boston 272p.

Alonso-Zarza, A.M. and Calvo, J.P., 2000, Palustrine sedimentation in an episodically subsiding basin; the Miocene of the northern Teruel Graben (Spain). Palaeogeography, Palaeoclimatology, Palaeoecology. 160; 1-2, Pages 1-21.

Anadón, P. Cabrtera, Ll., Julià, and Mazo, M., 1991, Sequential arrangement and asymmetrical fill in the Miocene Rubielos de Mora Basin (northeast Spain), Spec. Publs. Int. Ass. Sediment, 13, 257-278.

Anadon, P., Utrilla, R., and Vazquez, A., 2000, Use of charophyte carbonates as proxy indicators of subtle hydrological and chemical changes in marl lakes; example from the Miocene Bicorb Basin, eastern Spain. Sedimentary Geology. 133; 3-4, 325-347.

Anderson, R.Y., 1986, The varve microcosm: propagator of cyclic bedding, Paleoceanography, vol. 1, 4, p. 373-382.

Anderson, J.M. and Cruickshank, A.R.I., 1978 The biostratigraphy of the Permian and the Triassic; Part 5, A review of the classification and distribution of Permo-Triassic tetrapods. Palaeontologia Africana. 21; 15-44.

Ashley, G.M., Southard, J.B., and Boothroyd, J.C., 1982, Deposition of climbing-ripple beds: a flume simulation. Sedimentology, 29, 67-79.

Bayliss, P., 1986, Quantitative analysis of sedimentary minerals by powder X-ray diffraction, Powder Diffraction, 1, 2, 37-39.

Birkeland, P.W., 1999, Soils and Geomorphology, 3rd ed New York Oxford U P, 430p.

Bonaparte, J.F., 1997, El Triasico de San Juan-La Rioja Argentina y sus Dinosaurios, Museo Argentino de Ciencias Naturales, Buenos Aires, Argentina, 196p.

Bosworth, W.P., 1985, Geometry of propagating continental rifts: Nature, v. 316, p. 625-627.

Brindley, G.W. and Brown, G., 1980, Crystal structures of clay minerals and their X-ray identification.: Mineralogical Society. London, United Kingdom. Monograph - Mineralogical Society. 5, 495p.

Bristow, C.S. and Best, J.L., 1993, Braided rivers; perspectives and problems. In: Braided rivers. Best, J.L. and Bristow, C.S. (editors) Geological Society Special Publications. 75; 1-11.

Carroll, A.R. and Bohacs, K.M., 1997a, Lacustrine source quality and distribution; lake type controls on hydrocarbon generation, Annual Meeting Abstracts- American Association of Petroleum Geologists and Society of Economic Paleontologists and Mineralogists, v. 6, p. 18.

Carroll, A.R. and Bohacs, K.M., 1997b, Stratigraphic and biogeochemical cycles in ancient lake deposits: Annual Meeting Abstracts- American Association of Petroleum Geologists and Society of Economic Paleontologists and Mineralogists, v. 6, p. 18.

Carroll, A.R. and Bohacs, K.M., 1999, Stratigraphic classification of ancient lakes: balancing tectonic and climatic controls, Geology, v. 27, 99-102.

Cerling, T.E., 1986, A mass balance approach to basin sedimentation: constraints on the recent history of Lake Turkana, Palaeogeography, Palaeoclimatology, Palaeoecology, 54, 63-86.

Chamley, H., 1989, Clay Sedimentology, New York: Springer-Verlag, 623p.

Cohen, A.S., 1982, Paleoenvironments of root casts from the Koobi For Formation, Journal of Sedimentary Petrology, 52, 2, 401-414.

Cohen, A.S., 1990, Tectono-stratigraphic model for sedimentation in Lake Tanganyika, Africa, BJ Katz (ed) Lacustrine Basin Expolration: case studies and modern analogs, AAPG Memoir 50, 137-150.

Collinson, J.D., 1996, Alluvial sediments in Reading, H.G. (ed) Sedimentary Environments: Processes, Facies, and Stratigraphy, 3rd edOxford Blackwell science 37-82.

DeCelles, P.G., Langford, R.P., and Schwartz, R.K., 1983, Two new methods of paleocurrent determination from trough cross-stratification, Journal of Sedimentary Petrology, v. 53, p. 629-642.

Demko, T.M., Dubiel, R.F., and Parrish, J.T, 1998, Plant taphonomy in incised valleys: implications for interpreting paleoclimate from fossil plants. Geology. 26; 1119-1122.

Dickinson, W.R., 1985, Interpreting provenance relations from detrital modes of sandstones in Zuffa GG (ed.) Provences of Arenites, NATO Advanced Study Institutes Series C, Mathematical and Physical Sciences, 148, 333-361.

Dickinson, W.R. and Suczek, C.A., 1979, Plate tectonics and sandstone compositions, AAPG 63, 2164-2182.

Drever, J., 1973. The preparation of oriented clay mineral specimens for X-ray diffraction analysis by a filter-membrane peel technique. American Mineralogist, 58, 553-554.

Dubiel, R.F. and Smoot, J.P., 1994, Criteria for interpreting paleoclimate from red beds; a tool for Pangean reconstructions. In: Pangea; global environments and resources. Embry, A.F., Beauchamp, B. and Glass, D.J. (editors) Canadian Society of Petroleum Geologists Memoir. 17, 295-310.

Dubiel, R.F., Parrish, J.T., Parrish, J.M., and Good, S.C., 1991, The Pangean megamonsoon- evidence from the Upper Triassic Chinle Formation, Colorado Plateau, Palaios, v. 6., p. 347-370.

Ékes, C., 1993, Bedload-transported pedogenic mud aggregates in the Lower Old Red Sandstones in Southwest Wales, J Geol. Soc. London 150 Part 3: 469-471.

Eugster, H. P. and Hardie, L.A., 1978, Saline Minerals in A. Lerman (eds) Lakes: Chemistry, Geology, Physics, New York: Springer-Verlag, 237- 294.

Fastovsky, D. E., Jones, M. M., Therrien, F., Herrick, A. S., McSweeney, K., 2000, Thick B-Horizons in Late Triassic Paleosols, Chinle Formation, Petrified Forest National Park, Arizona, USA, GSA Abstracts with Programs, 32, 7.

Francis, J.E., 1994, Paleoclimates of Pangea- Geological Evidence, *in* A.F. Embry, B. Beauchamp, and D.J. Glass (eds.) Pangea: Global Environments and Resources, Canadian Soc. of Petroleum Geologists Memoir 17, 265-274.

Gierlowski-Kordesch, E.H., 1998, Carbonate deposition in an ephemeral siliciclastic alluvial system; Jurassic Shuttle Meadow Formation, Newark Supergroup, Hartford Basin, USA. Palaeogeography, Palaeoclimatology, Palaeoecology. 140; 1-4, 161-184.

Gierlowski-Kordesch, E. and Kelts, K, 1994, Introduction. In: Global geological record of lake basins; Volume 1. Gierlowski-Kordesch, E. and Kelts, K. (editors) 4; Cambridge University Press. Cambridge, United Kingdom., xvii-xxxiii.

Gierlowski-Kordesch, E. and Rust, B.R., 1994, The Jurassic East Berlin Formation, Hartford Basin, Newark Supergroup (Connecticut and Massachusetts); a saline lake-playa-alluvial plain system, *in* Sedimentology and geochemistry of modern and ancient saline lakes. Renaut, R.W and Last, W.M. (editors) Special Publication - SEPM (Society for Sedimentary Geology). 50; P.249-265.

Glenn, C.R. and Kelts, K., 1991, Sedimentary rhythms in lake deposits, *in* G. Einsele, W. Ricken, and A. Seilacher (eds.) Cycles and Events in Stratigraphy, Springer-Verlag: Berlin, 188-221.

Gore, P.J.W., 1988a, Lacustrine sequences in an Early Mesozoic rift basin: Culpeper Basin, Virginia, *In* AJ Fleet, K. Kelts, and MR Talbot (eds.), Proceedings of Symposium on Lacusrine Petroleum Source Rocks. Geol. Soc. London Spec. Pub., Blackwell Scientific Publications, London, 7-41.

Gore, P.J.W., 1988b, Late Triassic and Early Jurassic lacustrine sedimentation in the Culpeper basin Virginia, in W. Manspeizer (ed) Triassic-Jurassic Rifting: Contintntal Breakup the Origin of the Atlantic Ocean and Passive Margins Part A New York Elsevier Press, 369-400.

Gore, P.J.W., 1989, Toward a model for open- and closed-basin deposition in ancient lacustrine sequences; the Newark Supergroup (Triassic-Jurassic), eastern North America. Palaeogeography, Palaeoclimatology, Palaeoecology. 70; 1-3, 29-51.

Hay, W., 1996, Tectonics and climate, Geol. Rundsch. 85:409-437.

Heward, A.P. 1978, Alluvial fan and lacustrine sediments from Stephanion A and B (La Magdalena, Cinera-Matallana and Sabero) coalfields, northern Spain. Sedimentology, 25, 451-488.

Hubert, J.F. and Hyde, M.G., 1982, Sheet-flow deposits of graded beds and mudstones on an alluvial sandflat-playa system; Upper Triassic Blomidon redbeds; St. Mary's Bay, Nova Scotia. Sedimentology. 29; 4, 457-474.

Hoffman, J., 1976, Regional metamorphism and K/Ar dating of clay minerals in Cretaceous sediments of the undisturbed belt of Montana, unpublished Ph.D. dissertation, Case Western Reserve University, 266p.

Jordan, T. E., 2000, Deformation and topography in the Sierra Pampeanas, Argentina: Responses to flat-subduction, GSA Abstracts with Programs, 32, 7.

Jordan, T. E. and Allmendinger, R.W., 1986, The Sierras Pampeanas of Argentina; a modern analogue of Rocky Mountain foreland deformation. American Journal of Science. 286; 10, 737-764.

Kelts, K., and Hsü, K.J., 1978, Freshwater carbonate sedimentation, *in* A. Lerman (ed) Lakes: Chemistry, Geology, Physics, New York: Springer-Verlag, 295-324.

Kraus, M.K., 1999, Paleosols in clastic sedimentary rocks: their geologic applications, Earth-Science Reviews, 47, p. 41-70.

Kutzbach, J.E. and Gallimore, R.G., 1989, Pangean climates: megamonsoons of the megacontinent, J. Geophys. Res., 94, 3341-3357.

Lambiase, J.J., 1990, A model for tectonic control of lacustrine stratigraphic sequences in continental rift basins *in* Katz, B.J., ed., Lacustrine basin exploration: case studies and modern analogs, AAPG Memoir 50, 265-276.

Leeder, M. R. and Gawthorpe, R.L., 1987, Sedimentary models for extensional tilt-block/ half-graben basins. *In*: Continental extensional tectonics. Coward, M.P. (editor); Dewey-J-F (editor); Hancock-P-L (editor) Geological Society Special Publications. 28; Pages 139-152.

Lopez-Galamundi, O.R., Alvarrez, L., Andreis, R.R., Bossi, G.E., spejo, I., Seveso, F.F., Legarreta, L., Kokogian, D., Limarino, C.O., and Sessarego, H., 1989, Cuencas intermontanas, Cuencas Sedimentarias Argentinas 1989, p. 123-167.

Lopez-Galamundi, O.R., Espejo, I.S., Conaghan, P.J., Powell, C.M., and Veevers, J.J., 1994, Southern South America from Veevers, J.J. and Powell, C.McA., eds., Permian-Triassic Pangean Basins and Foldbelts along the Panthalassan Margin of Gondwanaland, Boulder, CO, Geological Society of America Memoir 184, p. 281-329.

Lorenz, J.C., 1988, Triassic-Jurassic Rift-Basin Sedimentation: History and Methods, Van Nostrand Reinhold New York 315p.

McPherson, J.G., Shanmugam, G., and Moiola, R.J., 1987, Fan-deltas and breaid deltas: varieties of coarse-grained deltas, Geological Society of America Bulletin, 99, 331-340.

Mack, G.H. and James, W.C., 1992, Paleosols for Sedimentologists, Geological Society of America Short Course Notes, 127p.

Mack, G.H. and Seager, W.R., 1990, Tectonic control on facies distribution of the Camp Rice and Palomas Formations (Pliocene-Pleistocene) in the southern Rio Grande rift, Geol. Soc. Amer. Bull, 102: 45-53.

Mack, G.H., James, W.C., and Monger, H.C., 1993, Classification of paleosols, Geological Society of America, v. 105, p. 129-136.

May, C.L., 1998, Applying hierarchy theory to macroevolutionary questions: examples from the Ischigualasto-Villa Union Basin (Triassic: NW Argentina, Ph.D. Thesis, University of California, Berkeley, 226 p.

Miall, A.D., 1996, The geology of fluvial deposits, sedimentary facies, basin analysis and petroleum geology. New York : Springer, 582 p.

Milana, J.P. and Alcober, O., 1994, Modelo tectosedimentario de la cuenca triásica de Ischigualasto (San Juan, Argentina), Revista de la Asociación Geológica Aregntina, 49 (3-4), 217-235.

Milana, J.P. and Lopez, S. (1995) Cyclostratigraphy of the Triassic lacustrine episode of the Ischigualasto Basin, western Argentina. 1st International Limno-geological Congress, Copenhagen, Dinamarca.Abstract vol., p.84.

Milana, J.P., 1998, Anatomía de parasecuencias en un lago de rift y su relación con la generación de hidrocarburos, Cuenca Triasica de Ischigualasto, San Juan. Revista Asociación Geológica Argentina, v. 53.

Moore, D.M. and Reynolds, R.C., 1989, X-ray diffraction and the identification and analysis of clay minerals. New York: Oxford University Press, 332 p.

Mount, J.F. and Cohen, A.S., 1984, Petrology and geochemistry of rhizoliths from Plio-Pleistocene fluvial and marginal lacustrine deposits, east Lake Turkana, Kenya. Journal of Sedimentary Petrology. 54; 1, Pages 263-275.

O'Brien , N.R., 1996, Shale lamination and sedimentary processes from AES Kemp (ed) Palaeoclimatology and Palaeoceanography from Laminated Sediments,Geological Society Special Publication No. 116, p. 23-36.

Odin, G.S. and Letolle, R., 1982, The Triassic time scale in 1981. In: Numerical dating in stratigraphy. Odin, G.S. (ed.) p. 523-533.

Olsen, P.E., 1990, Tectonic, climatic, and biotic modulation of lacustrine ecosystems-examples from Newark Supergroup of eastern North America, BJ Katz (ed)

Lacustrine Basin Exploration: case studies and modern analogs, AAPG Memoir 50, 209-224.

Parrish, J.T. and Curtis, R.L., 1982, Atmospheric circulation, upwelling and organic-rich rocks in the Mesozoic and Cenozoic eras, Palaeo. Palaeo. Palaeo., v. 40, p. 31-66.

Parrish, J.T., 1993, Climate of the supercontinent Pangea, J. Geol., 101, 215-233.

Pettijohn, F.J., Potter, P.E., and Siever, R., 1987, Sand and Sandstones 2nd edition, Springer-Verlag: New York, 553p.

Platt, N.H., 1989a, Lacustrine carbonates and pedogenesis: sedimentology and origin of palustrine deposits from the Early Cretaceous Rupleo Formation, W Cameros Basin, N Spain, Sedimentology, 36, 665-684.

Platt, N.H., 1989b, Climatic and tectonic controls on sedimentation of a Mesozoic lacustrine sequence; the Purbeck of the western Cameros Basin, northern Spain. Palaeogeography, Palaeoclimatology, Palaeoecology. 70; 1-3, 187-197.

Platt, N.H. and Wright, V.P., 1991, Lacustrine carbonates: facies models, facies distributions and hydrocarbon aspects, Spec. Publs. Int. Ass. Sediment, 13, 57-74.

Ramos, V.A. and Kay, S.M., 1991, Triassic rifting and basalts of the Cuyo basin, central Argentina, in Symposium of Andean Magmatism, Geological Society of America Special Paper 265, p. 79-91.

Retallack, G.J., 1977, Triassic palaeosols in the upper Narrabeen Group of New South Wales; Part II, Classification and reconstruction. Journal of the Geological Society of Australia. 24, Part 1; 19-36.

Retallack, G.J., 1988, Field recognition of paleosols in J. Reinhardt and W.R. Sigleo, Paleosols and weathering Through Time: Principles and Application, Geological Society of Maerica Special Paper 216, p. 1-20.

Retallack, G.J., 1990, Soils of the Past: an introduction to paleopedology, Unwin Hyman: Boston, 520p.

Reynolds, R.C., Jr., 1985, NEWMOD© a Computer Program for the Calculation of One-Dimensional Diffraction Patterns of Mixed-Layered Clays: R.C. Reynolds Jr., 8 Brook Drive, Hanover, New Hampshire.

Rogers, R.R., Swisher, C.C., Sereno, P.C., Monetta, A.M., Forster, C.A., and Martínez, R.N., 1993, The Ischigualasto tetrapod assemblage (Late Triassic) and 40Ar/39Ar dating of dinosaur origins, Science, 260, p. 794-797.

Rust, B.R. and Nanson, G.C., 1989, Bedload transport of mud as pedogenic aggregates in modern and ancient rivers, Sedimentology, 36, p. 291-306.

Smith, N.D., 1972, Flume experiments on the durability of mud clasts, Journal of Sedimentary Petrology, 42; 2, 378-383.

Smoot, J.P, 1985, The closed basin hypothesis and its use in facies analysis of the Newark Supergroup, *in* G.R. Robinson Jr and S.J. Froelich (eds.), Proceedings of the Second U.S. Geological Survey Workshop on the Early Mesozoic basins of the Eastern United States, USGS Circular 946, p 4-10.

Smoot, J.P., 1991, Sedimentary facies and depositional environments of early Mesozoic Newark Supergroup basins, eastern North America: Palaeogeography, Paleoclimatology, and Palaeoecology, 84, p. 369-423.

Smoot, J.P., 1993, Field trip guide: Quaternary-Holocene lacustrine sediments of Lake Lahontan, Truckee River canyon north of Wadsworth, Nevada, USGS Open-File Report 93-689, 35p.

Smoot, J.P. and Olsen, P.E., 1988, Massive mudstones in basin analysis and paleoclimatic interpretation of the Newark Supergroup, in Manspeizer, W (ed.) Triassic-Jurassic Rifting: continental break-up and the origin of the Atlantic Ocean and Passive Margins Part A Developments in Geotectonics 22, 249-274.

Stipanicic, P.N. and Bonaparte, J.F., 1979, Cuenca triásica de Ischigualasto-Villa Union (Provincias de La Rioja y San Juan), in Turner, J.C., ed., Segundo Simmposio de Geología Regional Argentina: 1, Córdoba, Academia Nacional de Ciencias, 253-575.

Talbot, M.R and Kelts, K., 1990, Paleolimnological signatures from carbon and oxygen isotopic ratios in carbonates from organic carbon-rich lacustrine sediments. *in* Lacustrine basin exploration; case studies and modern analogs. Katz, B.J. (editor) AAPG Memoir. 50; Pages 99-112.

Talbot, M.R. and Allen, P.A., 1996, Lakes in H.G. Reading, Sedimentary Environments: Processes, Facies and Stratigraphy, Blackwell Science, Oxford, p. 83-124.

Tucker, M.E., 1996, Sedimentary Rocks in the Field, John Wiley and Sons, NY, 153p.

Tye, R.S. and Coleman, J.M., 1989, Depositional processes and stratigraphy of fluvially dominated lacustrine deltas: Mississippi Delta Plain, Journal of Sed. Petrol., 59, 6, 973-996.

Uliana, M.A., Biddle, K.T., and Cerdan, J., 1989, Meoszoic extension and the formation of Argentine sedimentary basins, *in* A.J. Tankard and H.R. Balkwill (eds.) Extensional Tectonics and stratigraphy of the North Atlantic Margins, AAPG Memoir 46, p. 599–614.

Valencoi, D.A, Mendía, J.E., and Vilas, J.F., 1975, Paleomagnetism and K-Ar of Triassic Igneous rocks from the Ischigualasto-Ischichuca and Puesto Viejo Formations, Argentina, Earth and Planetary Science Letters, 26, 319-330.

Volkheimer, W., 1967, Paleoclimatic evolution in Argentina and relations with other regions of Gondwana, Gondwana stratigraphy, IUGS Symposium, Buenos Aires, p. 551–574.

Zapata, T.R. and Allmendinger, R.W., 1996, Growth stratal records of instantaneous and progressive limb rotation in the Precordillera thrust belt and Bermejo Basin, Argentina. Tectonics. 15; 5, 1065-1083.

APPENDIX B: EVALUATION OF PROVENANCE, CLIMATE AND POST-DEPOSITIONAL CONTROLS ON THE COMPOSITION OF COEVAL FLUVIO-LACUSTRINE DEPOSITS AND PALEOSOLS

Abstract

Conglomerate, sandstone, and clay mineral assemblages of the coeval Middle Triassic Ischichuca and Chañares Formations from the Ischigualasto Basin, NW Argentina suggest that information about sandstone provenance and burial diagenesis are preserved. Triassic rifting formed the Ischigualasto Basin and produced an elongate basin that was filled in by coarse-grained alluvial, fluvial, and lacustrine sediments and paleosols. Sandstone provenance studies and paleocurrent indicators suggest that the source of the sediment was mainly from Precambrian crystalline basement rocks (gneiss, schist, and minor phyllite), and Paleozoic plutons (granodiorite and tonalite), with a minor contribution from reworked Upper Paleozoic marine and Early Triassic nonmarine sedimentary rocks. The source of the sediment remained relatively unchanged throughout deposition.

Authigenic clay minerals in the paleosols of the Chañares Fm include smectite and, rarely, minor kaolinite. The abundance of smectite in the eastern and southern part of the basin reflects the extent of the silicic volcanic ash dispersal and subsequent pedogenic and diagenetic alteration. Bentonites occur in all paleoenvironments across the basin and are composed of either smectite $\pm$ kaolinite in the southern and eastern regions and mixed-layered illite-smectite close to the basin-bounding fault to the west. The Ischichuca Fm has the most diverse suite of clay minerals. Deep-water lacustrine

facies contain mixed-layered illite-smectite and shallow water facies have mixed-layered illite-smectite ± kaolinite ± chlorite ± mixed-layered chlorite-smectite. The absence of temperature/depth-related clay mineral assemblages in the vertical sequences of Middle Triassic rocks indicates that classic burial diagenesis did not play a major role in alteration. The distribution of clay mineral assemblages is likely, in part, a reflection of depositional environment. Pore water chemistry and burial depth may have significantly influenced the degree of alteration of the clay minerals.

1. Introduction

Chemical weathering of bedrock is strongly dependent the amount and duration of precipitation. The susceptibility of different rock types to physical and chemical weathering influences the types of composition of detrital sediments and weathering products (Suttner, 1974; Pettijohn, Potter, and Siever, 1987; Johnsson, 1993; Birkeland, 1999). The purpose of this study is to evaluate the role of provenance, climate, and diagenesis on the composition of sandstone and conglomerate and authigenic clay formation in coeval Middle Triassic fluvio-lacustrine sediments and paleosols from the Ischigualasto rift basin, NW Argentina. Interpretation of the transport, climatic, and diagenetic effects on sandstone composition is coupled with the study of clay mineral assemblages and carbonate diagenesis. Rift basins have an especially high potential for recording information about paleoclimate because of their relatively high subsidence and sedimentation rates (Suttner and Dutta, 1986; Kelts, 1988).

Sandstone composition is strongly related to the surficial weathering processes of the source area and provides useful information about the provenance, transport,

deposition, and diagenesis (Dickinson, 1970; Pettijohn, Potter, and Siever, 1987; Johnsson, 1993). Although climate is often thought to be one of the factors controlling sandstone composition, studies of sands derived from coarse crystalline basement rocks suggest source rock texture and slope angle may play a more dominant role than climate (Suttner, 1974; Basu, 1985; Suttner and Dutta, 1986; Devaney and Ingersoll, 1993). Trends in the sandstone composition from coarse grained fluvial to fluvio-deltaic and fine-grained lacustrine rocks in the Ischigualasto Basin provide useful information about the changes in transport processes controlling the composition of the sandstones basinward. The mineralogical assemblage of lake sediments is dependent on the watershed bedrock, the amount of erosion in the watershed, and lake's physical conditions (Jones and Bowser, 1978). Lacustrine sands are generally composed of silicate materials including lithic fragments, fine-grained sand and silt-sized grains of quartz, feldspar, and clay minerals (Jones and Bowser, 1978).

Clay minerals are often used as indicators of climate in both soils and lake deposits and a means of inferring the degree of diagenetic alteration (Hower et al., 1976; April, 1981; Singer, 1984; Yuretich, 1988; Chamley, 1989; Abercrombie et al., 1994; Mack and James, 1994; Yuretich et al., 1999). The clay mineral composition of soils depends on climate because clays express the intensity of weathering on land (Birkeland, 1999; Chamley, 1989). For example, kaolinite, gibbsite, and hematite are thought to represent extreme leaching in a tropical to subtropical climate whereas smectite forms in a more arid climate (Jenny, 1941; Singer, 1984; Wright, 1986). The clay mineral that forms in the soil, however, may not be stable because it may alter during burial

diagenesis (Mack and James, 1992). Illitization of smectite is the most common diagenetic process in sedimentary basins, but is thought to occur at depth, high temperatures, or reduction of silica activity during quartz precipitation (Hower et al., 1976; Abercrombie et al., 1994).

Clay mineral assemblages in lacustrine rocks can provide important information about the paleochemistry of the lake and the climate of the lake's watershed (April, 1981;Yuretich, 1988; Chamley, 1989; Yemane et al., 1996; Yuretich et al., 1999). In freshwater lakes, the mineralogy directly corresponds to the clay mineralogy of the surrounding drainage basin (Chamley, 1989). Detrital clay mineral type and abundance is used to determine paleoclimatic conditions of the watershed because humid climates produce more extensive chemical weathering, resulting in kaolinite whereas the dominance of smectite may suggest contrasting seasons and a pronounced dry season unless there is abundant altered volcanic glass in the watershed (Singer, 1984). In most freshwater lakes, the detrital clays do not undergo significant alteration in the lake (Chamley, 1989; Yemane et al, 1996).

In this study, we present conglomerate and sandstone petrologic and clay mineral data from the southern region of the Triassic Ischigualasto Basin in NW Argentina in order to assess the relative importance of provenance and climate on sandstone composition and clay mineral assemblages in the Ischigualasto rift basin. Stable carbon and oxygen isotopic data of carbonate rocks provides additional information about diagenetic processes in the basin.

2. Geologic History and Previous Work

The Ischigualasto Basin is located in northwestern Argentina in the San Juan and La Rioja provinces near the border of the Sierras Pampeanas and Precordillera terranes (Fig. 1). The Sierra Pampeanas consist mostly of Precambrian crystalline and Paleozoic cover rocks. In the western Sierra Pampeanas, the exposed basement includes schist, gneiss, migmatite, amphibolite, and granulite (Teruggi et al., 1967; Jordan and Allmendinger, 1986; Ragona et al., 1995). Mylonitic zones juxtapose the basement rocks. Paleozoic plutons of granodiorite and tonalite are predominant in the Sierra de Valle Fértil (Ragona et al., 1995). Paleozoic sedimentary rocks including cherty limestone of the Ordovician San Juan Formation (Fm) and quartzo-feldspathic to lithofeldspathic sandstone and organic-rich shale of the Carboniferous Guandacol and Tupe Formations (Fms) crop out in southwest and west of the Ischigualasto Basin (Teruggi et al., 1967; Lopez-Gamundi et al., 1990; Ragona et al., 1995). The Permian Patquía Fm contains sandstone with a similar composition and grades vertically to playa-lake siliciclastic-evaporite deposits and eolian sandstone (Lopez-Gamundi et al., 1990). Doubly plunging anticlines expose the Paleozoic and Triassic rocks in the Ischigualasto Basin and Sierra de Valle Fértil (Jordan and Allmendinger, 1986; Ragona et al., 1995).

The Ischigualasto Basin is one of a series of NNW trending nonmarine Triassic rift basins that formed in response to extension along the margins of Gondwanaland and is thought to be the northern extension of the Cuyo rift basin located to the south (Uliana et al., 1989). The Valle Fértil fault is the basin bounding master fault located on the western side of the basin (Fig. 2). The Ischigualasto Basin is an elongate basin that is

~100 km in length and ~45 km in width. Analysis of two-dimensional seismic lines orthogonal to the Valle Fértil border fault indicates half graben asymmetry and growth faulting in the Ischigualasto Basin (Stipanicic and Bonaparte, 1979; Milana and Alcober, 1994; López-Gamundí, 2001). The basin fill reaches a maximum of ~4-9 km in thickness in the west-central part of the basin, near the Valle Fértil fault margin, and thins to the NE (Stipanicic and Bonaparte, 1979; Uliana et al., 1989; Ruiz and Introcaso, 1999). Overall thickening of the basin fill to the west suggests that the Valle Fértil fault was active throughout Triassic sedimentation and there was differential subsidence across the basin. East- and northeast-directed paleocurrents from the fault basin margin suggest strong transverse sediment supply during the Early and Middle Triassic and both axial and transverse sediment transport during the Late Triassic (Milana and Alcober, 1994; Alcober, 1996). The basin fills comprises seven formations: the Talampaya, Tajardos, Chañares, Ischichuca, Los Rastros, Ischigualasto, and Los Colorados Fms. This study focuses on the coeval Middle Triassic Ischichuca and Chañares Fms.

Previous studies of the composition of the framework grains of sandstone and clay mineralogy examined the Chañares and Ischichuca Fms that crop out in the southern Ischigualasto Basin in the Cañon de la Peña and Ischigualasto River. The framework grains of the sandstone of the Ischichuca Fm are dominantly quartzose and/or feldspathic and primarily derive from crystalline basement rock and pyroclastic material (Bossi, 1970). The clay in the Chañares Fm consists of beidillite with minor amounts of smectite and kaolinite (Bossi, 1970). The clay mineralogy of the carbonaceous shale and sandstone of the Ischichuca and Los Rastros Fms is dominated by kaolinite and illite

(Bossi, 1970). Three tuffaceous deposits from the Ischichuca and Los Rastros Fms are dominated by mixed-layered illite-smectite, but also contain minor amounts of chlorite, kaolinite, illite, smectite, and beidellite (Bossi, 1970). Illitization is thought to be an important diagenetic process in these rocks. Bossi (1970) uses these clay mineral assemblages to infer the climate of the basin to have alternating between hot and dry to humid during the Middle Triassic. This study presents a more detailed study of the conglomerate and sandstone provenance and the variation in clay mineral assemblages of the Ischichuca and Chañares Fms as a function of source area, diagenesis, and climate.

3. Methods

Mineralogical analyses of bulk rock and size-fractionated samples were preformed using a Siemens D-500 X-ray diffractometer (XRD) equipped with a Cu tube and a graphite monochromometer. Two hundred and fifty bulk rock samples were first ground with a mortar and pestle, and then micronized with a micronizing mill using agate grinding elements in isopropyl alcohol. Relative mineral abundances were determined using selected peak areas and mineral intensity factors for each mineral (Bayliss 1986). All mineral abundances are within $\pm$10% (Bayliss, 1986). Mineral intensity factors of quartz, feldspars, and micas were taken from Bayliss (1986) and all phyllosilicate values were from Hoffman (1976). The Mg^{2+} content in calcite was estimated from the position of the [104] peak (Brindley and Brown, 1980). One hundred and fifty size-fractionated samples were prepared by centrifuging ground and sonified sample dispersions. I used the filter transfer method of preparing clay films on glass slides (Drever, 1973). Clay-sized fractions were subjected to standard gylcolation techniques for identification. Clay

minerals were size-separated, oriented, and x-rayed (air-drying and glycol solvation) to study characteristic 00l d-spacings. XRD analysis of 10 samples for randomly oriented clays was used to determine the b-axis dimension [060], which is useful to distinguish between dicoctahedral and trioctahedral clay minerals because the b-axis dimension is sensitive to the size of the cations and the site occupancy in the octahedral sheet (Moore and Reynolds, 1989). XRD patterns of clay-sized samples were modeled with the computer program, NEWMOD®, to determine the percent of illite in mixed-layered illite-smectite and interlayer ordering and abundance of each clay mineral found in the sample (Reynolds, 1985).

Petrographic studies of one hundred and fifty samples were conducted using an optical microscope. Standard thin sections were prepared from freshly cut rock samples to study the mineralogy, paragenesis, and diagenetic features. Thirty polished thin sections were examined using cathodoluminesence (CL) to evaluate the extent of carbonate diagenesis.

Forty sandstone samples were analyzed using an automated point-counter with 375-450 counts per thin section, depending on the grain size of the sample. There was ~1mm between each point counted. A range of fine- to coarse-grained sandstone was analyzed. I simultaneously used the traditional (e.g., Suttner et al., 1981; Suttner and Basu, 1985) and the Gazzi-Dickinson method of point counting (e.g., Dickinson, 1970; Ingersoll et al., 1984).

Microsamples of primary and secondary carbonate were taken from thirty samples using a 0.5 mm diameter dental drill. Samples were selected for two reasons: 1) to

characterize the isotopic composition of the diverse set of lithofacies present in the lacustrine deposits and paleosols and 2) to evaluate the possibility of pervasive diagenesis by analyzing the cross-cutting veins and calcite cements in sandstone and comparing this data with primary carbonate. Between 0.5 and 1.5mg of carbonate powders was roasted at ~200°C under vacuum to drive off volatiles. Then, samples were reacted with 4 drops of 100% phosphoric acid for 15 minutes. The stable carbon ($\delta^{13}C$) and oxygen ($\delta^{18}O$) isotopic composition of carbonates was determined using a mass spectrometer linked to a Kiel carbonate preparation device. All isotopic data are reported relative to the PDB (PeeDee Belemnite) standard.

4. Results

4.1 Sandstone framework composition

The sandstone and conglomerate was sampled from the escarpment margin of the rift basin. In general, the framework grains are quartzose-rich and cluster in the upper part of the QFL ternary diagram (Fig. 3), and can be classified as compositionally moderately mature. There is significant overlap between the different size fractions of sandstone and conglomerate, which represent different depositional environments. In coarse-grained channel sandstone and conglomerate, monocrystalline quartz, unstrained igneous polycrystalline quartz, and strained metamorphic polycrystalline quartz are the most dominant clasts observed and comprise, on average, ~78% of the framework grains. Chert clasts are rare (average: <1%). Lithic fragments comprise, on average, ~11% of the clasts and the most common rock fragments include schist, gneiss, granite, and rarely, phyllite. Plagioclase and microcline are both found in these sandstones (average: ~11%),

but plagioclase is more common than microcline. Both types of feldspars occur as altered and unaltered clasts. Feldspars are calcitized or have altered to kaolinite. Detrital micas in these rocks include chlorite, biotite, and muscovite. There is no systematic change in abundance of any clast type vertically or laterally in the Cañon de la Peña and Rio Marco sections. The most common cements observed include quartz overgrowths, poikilotopic calcite, and coarse, equant calcite. The lithic grains are more angular than the quartzose grains. Both the sandstone and conglomerate are moderately-well to well-sorted.

In the finer-grained overbank and prodeltaic deposits, lithic clasts include mica fragments of biotite, muscovite, and chlorite, and rarely schist fragments (average: ~17%). Micas are more common in the overbank and prodeltaic deposits than the channel facies. Polycrystalline quartz and metamorphic clasts are not as common in these samples as in the channel facies. Monocrystalline quartz and chert are the most common clasts (average: ~69%). Both microcline and plagioclase occur as both altered and unaltered grains (average: ~14%). Plagioclase is more abundant than the K-feldspars. There is no systematic change in abundance of any clast type vertically or laterally in the Cañon de la Peña and Rio Marco sections. Cements include hematite, chlorite and other clay minerals, and chert. The framework grains are subangular to subrounded in shape and are moderately well-sorted.

4.2 Clay mineralogy

The clay-sized minerals comprise a small percentage of each of the 145 samples studied, between 1-20%, but on average, 5-10%. The clay minerals identified in 145

samples are illite, kaolinite, chlorite, smectite, mixed-layered chlorite/smectite (C/S), and mixed-layered illite/smectite (I/S; I: illite in I/S) (Figs. 4 and 5). In general, the rocks are dominated by dioctahedral smectite and I/S (Fig. 4). Bentonites occur in all measured sections and paleoenvironments across the basin. The clay minerals found in the bentonites are 70-80% I in I/S with R1 ordering near the western side of the Ischigualasto Basin in the Rio Marco and Cañon de la Peña sections and dioctahedral smectite ± kaolinite along the southern and eastern margins of the basin in the Cerro Morado and Rio Gualo sections. One occurrence of 70% I in I/S with R 1 ordering in a bentonite from the Rio Gualo section was observed. In the paleosol mudrock from the Rio Marco, Cerro Morado, and Rio Gualo sections, the dominant clay mineral present is dioctahedral smectite. In the same paleosols in Cañon de la Peña, illite, 70-80% I in I/S R1 ordering, dioctahedral smectite, and minor chlorite are present.

In the Rio Marco and Cañon de la Peña sections, the fluvial sandstone and conglomerate have kaolinite and illite cement. In the fine- to medium-grained overbank sandstone, kaolinite, illite, 70%I in I/S with R1 ordering, and minor C/S (60% chlorite in C/S, R1 ordering) occur. The mean half-height peak width of the basal (001) of the illite ranges from 0.157 to 0.218 mm. Laminated fine- to medium-grained deltaic sandstone and laminated and massive lacustrine mudrock have a relatively homogenous clay mineral assemblage. These rocks are dominated by 70%I in I/S with R1 ordering, but kaolinite, illite, 60% C in C/S with R1 ordering, and chlorite may also present. The percent I in I/S is relatively uniform (between 70-80% I) throughout the Cañon de la Peña and Rio Marco sections.

4.3 Carbonate diagenesis

All the carbonate samples are composed of low Mg-calcite based on XRD analysis. Analysis of the stable carbon and oxygen isotopic composition of micrites, veins, cements and spar indicate that the stable carbon and oxygen isotopic composition are not significantly different (Fig. 6). The stable carbon and oxygen isotopic data fall in a restricted range of oxygen isotopic values. The $\delta^{13}C$ values range widely, from -0.2 to −13.1‰. There is no systematic trend for the $\delta^{13}C$ values for individual sets of primary or secondary carbonate components. The $\delta^{18}O$ values are not as variable as the $\delta^{13}C$ values, and range from −18.5 to −19.9‰.

There is no correlation between isotopic signatures and degree of luminescence of the carbonate samples. CL study of the carbonate samples does not show any evidence of relict textures or zonation in the cements or primary carbonate. The degree of luminescence of the carbonate seems to reflect crystal size. Bright pink to red luminescence is characteristic of the coarse crystals of the vein calcite in lacustrine claystone samples and poikilotopic calcite cement found in the coarse-grained channel sandstone.

5. Discussion

5.1 Framework conglomerate and sandstone composition

Channel sandstone and conglomerate compositional data indicate derivation was primarily from polycrystalline quartz of igneous and metamorphic rocks. The most likely source of the sands and granules is Precambrian metamorphic rocks and Paleozoic plutonic rocks of the Sierra de Valle Fértil located to the south and southwest of the

Ischigualasto Bain (Figs. 1 and 2). Subordinate amounts of schist, gneiss, and phyllite clasts were probably derived from local Precambrian metamorphic rocks. Feldspars are both altered and unaltered. The main sources of the unaltered feldspar grains probably were the Paleozoic granodiorite or, less likely, Precambrian metamorphic rocks. The altered feldspar grains may be reworked from Upper Paleozoic feldspathic sandstone of the Guandacol, Tupe, or Patquía Formations or feldspathic sandstone from the Lower Triassic Talampaya or Tarjados Fms. Differentiation of the possible sources of the altered feldspars is not possible because of the degree of alteration to kaolinite or calcite. Paleocurrent data of trough cross-beds from Milana and Alcober (1994) and this study (Appendix A) are consistent with these source rock interpretations. The majority of these conglomerate and sandstone overlap the Transitional Continental and Recycled Orogen tectonic provenance fields of Dickinson et al. (1983), typical of many rift systems (e.g., Triassic Hartford Basin, Hubert et al., 1992; Lake Tanganyika, Soreghan and Cohen, 1993; Red Sea and Gulf of Aden, Garanti et al., 2001). In general, the average composition of first cycle medium-grained sands derived from metamorphic and plutonic rocks in a humid climate are more quartzose than those sands that form in an arid climate (Suttner et al., 1981; Fig. 1). The escarpment margin side of Lake Tanganyika has small drainage basins along a steep margin that are thought to produce sands with more lithic fragments than any other rift basin margin because of the dominance of mechanical weathering processes (Soreghan and Cohen, 1993). Lower gradient margins are expected to produce sands that underwent more modification from the original parent material

(Basu, 1985). Low gradient margins in the Ischigualasto Basin are consistent with the sedimentological evidence presented in Appendix A.

Overbank and prodeltaic deposits have a very different composition compared to the channel lithofacies because they are finer-grained and have fewer polycrystalline rock fragments than the coarse-grained facies, excluding chert. Compositional data of the fine- to medium-grained sandstone indicate derivation primarily from quartzose sources. Monocrystalline quartz fragments indicate significant amounts of both igneous and metamorphic rocks based on morphology and undulatory extinction. Possible sources of the quartzose clasts could be Precambrian metamorphic rocks or Paleozoic plutons. The quartz grains could also be recycled from a sedimentary source such as the Upper Paleozoic or Lower Triassic sandstones, but most of the grains are not well-rounded, suggesting minimal recycling. Micas are most likely derived from Precambrian metamorphic basement rock or Paleozoic plutons and preferentially accumulated in the overbank and prodeltaic facies because of hydraulic sorting. The altered feldspars may reflect reworked feldspathic sandstones whereas unaltered feldspars are most likely derived from Paleozoic plutons or Precambrian metamorphic rocks. The abundance of chert in the finer-grained fraction may indicate one of three things: 1) a shift in the source rock from predominantly Precambrian metamorphic basement rocks to a mixture of Precambrian and Paleozoic granitoids and Ordovician cherty limestone (San Juan Fm) as a result of uplift; 2) increased erosion, exposing the Paleozoic rocks, or 3) alteration of silicic volcanic ash. Similar to the conglomerates and coarse-grained sandstone, the majority of these sandstones also overlap the Transitional Continental and Recycled

Orogen tectonic provenance fields of Dickinson et al. (1983), typical of sediments more basinward in rift systems.

5.2 Sandstone and conglomerate cementation

Most of the sandstone and conglomerate underwent considerable compaction prior to cementation. In most of the sandstone samples, it is impossible to establish paragenesis of cement formation because younger cements often replace earlier cements and grains and as a result, only one type of cement is present in most samples. In the coarse-grained channel sandstones and conglomerates, early-stage quartz overgrowths and late-stage poikilotopic calcite is common. Either pressure solution by compaction of quartzose grains or the quantity of volcanic ash may account for silica-saturated water and precipitation of quartz overgrowths. Calcite is interpreted to be a late-stage cement based on the presence of calcite veins that cross-cut through fine-grained lacustrine rocks. Feldspar grains are also calcitized at a late stage. In thin section, kaolinite replaces feldspar, which suggests an authigenic origin. Locally, authigenic books of kaolinite are present in pore spaces of coarse-grained sandstone and conglomerate, but the relative timing of cementation cannot be determined. Kaolinite is stable in dilute, acidic, organic-rich, and silica-saturated conditions (Drever, 1988; Krauskof and Bird, 1995). Acidic pore waters could arise from oxidation of organic material in laterally equivalent lacustrine units. Dilute, acidic water expelled from the lacustrine rocks during burial may have migrated to the channel conglomerate and sandstones.

Overbank sandstone shows significant pseudomatrix development during compaction. Detrial mica and schist grains are bent around more durable clasts of

quartzose and feldspar grains. Clay cements, such as chlorite and I/S, and hematite are common in these sandstones. In the prodeltaic sandstone, compaction is also significant based on the presence of mica pseudomatrix. Cementation by clays (dominantly I/S) is common. The clay mineral assemblages of the finer grained lacustrine facies are described more thoroughly in the next section.

5.3 Clay mineral assemblages- provenance vs. diagenesis

5.3a Paleosol massive mudrock

The paleosol mudrock from the southwestern, eastern, and southern part of the Ischigualasto Basin contains dioctahedral, fully expandable smectite at every stratigraphic level in the Rio Marco, Cerro Morado, and Rio Gualo sections. Near the top of the Rio Gualo section, minor kaolinite (<5%) is also present (Fig. 4). Although the smectite could be detrital in the paleosols, smectite derived from the hydrolysis of volcanic ash is the favored interpretation. The smectite displays a high degree of crystallinity based on XRD patterns and cornflake-like morphology, typical of authigenic smectite, in scanning electron images. Incorporation of significant amounts of silicic ash into these rocks is noted based on the presence of relict, thin, bubble wall shard shapes observed in some of the thin sections. Alteration of silicic ash often results in formation of smectites (Fischer and Schminke, 1984). A number of factors may be responsible for diagenetic reactions in a terrestrial environment including temperature, pH, silica activity, pore fluid composition, and burial rate (Hower et al., 1976; Boles and Franks, 1979; Abercrombie et al., 1994). Dissolution of volcanic glass raises silica activity above quartz saturation. Early diagenesis of volcanic ash at low temperatures (~25°C) often results in the precipitation of opalline material and smectite (Bish and Aronson, 1993).

The clay mineral assemblage of the mudrock is not overprinted by progressive burial diagenesis in these regions of the basin based on the presence of fully expandable smectite. This is consistent with the degree of burial and maximum inferred depths of those regions, between 0 and 0.8 km (Uliana et al, 1989; Milana and Alcober, 1994; Ruiz and Introcaso, 1999). The deepest part of the basin is located in the west-central part of the Ischigualasto Basin, close to the basin bounding Valle Fértil fault, and is estimated to be between a maximum of ~4.5-9 km deep, but more likely <1.5km of sediment accumulated after deposition of Middle Triassic rocks (Uliana et al, 1989; Milana and Alcober, 1994 Fig.1a; Ruiz and Introcaso, 1999, Fig. 1).

The massive mudrocks of the Cañon de la Peña section contains a diverse clay assemblage: I/S ± illite ± kaolinite ± C/S. Unlike the other paleosol mudrocks in the Ischigualasto Basin that display bluish gray colors typical of waterlogged soils, these paleosols are red-colored. Thermal and chemical alteration of the mudrock as a result of the basalt sill is likely in the Cañon de la Peña section. Basalt dikes altered Triassic mudrock in the Late Triassic Hartford Basin (USA). Progressive alteration of I/S in unaltered red mudstone to corresnite at the contact of the basalt and mudrock is interpreted to form as a result of hydrothermal fluids rich in iron and magnesium associated with basalt flows (Vergo and April, 1982). A similar situation likely occurred in the Cañon de la Peña section in order to form illite, I/S, kaolinite, and C/S.

5.3b Lacustrine siliciclastic and carbonate rocks

The clay mineral assemblage of the shallow water lacustrine facies includes I/S, illite, kaolinite, and minor C/S (Fig. 4); however, I/S is the most abundant clay mineral.

The deep-water lacustrine facies contain only I/S. Variation in the clay mineral assemblages of lacustrine sediments may be the result of migrating sediment facies through time, changes in weathering processes in the watershed, or variations in the lake water chemistry, which can have a major effect on burial diagenesis (April, 1981; Yuretich, 1989). Lateral changes in clay mineral assemblages are also seen in sediments from Lake Constance (Chamley, 1989). In Lake Constance, the abundance of chlorite and illite decreases and the abundance of smectite increases away from Rhine river input (Chamley, 1989). Grain size and density of the clay minerals are thought to have a major control on clay mineral distribution if the source area of the clay minerals remains constant as is observed in the Ischichuca Fm. Some combination of depositional environment, climate, and diagenesis likely played a role on the clay mineral assemblages.

If the effects of burial diagenesis are insignificant, then climate in the watershed can be inferred from clay mineral assemblages. The detrital micas, muscovite and chlorite, reflect erosion in the surrounding uplands and accumulation in the lake during periods of rainfall (Chamley, 1989). I/S is generally thought to occur in warm climates with seasonal aridity (Dunoyer de Segonzac, 1970). However, this assumption of a climatic signal preserved in the lacustrine rocks is unrealistic because simple kinetics could have driven diagenetic reactions to a stable state since deposition during the Triassic (~240 Ma).

Diagenesis most likely played some role in the clay mineral assemblages observed. The relative proportion of illite in I/S in all of the lacustrine facies shows no

consistent change with stratigraphic height. Other diagenetic studies of argillaceous rocks have shown that the percent of illite in I/S increases with increasing depth and temperature (Hower et al., 1976). Other studies indicate that the supply of K^+ is a limiting factor of illite formation (Hower et al., 1976; Altaner and Bethke, 1988). In the sandstone and conglomerate facies, possible sources of K^+ include potassium feldspar, detrital muscovite, and lithic fragments that contain these minerals. Potassium does not appear to limit the illitization reaction.

Pore fluid composition has been shown to have a major impact on clay mineral assemblages observed in other Triassic lake sequences (April, 1981). In general, dilute fluids are found in pore spaces of the lacustrine mudrock and sandstone of freshwater lakes (Yuretich, 1988). April (1981) used the authigenic clay mineral assemblages of Late Triassic lacustrine shale and mudrock to determine the pore water chemistry of the lakes that influenced clay authigenesis in lake sediments in the Hartford Basin. He suggested that Mg-rich, saline fluids influenced corrensite formation (April, 1981). The presence of dilute pore fluids is thought to inhibit smectite illitization under normal burial conditions (Yuretich, 1988), and may account for lack of increasing illitization with depth in the Ischigualasto Basin rocks. The pH of the pore fluids has a significant impact on the stability fields of silicate minerals. At neutral conditions, typical of freshwater lakes, smectite is a stable phase. With increasing pH, illite is the more stable phase. Near neutral pH waters inherited from the freshwater lake may have been an important component of diagenesis in the Ischichuca Fm. Upward migration of pore fluids during compaction supplied near neutral fluids. The presence of I/S in the lacustrine sediments

most likely can be attributed to two factors: 1) alteration of silicic ash in the lake sediments by near neutral fluids inherited from freshwater lakes and 2) differential burial conditions (e.g., temperature and depth) across the basin. Alteration of silicic ash during diagenesis most likely accounts for the presence of I/S because relict volcanic shards are preserved in lacustrine claystone. The clay mineral assemblages record geochemical conditions related to inherited lake pore water composition and increased burial depths close to the basin bounding Valle Fértil border fault.

As smectite illitization progresses, silica and other cations are released between temperatures of 25-200°C (Abercrombie et al., 1994). Excess Si^{4+} released during smectite illitization in lacustrine rocks could have been transferred to the channel sandstones to be precipitated as quartz overgrowths or kaolinite, as observed in the Eocene Wilcox sandstone in Texas (Boles and Franks, 1979). Precipitation of low silica phases such as illite and quartz occurs as opal and smectite dissolve (Abercrombie et al., 1994).

5.3c Bentonites

The bentonites comprise a small fraction of the lithologies observed in all the measured stratigraphic sections. In the southern and eastern parts of the basin, smectite $\pm$ kaolinite occur in the altered ash layers. Both these clay minerals form in freshwater environments, although silicic ash may also alter to kaolinite in acidic conditions (Chamley, 1989). Smectite formation from a volcanic ash precursor is favored by relatively dilute fluids, with low concentrations of K^+, Na^+, and Ca^{2+} (Drever, 1988; Altaner and Grim, 1990). Smectite and kaolinite are characteristic of burial temperatures

≤ ~50°C (Hoffman and Hower, 1979), and slow rates of burial (Abercrombie et al., 1994), which corresponds to depths between 0.7-1.5 km, depending on the geothermal gradient (10-30°C) and Earth surface temperatures (15-25°C). This range of temperature is too low to produce significant mineralogical alteration.

In the western region of the Ischigualasto Basin, the clay mineral assemblage of the bentonites is composed of ordered I/S. I/S may form either directly from a volcanic glass precursor or is transformed from smectite. Progressive illitization of smectite has been documented with depth in argillaceous sediments from the Gulf Coast (Hower et al., 1976) and volcaniclastic rocks (Inoue, 1987). The illitization of smectite may also be associated with rapid burial and temperatures of 110-120°C (Hoffman and Hower, 1979; Abercrombie et al., 1994). Assuming a maximum of ~4.5 km of sediment thickness in the Ischigualasto Basin near the western basin bounding Valle Fértil border fault based on 3D gravity models, seismic studies, and measured sections of the Triassic rocks (Milana and Alcober, 1994; Ruiz and Introcaso, 1999), and a geothermal gradient of 25°C, temperatures likely reached a maximum of 138°C, enough to produce significant alteration of smectite to I/S. However, progressive smectite illitization is not observed. The lack of a systematic trend in the clay mineral assemblages in the bentonites from the measured sections suggests that the effects of burial diagenesis were minimal. We suggest that differences in the clay mineral assemblages of the bentonites across the basin may be the result of differences in pore water composition.

5.4 Carbonate diagenesis

CL study of the primary and secondary carbonate does not show any evidence of relict textures or zonation in the cements or primary carbonate. Dull to bright luminescence of primary limestone is compatible with the presence of divalent manganese. The variety of CL colors observed may be due to the relative abundance of Fe^{2+}, which will quench the Mn^{2+} activator present in the calcite, producing a wide variety of CL colors (Walker and Burley, 1991). Dull red to brown luminescence of the primary carbonate components is consistent with pervasive recrystallization (Machel and Burton, 1991).

Stable isotopic analysis of primary and secondary carbonate with the same intensity of luminescence yielded similar $\delta^{18}O$ results, suggesting that secondary growth of calcite as cements and veins significantly affected the $\delta^{18}O$ values of the original, primary carbonate (Fig. 6). The $\delta^{13}C$ and $\delta^{18}O$ values likely reflect an isotopic exchange between the original carbonate rocks and diagenetic fluids because the carbonate has a consistently low $\delta^{18}O$ values and display a narrow range in isotopic composition. The oxygen isotope composition of diagenetic calcite is is dependent on many factors, including the $\delta^{18}O$ value of meteoric water, evaporation, temperature of precipitation of calcite, and diagenesis. In this case, the temperature of recrystallization during diagenesis probably is the dominant factor in controlling the $\delta^{18}O$ of the carbonates. The maximum burial temperatures must be estimated in order to evaluate the oxygen isotopic composition of the water responsible for recrystallization of the primary carbonates and precipitation of the secondary cements. We use the following fractionation between calcite and water to constrain the water $\delta^{18}O$ and temperature:

$$1000\ln\alpha_{c\text{-}w} = 2.78\text{x}10^{6}T^{-2}\text{-}2.89 \text{ (Friedman and O'Neil, 1977)}$$

where $\alpha_{c\text{-}w} = (^{18}O/^{16}O)_c/(^{18}O/^{16}O)_w$ and T = temperature in °Kevin (Friedman and O'Neil, 1977). The current mean annual temperature in San Juan, Argentina, located ~150km SW of the Ischigualasto Basin, is 18°C, at 880m above sea level (Alcober, 1996). The mean elevation in the Ischigualasto Basin is 1300m. If the mean $\delta^{18}O$ value of lacustrine micrite is –18.8‰ (PDB), and a similar $\delta^{18}O$ value of precipitation fell during the Triassic as in Mendoza, Argentina today (average: -5.97‰ (SMOW) at 760 m above sea level), then precipitation of the calcite would have occurred at 98°C. This calculated temperature is unreasonable for Earth surface temperatures, but does correspond to possible burial paleotemperatures in the western part of the basin.

Conclusions

1. Combined paleocurrent and provenance data provide information about the composition and location of the source terrane. The overall drainage pattern of the rivers in the southern part of the Ischigualasto Basin is to the N-NE, transverse to the rift basin. Based on point count data, the main sources of sediment are likely from Precambrian gneiss and schist and Paleozoic granodiorite and tonalite. Minor influx of recycled (altered) feldspar and quartzose grains from Upper Paleozoic and Lower Triassic sedimentary rocks is possible. Provenance data from the fluvial sandstone demonstrate that the main sources of sand and granules did not change upsection. A moderately humid to semi-humid climate may be responsible for the dominance of quartzose grains in the conglomerate and sandstone rather than lithic fragments observed in most modern

rift basins. The lithic component of the conglomerate and sandstone directly reflects the source area.

2. The clay mineral composition of paleosols reflects the abundance of silicic ash deposited across the basin, except in the Cañon de la Peña section. In the Cañon de la Peña section, thermal and chemical alteration of the mudrock by a basalt sill affected the clay mineral assemblage.

3. Lacustrine clay mineral assemblages reflect proximity to shoreline, burial depth, and pore fluid composition. Increased illite and chlorite content may reflect proximity to shoreline and increased I/S content may reflect seasonally wet conditions or, more likely, an influx of silicic ash. Kaolinite likely formed from alteration of feldspar with acidic pore waters, which resulted from high organic matter content in the lacustrine rocks during diagenesis.

4. The clay mineral assemblage of the bentonites reflects differential burial conditions across the basin. In the shallow parts of the Ischigualasto Basin, smectite is the dominant clay mineral whereas in the deep part of the basin, I/S is dominant.

5. Diagenetic fluids did migrate through pore spaces in these rocks in order to pervasively alter the carbonate rocks and precipitate poikilotopic calcite cement in the coarse-grained fluvial facies and form calcite veins in fine-grained lacustrine claystone. The original stable carbon and oxygen composition of the carbonate rocks was altered after burial.

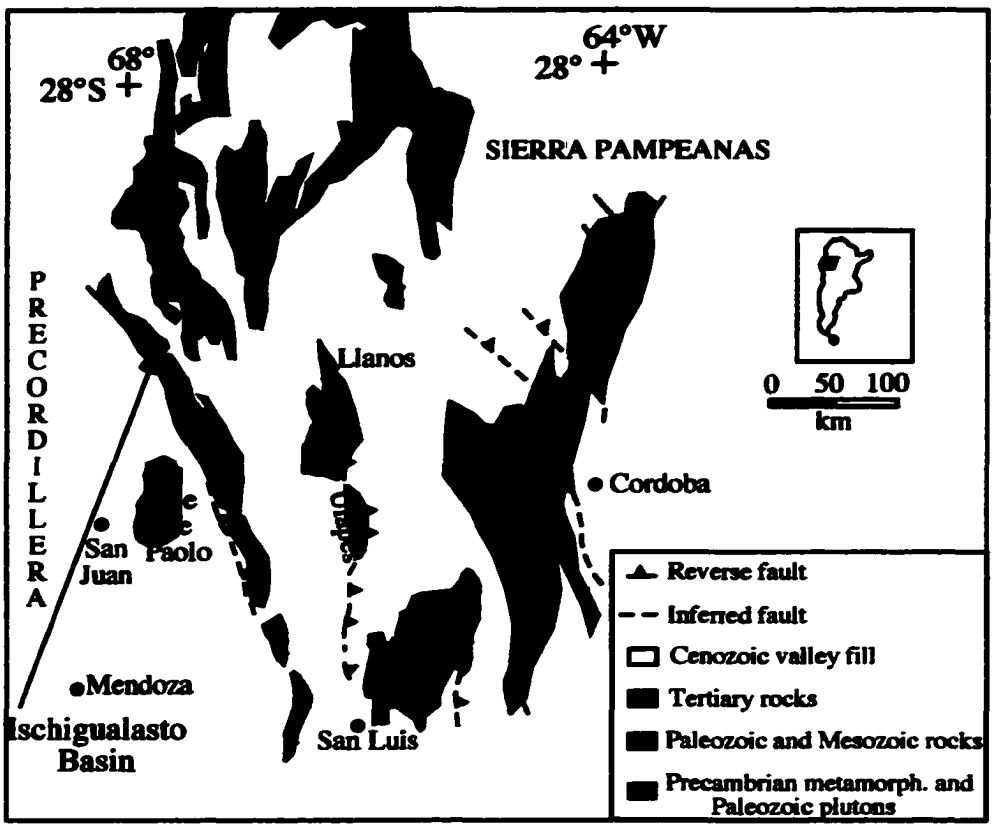

FIGURE B-1. Generalized geologic map of some of the Sierras Pampeanas basement uplifts and location of the Ischigualasto Basin (modified from Jordan and Allmendinger (1986); Figs. 2 and 5; and Ragona et al.,(1995)).

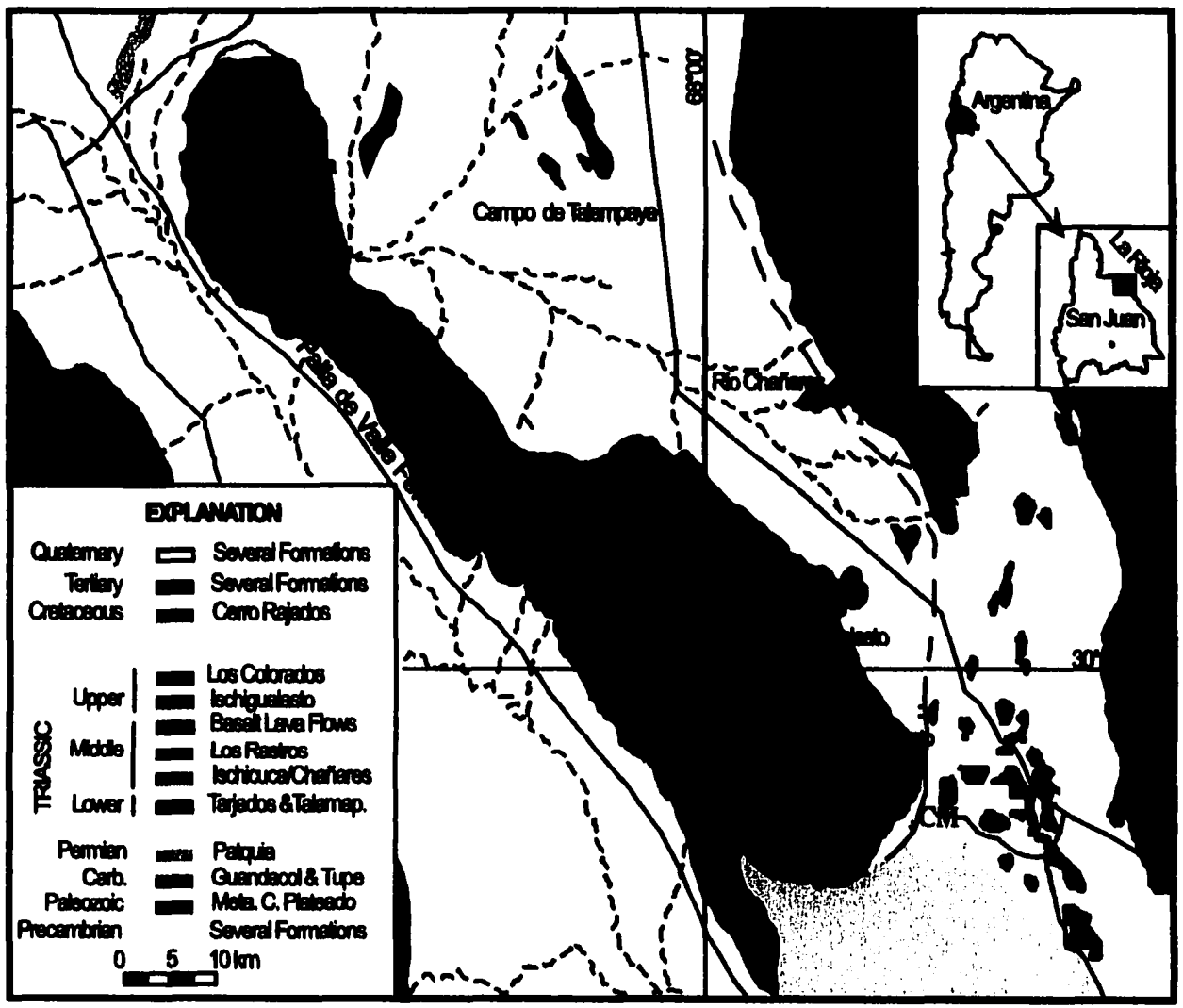

FIGURE B-2. Geologic map of the Ischigualasto Basin(location in Fig 1a) in the Sierras Pampeanas region of NW Argentina (from Milana and Alcober, 1994). Measured sections are labeled on the map as follows: CP- Canon de la Pena, RM- Rio Marco, CM- Cerro Morado, and RG- Rio Gualo.

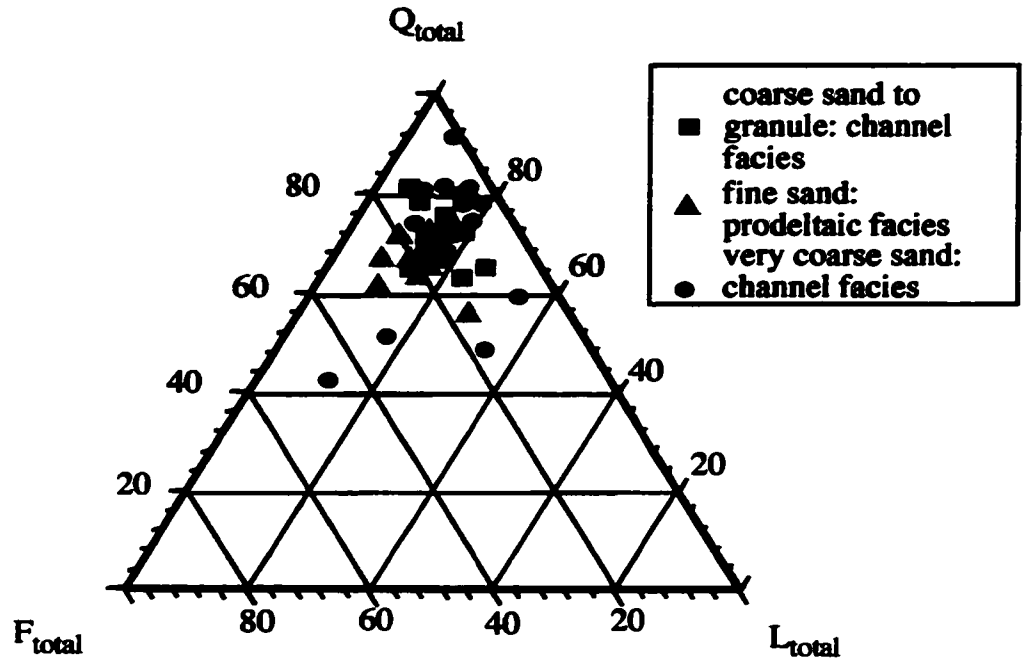

FIGURE B-3. Ternary plot of sandstone and conglomerate by grain size. Q_{total}= total quartzose grins; F_{total} = total feldspar grains; L_{total} = total lithic grains.

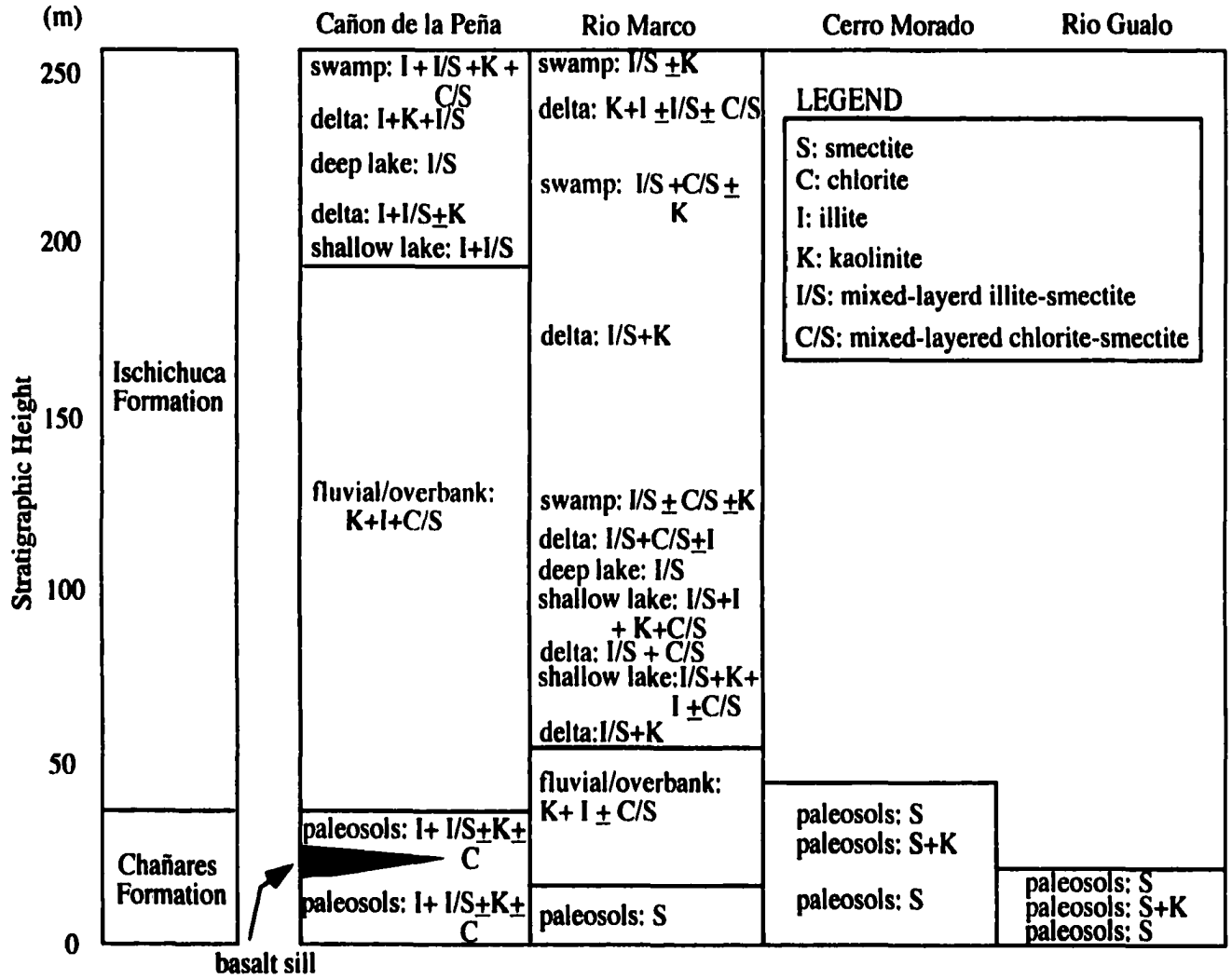

FIGURE B-4. Generalized distribution of clay minerals across the Ischigualasto Basin. The Chañares Fm has a distinct claymineral assemblage compared to the Ischichuca Fm, except in Cañon de la Peña. The paleosols in Cañon de la Peña reflect a higher grade of alteration than at the other measured sections. The Ischichua Fm represents both fluvial and lacustrine deposits. I/S is characteristic of all of the lacustrine units whereas illite andkaolinite are typical of the cements of the fluvial deposits.

FIGURE B-5. Representative X-ray diffraction patterns of the ethylene glycol -solvated <0.5 mm fraction of samples from the Ischigualasto Basin. a)70%I in I/S R1 and kaolinite. b) 70%I in I/S R1. c) illite, 50% I in I/S R1, and kaolinite, d) smectite. Mineralogical abbreviations same as in FIGURE B-4.

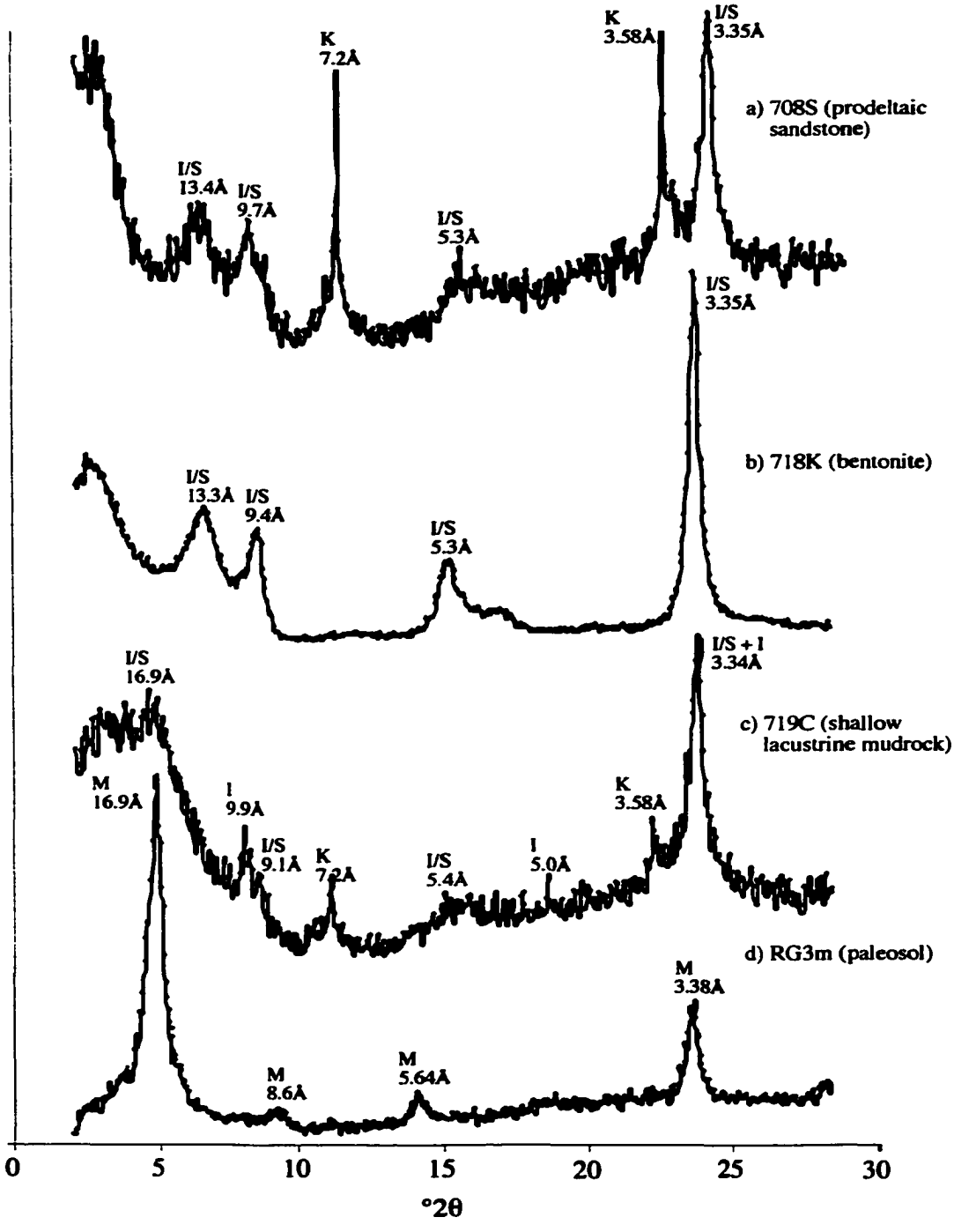

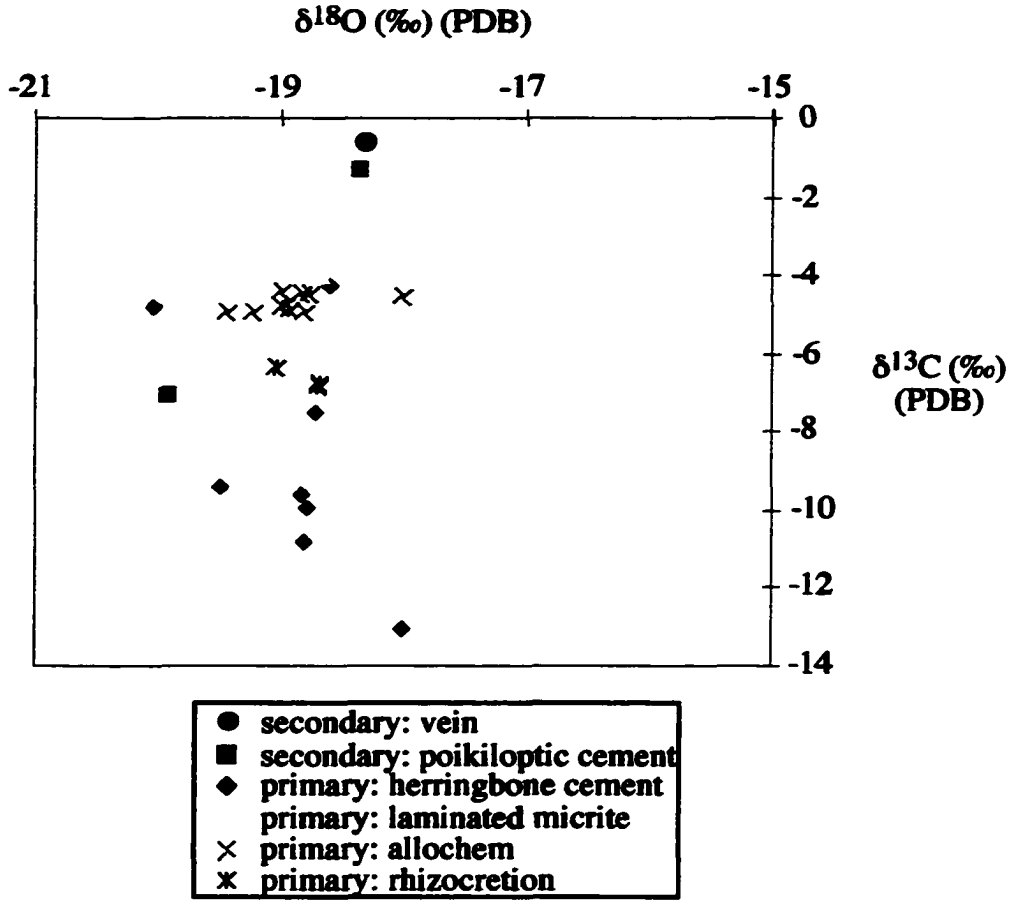

FIGURE B-6. $\delta^{18}O$ (‰) (PDB) versus $\delta^{13}C$ (‰) (PDB) for primary cements and allochems and secondary cements and veins composed of low-Mg calcite. Note the overlap between primary and secondary components of limestones.

Works Cited

Abercrombie, H.J., Hutcheon, I.E., Bloch, J.D., and de-Caritat, P., 1994, Silica activity and the smectite-illite reaction: Geology, v. 22; n. 6, Pages 539-542.

Altaner, S.P., and Bethke, C., 1988, Interlayer ordering in I/S, American Mineralogist, 73, 7-8, 766-774.

Altaner, S.P. and Grim, R.E., 1990, Mineralogy, chemistry, and diagenesis of tuffs in the Sucker Creek Formation (Miocene), Eastern Oregon, Clays and Clay Minerals, 38, 6, 561-572.

April, R.H., 1981, Clay petrology of the Upper Triassic/Lower Jurassic terrestrial strata of the Newark Supergroup, Connecticut Valley, U.S.A, Sedimentary Geology. 29; 4, 283-307.

Alcober, O., 1996, Revision de los Crurotarsis, estratgrafia y tafonomia de la formacion ischigualasto, Thesis docoral, Universidad Nacional de San Juan Facultad de Ciencias Exactas Fisicas y Naturals. 254p.

Basu, A., 1985, Influence of climate and relief on compositions of sands released at source areas, *in* G.G. Zuffa (ed.), Provenance of arenites. NATO ASI Series. Series C: Mathematical and Physical Sciences. 148, 1-18.

Bayliss, P., 1986, Quantitative analysis of sedimentary minerals by powder X-ray diffraction, Powder Diffraction, 1, 2, 37-39.

Birkeland, P.W., 1999, Soils and Geomorphology, 3rd edition, Oxford University Press, New York, 430p.

Bish, D.L. and Aronson, J.L., 1993, Paleogeothermal and paleohydrologic conditions in silicic tuff from Yucca Mountain, Nevada. Clays and Clay Minerals. 41; 2, 148-161

Boles, J.R. and Franks, S.G., 1979, Clay diagenesis in Wilcox sandstones of Southwest Texas; implications of smectite diagenesis on sandstone cementation. Journal of Sedimentary Petrology. 49; 1, 55-70

Bossi, G.E., 1970, Asocianes mineralogicas de las arcillas en la cuenca de Ischigualasto-Ischichuca Parte II: Perfiles de la Hoya de Ischigualasto, Acta Geologica Lillonana XI:4, 75-100.

Brindley, G.W. and Brown, G., 1980, Crystal structures of clay minerals and their X-ray identification, Mineralogical Society. London, United Kingdom. Monograph - Mineralogical Society. 5, 495p.

Callender, E., 1997, Geochemical mass balances of major elements in Lake Baikal, Limnol. Oceanogr., 42, 1, 148-155.

Chamley, H., 1989, Clay Sedimentology, Springer Verlag, NY, 623p.

Devaney, K.A. and Ingersoll, R.V., 1993, Provenance evolution of Upper Paleozoic sandstones of north-central New Mexico, *in* M.J. Johnsson and A. Basu (eds.), Proceses Controlling the Composition of Clastic Sediments: Boulder, Colorado, Geological Society of America Special Paper 284, 91-108.

Dickinson, W.R., 1970, Interpreting detrital modes of greywacke and arkose, J Sed Pet 40 2 695-707.

Dickinson, W.R., 1985, Interpreting provenance relations from detrital modes of sandstones *in* Zuffa GG (ed.) Provences of Arenites, NATO Advanced Study Institutes Series C, Mathematical and Physical Sciences, 148, 333-361.

Dickinson, W.R. and Suczek, C.A., 1979, Plate tectonics and sandstone compositions, AAPG 63, 2164-2182.

Dickinson, W.R. and 8 others, 1983, Provenance of North American Phanerozoic sandstones in relation to tectonic setting, Geological Society of America Bulletin, 94, 222-235.

Drever, J.I., 1973. The preparation of oriented clay mineral specimens for X-ray diffraction analysis by a filter-membrane peel technique. American Mineralogist, 58, 553-554.

Drever, J.I., 1988, The Geochemistry of Natural Waters, Prentice Hall, Englewood Cliffs, New Jersey, 437p.

Dutta, P.K. and Suttner, L.J., 1986, Alluvial sandstone composition and paleoclimate, II. authigenic mineralogy. J. Sed. Pet., 56, 346-358.

Dunoyer de Segonzac, G., 1970, The transformation of clay minerals during diagenesis and low grade metamorphism: a review, Sedimentology, 15, 281-346.

Fisher, R.V. and Schmincke, H.U., 19884, Pyroclastic Rocks, Springer-Verlag, New York, 472p.

Friedman, I. and O'Neil, J.R., 1977, Compilation of stable isotope fractionation factors of geochemical interest, *in* Fleischer, M. (ed.) Data of Geochemistry, Chapter KK: U.S. Geological Survey Professional Paper 440-K, 12p.

Garzanti, E., Vezzoli, G., Andò, S., and Castiglioni, G., 2001, Petrology of rifted-margin sand (Red Sea and Gulf of Aden, Yemen), J. of Geol., 109, 277-297.

Hoffman, J., 1976, Regional metamorphism and K/Ar dating of clay minerals in Cretaceous sediments of the undisturbed belt of Montana, unpublished Ph.D. dissertation, Case Western Reserve University, 266p.

Hoffman, J. and Hower, J., 1979, Clay mineral assemblages as low grade metamorphic geothermometers; application to the thrust faulted disturbed belt of Montana, U.S.A. In: Scholle, P.A. and Schluger, P.R. (eds.) Aspects of diagenesis. Special Publication - Society of Economic Paleontologists and Mineralogists. 26, 55-79.

Hower, J., Eslinger, E.V., Hower, M.E., Perry, E.A., 1976, Mechanisms of burial metamorphism of argillaceous sediment: mineralogical and chemical evidence. Geol. Soc. Am. Bull., 87, 725-737.

Hubert, J.F., Feshbach-Meriney, P.E., and Smith, M.A., 1992, The Triassic-Jurassic Hartford Basin, Connecticut and Massachusetts, sandstone diagenesis, and hydrocarbon history. Am. Assoc. Pet. Geo. Bull. 7. 1710-1734.

Ingersoll, R.V., Bullard, T.F., Grimm, R.L., Pickle, J.D., and Sares, S.W., 1984, The effect of grain size on detrital modes: a test of the Gazzi-Dickinson point-counting method: Jour. Sed. Petrology, 54, 103-116.

Inoue, A., 1987, Conversion of smectite to chlorite by hydrothermal and diagenetic alterations, Hokuroku Kuroko mineralization area, Northwest Japan. Proc. Int. Clay Conference, Denver 1985, 158-164.

Jenny, H., 1941. Factors of Soil Formation. McGraw-Hill, New York, 281 p.

Johnsson, M.J., 1993, The system controlling the composition of clastic sediments *in* M.J. Johnsson and A. Basu (eds.), Processes Controlling the Composition of Clastic Sediments: Boulder, Colorado, Geological Society of America Special Paper 284, 1-19.

Jones, B.F. and Bowser, C.J., 1978, The mineralogy related chemistry of lake sediments, *in* A. Lerman (ed.), Lakes: Chemistry, Geology, Physics, Springer, New York, 194-235.

Jordan, T. E. and Allmendinger, R.W., 1986, The Sierras Pampeanas of Argentina; a modern analogue of Rocky Mountain foreland deformation. American Journal of Science. 286; 10, 737-764.

Kelts, K., 1988, Environments of deposition of lacustrine petroleum source rocks; an introduction, *in* Fleet, A.J., Kelts, K., and Talbot, M.R., eds., Lacustrine petroleum source rocks, Geological Society of London, Geological Society Special Publications, 40, p. 3-26.

Krauskopf, K.B. and Bird, D.K., 1995, Introduction to Geochemistry, McGraw-Hill, Inc., NY, 647.

López-Gamundí, O.R., Espejo, I.S., and Alonso, M.S., 1990, Sandstone composition changes and paleocurrent reversal in the Upper Paleozoic and Triassic deposits of the Huaco area, western Paganzo Basin, west-central Argentina, Sedimentary Geology, 66, 99-111.

López-Gamundí, O.R., 2001, Asymmetric half graben fill in Triassic rifts of Western Argentina: Interaction between sedimentation and tectonics, AAPG abstract.

Machel, H.G. and Burton, E.A., 1991, Factors governing cathodoluminescence of calcite and dolomite, and their implications for studies of carbonate diagenesis, *in* C.E. Barker and O.C. Kopp (eds.) Luminescence microscopy and spectroscopy: qualitative and quantitative applications, SEPM Short Course Notes No. 25, Dallas Texas, 37-57.

Mack, G.H. and James, W.C., 1992, Paleosols for sedimentologists, Geological Society of America Short Course Notes, 127p.

Mack, G.H., James, W.C., and Monger, H.C., 1994, Classification of paleosols, Geological Society of America Bulletin, 105 129-136.

Milana, J.P. and Alcober, O., 1994, Modelo tectosedimentario de la cuenca triásica de Ischigualasto (San Juan, Argentina), Revista de la Asociación Geológica Aregntina, 49 (3-4), 217-235.

Moore, D.M., and Reynolds, R.C. Jr., X-Ray Diffraction and the Identification and Analysis of Clay Minerals, Oxford University Press, New York, NY, 332pp.

Pettijohn, F.J., Potter, P.E., and Siever, R., 1987, Sand and Sandstones ,2nd edition, Springer-Verlag: New York, 553p.

Ragona, D., Anselmi, G., Gonazález, P., and Vujovich, G., 1995, Mapa Geológico de la Provincia de San Juan, República Argentina.

Retallack, G.J., 1990, Soils of the Past- an introduction to paleopedology, Unwin Hyman, Boston, 520 p.

Retallack, G.J., 1991, Untangling the effects of burial alteration and ancient soil formation, Annual Review of Earth and Planetary Sciences, 19, 183-206.

Reynolds, R.C., 1985, Newmod, a Computer Program for Calculation of One-Dimensional Diffraction Patterns of Mixed-Layered Clays, 8 Brook Road, Hanover, NH 03755.

Ruiz, F. and Introcaso, A., 1999, Un modelo gravimétrico 3D de la profunda cuenca sedimenaria de Ischigualasto-Villa Unión (San Juan y La Rioja)- Argentina, Revista Brasileira de Geofisica, 17, 3-11.

Singer, A., 1984, The paleoclimatic interpretation of clay minerals in sediments - a review: Earth-Science Reviews, 21, p. 251-293.

Soreghan, M.J. and Cohen. A.S., 1993, The effects of basin asymmetry on sand composition; examples from Lake Tanganyika, Africa. *in* Johnsson, M.J. and Basu, A. (eds.), Processes controlling the composition of clastic sediments, Geological Society of America Special Paper. 284, 285-301.

Stipanicic, P.N. and Bonaparte, J.F., 1979, Cuenca triásica de Ischigualasto-Villa Union (Provincias de La Rioja y San Juan), *in* Turner, J.C., ed., Segundo Simmposio de Geología Regional Argentina, 1, Córdoba, Academia Nacional de Ciencias, 253-575.

Suttner, L.J., 1974, Sedimentary petrographic provinces: an evaluation; Soc. Econ. Paleontologists Mineralogists, Spec. Pub. No 21, 75-84.

Suttner, L.J. and Basu, A., 1985, The effect of grain size on detrital modes: a test of the Gazzi-Dickinson point-counting method, Discussion, J. Sed Pet. 55, 4, 616-627.

Suttner, L.J. and Dutta, P.K., 1986 Alluvial sandstone composition and paleoclimate; I, Framework mineralogy. Journal of Sedimentary Petrology. 56; 3, 329-345.

Suttner, L.J., Basu, A., and Mack, G.H., 1981, Climate and the origin of quartz arenites, J of Sed. Pet. 51, 4, 1235-1246.

Teruggi, M.E., Andreis, R.A., Iñiguez, A.M., Abait, J.P., Mazzoni, M.M., and Spalletti, L.A., 1967, Sedimentology of the Paganzo beds at Cerro Guandacol, Province of La Rioja, *in* Gondwana Stratigraphy, 2, IUGS Symposium Buenos Aires 1967, 857-880.

Uliana, M.A., Biddle, K.T., and Cerdan, J., 1989, Mesozoic extension and the formation of Argentine sedimentary basins, *in* A.J. Tankard and H.R. Balkwill (eds.) Extensional Tectonics and stratigraphy of the North Atlantic Margins, AAPG Memoir 46, p. 599–614.

Vergo, N. and April, R.H., 1982, Interstratified clay minerals in contact aureoles West Rock, Connecticut, Clays and Clay Minerals, 30, 237-240.

Walker, G. and Burley, S.D., 1991, Luminescence petrography and spectroscopic studies of digenetic minerals, *in* C.E. Barker and O.C. Kopp (eds.) Luminescence microscopy and spectroscopy: qualitative and quantitative applications, SEPM Short Course Notes No. 25, Dallas Texas, 83-96.

Weaver, C.E., 1989, Clays, Muds, and Shales: Developments in Sedimentology, 44, Elsevier, NY, 819pp.

Wright, V.P., 1986, Paleosols: their recognition and interpretation: Princeton University Press, Princeton, NJ, 315p.

Yemane, K., Kahr, G., and Kelts, K., 1996, Imprints of post-glacial climates and paleogeography in the detrital clay mineral assemblages of an Upper Permian fluviolacustrine Gondwana deposit from northern Malawi, Palaeogeography, Palaeoclimatology, Palaeoecology, 125, 27-49.

Yuretich, R.F, 1988, Possible relationships of stratigraphy and clay mineralogy to source rock potential in lacustrine sequences. In: Lacustrine petroleum source rocks. Fleet, A.J., Kelts, K., and Talbot, M.R. (eds.) Geological Society Special Publications. Geological Society of London. London, United Kingdom, 40; p. 139-151.

Yuretich, R.F., Melles, M. Sarata, B., and Grobe, H., 1999, Clay minerals in the sediments of Lake Baikal; a useful climate proxy. Journal of Sedimentary Research. 69; 3, 588-596.

APPENDIX C: PRESERVATION OF A SEASONAL CLIMATE SIGNATURE IN ORGANIC MATTER OF MIDDLE TRIASSIC LACUSTRINE DEPOSITS, NW ARGENTINA

Abstract

The C_{org} and $\delta^{13}C_{org}$ values, and C_{org}/S_{total} and C/N ratios of the organic matter from Middle Triassic lacustrine rocks of the Ischichuca Formation from the southern region of the Ischigualasto Basin provide useful information for paleoclimate reconstruction. The C_{org} of the lacustrine deposits indicates a wide range of organic abundance related to position from the shoreline. These lacustrine deposits contain significant amounts of organic matter, up to 9.1 weight %. The highest C_{org} values occur in lake-margin coal and coaly shale. The C/N ratios of all the lacustrine deposits ranged from 4.7 to 32.6, typical of lakes that undergo changes in the source of organic matter. Most lacustrine samples had C/N values > 18, indicative of a significant proportion of terrestrial organic matter in the lake sediments. The source of this organic matter to the lake is likely fluvial input of terrestrial plants and lake-marginal vegetation. Observed shifts in the $\delta^{13}C_{org}$ of the lacustrine rocks are related to the source of the plant material (land or aquatic plants). In these deposits, the $\delta^{13}C_{org}$ of the land plants ranges from –22.1 to –24.9‰ and the $\delta^{13}C_{org}$ of the aquatic lacustrine plants ranges from –19.7 to –24.4‰. The relatively high $\delta^{13}C_{org}$ values of the land plants suggest that water stress was a significant environmental condition in the Ischigualasto Basin. The $\delta^{13}C_{org}$ values of algal matter indicate

productivity levels were not high, which may be attributed to the sediment, nutrient, and water supply to the lake.

Data from this study suggest that during the Middle Triassic, continental regions between 40°and 50°S were warm enough and received enough water for extensive plant growth along rivers and lakes even under a seasonal climate regime.

1. Introduction

Both climate models and geological evidence of the Triassic suggest large-scale monsoon circulation existed on Pangea (Kutzbach and Gallimore, 1989; Parrish, 1993; Francis, 1994). Monsoons are characterized by extreme seasonal changes in wind direction that are driven by differential heating of the continents and oceans, the Coriolis effect, and storage and release of latent heat (Webster, 1987). During the Triassic, the extremely large landmass, Pangea, was almost equally divided between the northern and southern hemispheres (Parrish, 1993). The location of Pangea accentuated the seasonal contrast in solar radiation between hemispheres, and is thought to have been one of the main drivers of monsoonal circulation (Parrish, 1993). Strong cross-equatorial winds are predicted to have changed direction seasonally based on general circulation model (GCM) experiments (Kutzbach and Gallimore, 1989; Hay and Wold, 1998). This extreme form of monsoonal circulation would have kept the equatorial region dry (Parrish et al., 1982).

Moderately high to high amounts of rainfall would have been restricted to the coastlines of the Tethys Sea and the mid-latitude western coasts of Pangea in both the Northern and Southern Hemispheres; high rainfall also occurred along the western

equatorial region of Pangea, but only during the monsoon maximum (Parrrish et al., 1982; Parrish, 1993; Dubiel et al., 1991). The only significant sources of moisture were the Tethys and eastern Panthalassan Seas. Loessite-paleosol sequences found near the coast of western equatorial Pangea during the Early to Middle Triassic suggest successive periods of strong, dry winds followed by wet and humid conditions (Chan, 1999). Lithologic and biotic paleoclimate indicators should reflect humid climates along the edges of Pangea, seasonal in most places, and arid regions in Pangea's interior (Robinson, 1973; Parrish et al., 1982; Parrish, 1993; Francis, 1994).

Understanding when and how the monsoonal circulation attained its maximum is important for evaluating its effects on ecology, ocean and atmospheric chemistry, and sedimentation processes across Pangea through time (Parrish, 1993; Veevers, 1994; Wilson et al., 1994; Parrish et al., 1996). Most Triassic paleoclimate data are from the Northern and Eastern Hemispheres; few data exist from the southwest quadrant of Pangea. As a result, the timing of the monsoon maximum is not well understood. This study focuses on the Ischigualasto Basin, which lay between 40° to 50° south latitude, less than 200 km from the western coastline of Pangea, during the Triassic (Veevers, 1994). Climate models of the southwestern quadrant of Pangea indicate a warm, moist, and temperate with a dry summer season (Kutzbach, 1994). This is consistent with fossil plant evidence from southern and southeastern Pangea (Retallack and Alonso, 1998). The focus of this paper is: 1) to document climate variability related to the monsoon by analyzing the organic matter preserved in laminated lacustrine deposits from the southern region of the Ischigualasto Basin, located in the SW quadrant of Pangea during the

Middle Triassic; 2) to compare these data to other published evidence of climate change using organic matter as a proxy for paleoclimate; and 3) to synthesize the geologic and geochemical evidence from across Pangea for a monsoonal climate during the Middle Triassic.

2. Background

The $\delta^{13}C$ values of organic matter ($\delta^{13}C_{org}$) are a potentially useful indicator of paleoclimatic conditions in the Ischigualasto Basin during the Middle Triassic because they are determined by environmental factors controlled by climate, such as pCO_2, water and nutrient stress, light levels, seasonality, and temperature (McKenzie, 1985; Bochernes et al., 1993; Meyers, 1994, 1997; Arens et al., 2000). Organic matter in modern and ancient lacustrine sediments is often used to reconstruct paleoenvironmental conditions and climate change (Meyers and Ishiwatari, 1993; Meyers, 1994, 1997). The $\delta^{13}C_{org}$ values of lacustrine algal matter are most affected by the availability of dissolved nutrients and pCO_2 in the lake water (Meyers, 1997). The $\delta^{13}C_{org}$ values of terrestrial organic matter is controlled by both the photosynthetic pathways and environmental factors, such as water and nutrient stress, temperature, altitude, seasonality, and light availability in the watershed (Bocherens, et al., 1993; Arens et al., 2000). The primary source of particulate organic material in modern lakes is from vascular plants that are washed in from the lake watershed by rivers or wind, although a small percentage of organic matter may be autochthonous (Meyers and Ischiwatari, 1993). Elemental (C and N), isotopic ($\delta^{13}C_{org}$), and mineralogic information is stored in lacustrine sediments and

can be used to unravel the climate and depositional and diagenetic history in lakes and their watersheds.

3. Geologic Setting

The Ischigualasto Basin is located in NW Argentina in the Sierras Pampeanas tectonic province and is interpreted to be part of a series of Triassic rift basins that formed along the western and southern margins of South America (Figure 1a) (Uliana et al., 1989). The Ischigualasto Basin is located on Precambrian craton and was east of the rift highlands (Uliana et al., 1989). Triassic continental rocks comprise, on average, 1.5 km of sedimentary rocks in the basin, with a maximum of ~4.0 km that lie unconformably on Precambrian metamorphic to Permian sedimentary rocks (Stipanícic, 1983). The Lower to Middle Triassic stratigraphic sequence is conformable except between the Lower Triassic Tarjados Formation (Fm) and Middle Triassic Ischichuca and Chañares Formations (Fms) (Figure 1b), which are coeval. Structurally, the basin is bounded on the west by the Valle Fértil border fault, reactivated during the Neogene as a thrust fault, which separates Precambrian metamorphic rocks from Permian, Triassic, and Cenozoic rocks (Jordan and Allmendinger, 1986). The Ischichuca Fm is only well-exposed near the Valle Fértil fault, which is the western basin-bounding fault of the Triassic rift half graben. The Ischichuca Fm consists of conglomerate, sandstone, siltstone, and bentonitic shale (Stipanícic, 1983; López Gamundi et al., 1989) and is interpreted to be lacustrine and prodelatic deposits (López Gamundi et al., 1989; Milana, 1998). Most of the profundal lacustrine deposits are not observed because they are either buried by thick deposits of Cenozoic foreland basin fill or were eroded during Andean

fold-and-thrust belt evolution during the late Cenozoic (Jordan and Allmendinger, 1986; Zapata and Allmendinger, 1996). The coeval Chañares Fm crops out in the southern and eastern margins of the basin. The Chañares Fm is tuffaceous (Stipanícic, 1983) and was initially described as sheetflood and alluvial fan deposits (Romer and Jensen, 1966). Appendix A describes these units as stacked sequences of vertisols to palustrine deposits. The focus of this study is on the Middle Triassic Ischichuca Fm.

4. Depositional Framework

The Ischichuca and Chañares Fms were deposited in three different environments: 1) fluvial channels and overbank deposits, 2) palustrine-paleosol deposits, and 3) lacustrine deposits. Although organic matter is preserved in all of these environments, few plant fossils were observed in the fluvial channels and palustrine-paleosols. The fossil plants in the Ischichuca Fm are diverse, and correspond to the *Dicroidium* flora, including *Neocalamites*, *Zuberia*, *Dicroidium*, *Sphenopteris*, *Cladophlebis*, *Johnstonia*, cycads, and conifers (Stipanícic, 1983; Bonaparte, 1997). Plant hash horizons are common on bedding plane surfaces of the fluvial-deltaic and littoral lacustrine deposits. Most of these horizons are thin (<2mm) mats of unsorted and rarely oriented plant fragments that cannot be identified because the leaves were physically altered during transport and deposition. Fragments are typically coalified. Interpretation of depositional processes and settings of the lacustrine rocks indicates four major lacustrine subenvironments are represented: 1) profundal, 2) prodeltaic, 3) littoral, and 4) lake-margin swamps.

The profundal lacustrine deposits are characterized by laterally continuous, rhythmic, thinly laminated claystone and limestone. The lamination is visible because of the distribution of amorphous organic matter. The prodeltaic environment is represented by rhythmic laminations of mudrock and fine-grained sandstone, which are more common than in any other lithofacies. These laminations are defined by the difference in color and presence of organic matter in discontinuous to continuous layers. The littoral lacustrine environments include ripple-laminated limestone deposits and massive siltstones. Littoral zone carbonate rocks are laminated and exhibit ripples. Fragments of calcified charophyte stems and a few ostracods and gastropods compose the allochems found in the laminations. The charophytes were transported and reworked from their original sites of deposition based on the degree of fragmentation. The massive siltstone has *Unionidae* shell impressions, characteristic of freshwater environments. The lake-margin swamp environments are indicated by coaly shale and coal.

Lacustrine deposition is dominated by fluvial processes (Appendix A). Three major lacustrine phases are recognized by the presence of rhythmic laminations of mudrock and fine-grained sandstone identified in outcrop. Each lacustrine sequence is separated by fluvial-deltaic deposition in the Cañon de la Peña and Rio Marco measured sections (Appendix A). The three intervals of laucstrine deposition are referred to in this paper as Lake 1, Lake 2, and Lake 3, and refer to deposition in the lake in stratigraphic order. These lakes are distinguishable based on similar sedimentologic and mineralogic characteristics and may be stratigraphically correlated between the Cañon de la Peña and Rio Marco measured sections. Geochemical results are reported with respect to each of

the four lacustrine subenvironments in each lacustrine depositional interval in the Cañon de la Peña and Rio Marco measured sections.

5. Previous Work

Previous studies of the organic matter preserved in the Ischichuca Fm include identification of the fossil plants, total carbon content (TOC), and pyrolysis. The floral assemblage reflects typical Gondwanan Middle to Late Triassic Dicrodium assemblages, representing riparian to xeric terrestrial habitats (May, 1998). Shale from the Cañon de la Peña and Ischigualasto River was analyzed to determine the TOC and hydrocarbon potential (Milana, 1998). The TOC of twenty-four organic-rich shale samples ranged from 2.3 to 10.4 weight (wt.) % (Milana, 1998). The source of the organic matter in the shale was determined using hydrogen indices. Milana (1998) noted a change in the source of the organic matter within stacked sequences of prograding deltas. Oil-prone organic matter is characteristic of deeper lake deposits and is progressively diluted by land plants as the amount of gas-prone organic matter increased as a result of fluvial input in progradational sequences (Milana, 1998).

6. Methods and Analytical Procedures

Two measured stratigraphic sections in the southern Ischigualasto Basin, Cañon de la Peña and Rio Marco, contain abundant lacustrine deposits (Figure 1b). Seventy lacustrine samples were chosen for organic geochemical analyses because they represent the variation in the types of laminated lacustrine rocks observed in the basin.

Concentrations of inorganic and organic carbon and sulfur were measured simultaneously using a LECO® CS-244 analyzer. Both acid-soluble and -insoluble dry

sediment samples were analyzed. Total carbon and sulfur weight percent for each sample were measured using dry sediment. For the acid-insoluble fraction, 250 mg of sample was reacted with 50 ml of 1N HCl for twelve hours at 60°C to remove inorganic carbon. Samples were rinsed with 150-250 ml of deionized water and dried in an oven overnight at 60°C. Inorganic carbon weight percent was determined by subtraction of the total carbon and the insoluble carbon (C_{org}). Organic carbon is defined as the fraction that remains after all the inorganic carbon has been removed by hydrochloric acid.

Organic carbon was also measured using a Leeman CE 440 elemental analyzer. C, H, and N were simultaneously determined for each sample. Samples were first treated with 5N HCl to eliminate carbonate, rinsed with deionized water, and dried in an oven at 60°C for at least twelve hours. Between 25 and 50 mg of dried sediment was then combusted in the presence of pure O_2(g). The resulting oxides of C, H, and N were analyzed chromatographically, and the amount of gas was measured using a thermal conductivity detector. Duplicate analyses are within 0.5 wt. %.

The organic carbon $\delta^{13}C$ values of bulk rock samples were obtained after treatment with 5N HCl for twelve hours at room temperature to remove carbonate. Samples were rinsed and centrifuged with deionized water until the samples were at a pH between 5 and 6. Samples were dried in an oven for at least twelve hours at 60°C. Between 0.05 and 1g of sample (depending on the C_{org} content of the sample) was reacted with CuO in evacuated and sealed quartz tubes for twelve hours at 850°C. The CO_2(g) produced was analyzed with a Finnigan MAT 252 mass spectrometer. Ratios are reported with respect to the PDB standard. Duplicate analyses are within 0.1‰.

7. Results

7.1 C_{org}

The organic carbon concentrations are quite variable regardless of the depositional environment (Figs. 2 and 3). The lake-margin coal and coaly shale beds have significantly higher carbon concentrations (up to 9.1 wt. %) than all other depositional environments, even after all the deposits were normalized for grain size. The littoral carbonate has a narrower range of C_{org}, from 0.3 – 0.8 wt.% and has a similar grain size as the siliciclastic material in the coal deposits. The ranges of organic carbon concentrations of the littoral, prodeltaic, and profundal deposits of the lake are similar (littoral: 0.2 – 2.9 wt. %; prodeltaic: 0.1-4.9 wt.%; profundal: 0.4 –3.2 wt. %).

7.2 C_{org}/S_{total} Ratios

The S_{total} content of all of the lacustrine deposits is very low and falls in a narrow range (Fig. 4). Most of the deposits are characterized by high C_{org}/S_{total} ratios (>11), except where the samples had <0.1 wt. % C_{org}.

7.3 C/N Ratios

The atomic C/N ratios of most of the lacustrine deposits are relatively high, regardless of their C_{org} contents (Figs. 2 and 3). The lake-margin coals, littoral siltstone, and deltaic sandstone exhibit similar ranges of C/N values (coal: 12.5 –32.6; littoral siltstone: 15.5–25.7; deltaic: 11.8-31.6). The profundal deposits have a narrower range in C/N values (18.8-21.2). The littoral carbonates have low C/N ratios (4.7-14.1).

7.4 Organic Carbon Isotope Compositions

The $\delta^{13}C_{org}$ values are variable, even within individual lacustrine subenvironments. The $\delta^{13}C_{org}$ of the lake-margin coal ranges from –22.1 to –24.9‰, similar to the deltaic sandstone (-22.2 to -24.4‰). The profundal claystone and carbonate and littoral siltstone have a similar range of carbon isotopic compositions (profundal: -19.7 to -24.4‰; littoral: -23.3 to -24.7‰). The $\delta^{13}C_{org}$ values of the littoral carbonate range from –22.4 to –23.6‰.

8. Discussion

8.1 Preservation, Distribution, and Composition of Organic Matter in Lakes

The organic carbon concentration of lake sediments reflects a balance between the organic matter production and deposition within the lake and the rate of organic decomposition and degradation (Kelts, 1988; Bohacs et al., 2000). Primary production of organic matter in lakes is a function of many variables including solar input, wind, precipitation, water chemistry, and temperature (Kelts, 1988). However, solar input and water chemistry are thought to have the largest impact on primary productivity in lakes (Katz, 1990). The available solar input affects the photosynthetic ability of organic matter. In general, solar input decreases with increasing latitude, lake area/depth, and turbidity in the lake (Bohacs et al., 2000). Lake-water chemistry controls the nutrient availability necessary for organisms to grow. Preservation of organic matter is controlled by a number of parameters including the lake-water chemistry, type of organic matter (land plants vs. algal plants), rates of settling, lake depth, and recycling (Bohacs et al, 2000).

Lake-water composition may enhance or decrease the productivity rates and preservation potential of organic matter. Lake-water chemistry is a function of climate, hydrologic balance, and bedrock chemistry (Kelts, 1988; Talbot, 1988; Cerling, 1994). Algal productivity in hypersaline and saline lakes is high, but recycling of organic matter is rapid so that little organic matter actually accumulates on the lake bottom (Kelts, 1988). Alkaline lakes have a higher primary productivity than lakes with near-neutral pH because of the abundance of CO_3^{-2} available to plants (Kelts, 1988). Freshwater lakes tend to have low to moderate productivity levels (Kelts, 1988) compared to tropical alkaline lakes (Bohacs et al., 2000).

Although seasonal or permanent stratification in a lake may promote preservation of organic matter, it is not essential (Talbot, 1988). Anoxic conditions in lakes decrease the number of bioturbating organisms at the lake bottom, which enhances the preservation potential of organic matter (Kelts, 1988). Microbial degradation at the lake bottom controls the amount of organic matter that is preserved. Algal material is less likely to be preserved in lake sediments than terrestrial land plants because algal material is more reactive and more readily consumed by microbes and deposit feeders than land-derived material (Meyers and Ischiwatari, 1993; 1995).

Preservation of organic matter is also controlled by rates of settling. The settling or sinking rate of organic matter in the lake depends on the type of organic matter (autochthonous algae vs. allochthonous land plants), the lake depth, and recycling in the water column by other organisms. Algal phytoplankton tends to be consumed in the water column before it can settle. In contrast, land plant material tends to sink rapidly as

a result of having a larger particle size compared to algal organic matter. In Lake Michigan, sediment trap studies indicate less than 10% of the particulate matter reaches the lake bottom, which is typical of most lakes, at depths of 100 m (Kelts, 1988; Meyers and Eadie, 1993). Approximately 75-99% of the organic matter that does reach the lake bottom is destroyed during bioturbation or resuspension (Ischiwatari and Meyers, 1995; Bohacs et al., 2000).

Although variations in organic matter content in lakes have been attributed to the amount of organic productivity and preservation potential, other factors such as sediment transport mechanisms, including turbidity currents and onshore and offshore currents, are important (Huc, 1987). Many lake basins have a heterogeneous distribution of organic matter that does not mimic concentric zonation patterns observed in some lake basins, where the highest concentration of organic matter is in the center of the basin. Transport mechanisms of sedimentation in lake basins, such as turbidity flows and onshore or offshore currents, may alter the zonation of organic concentration, as is observed in Lake Tanganyika (Huc, 1987). As a result, sediments, such as those from Lake Tanganyika, exhibit a wide range of organic carbon content, from 1.2-13 wt. % (Katz, 1988).

8.2 Controls on the C_{org} of the Ischichuca Formation

In the Ischigualasto Basin, the C_{org} is strongly influenced by distance from shore, especially proximity to fluvial input near the lake coastlines. The highest organic carbon concentrations are associated with the lake-margin swamps and deltaic deposits. The lake-margin coal has the highest concentration of organic matter and littoral carbonate deposits the lowest and narrowest range of organic carbon concentration (Figs. 2 and 3).

Carbonate precipitation in lakes and algal production is often thought to result from a low siliciclastic input (Talbot and Allen, 1996). In low, wet, and thickly vegetated basins, swampy areas often develop along lake shores, and may often be composed of mostly plant remains (Reineck and Singh, 1980; Talbot and Allen, 1996). Profundal lacustrine deposits also have low organic carbon concentrations. The range in organic carbon concentrations in the littoral siliciclastic deposits, profundal rocks, and deltaic deposits of the Ischichuca Fm may reflect times of enhanced terrestrial organic matter supply by fluvial systems or dilution by siliciclastic sands, silts, and muds.

Based on the absence of evidence of bioturbation in profundal rocks, the lake bottom likely did not support infauna or bottom-dwelling organisms. This observation may be the result of anoxic bottom waters in the lake with a stagnant bottom layer. The reducing conditions should enhance organic preservation in the profundal zone. There is no evidence of lamina destruction from methane gas bubbles so methanogenesis may not be important in this lake. The absence of pyrite or other sulfur-bearing minerals is indicative of a paucity of either sulfate or iron-bearing minerals in the watershed. Sulfate reduction does not appear to be an important player based on the C vs. S analyses of lacustrine deposits. An alternative explanation was presented by May (1998), who did not distinguish the Ischichuca Fm from the Los Rastros Fm and included the former in the latter. She suggested that the taphonomic bias in the fossils preserved in the rocks is the result of the evolution of lake water from low to high pH during deposition of the Los Rastros Fm in the northern region of the Ischigualasto Basin. May (1998) suggested that the lake bottom water was acidic during most of lacustrine deposition of the Los Rastros

Fm. The abundance of organic material in the Ischichuca Fm may be the result of settling through the water column into moderately to well-oxygenated but acidic lake bottom waters during rapid sedimentation in the lake rift basin.

8.3 Source of the Organic Matter in the Ischichuca Fm Using Atomic C/N values

The origin of the organic matter in lacustrine sediments can be distinguished using atomic C/N ratios (Meyers and Ischiwatari, 1993). The primary source of organic matter in modern lakes is detritus from the lacustrine algae and the surrounding vegetation in the watershed; animal remains constitute an extremely small component (Meyers, 1994). Cellulose in vascular plants and the protein richness of algal material affect the atomic C/N ratio of sediments (Meyers, 1997). As a result, nonvascular plants typically have low atomic C/N ratios (4–10), and vascular plants have higher ratios (>20) (Meyers and Ischiwatari, 1993). Many lakes have a mixture of vascular and nonvascular plant material that accumulate on the lake bottom and have atomic C/N ratios between 10 and 20 (Meyers and Ischiwatari, 1993).

In modern and ancient lake sediments, the atomic C/N ratio can be used to differentiate between a dominantly algal or terrestrial plant input into the lake regardless of diagenetic alteratio (Meyers and Ischiwatari, 1993; Meyers and Kowalski, 1994). In Lake Michigan, Lake Bosumtwi, Lake Yunoko, and Mangrove Lake, bulk C/N ratios are not significantly affected by degradation in the water column (Meyers and Ischiwatari, 1993). Burial of organic matter at the lake bottom tends to limit diagenetic alteration (Meyers and Ischiwatari, 1993).

The effect of grain size on the atomic C/N ratio is significant (Meyers, 1997). Sandstone contains large fragments of land plants compared to siltstone and claystone (Meyers, 1997). Silicate minerals typically contribute very little nitrogen and hydrogen, except in clay-rich samples (Meyers, 1997, Krishnamurthy et al., 1999). Clay minerals, common in fine-grained rocks, tend to artificially depress the atomic C/N ratio because they have large surface areas and negative surface charges, which tend to hold onto nitrogen compounds such as ammonia (Meyers, 1997). As a result, fine-grained sediments tend to have lower C/N ratios than coarse-grained sediments. The Ischichuca Fm has a minor amount of clay-sized material, between 1-10 wt.% (Appendix D). In general, inorganic nitrogen is thought to be minimal compared to organic nitrogen concentrations except in samples with low organic concentrations, < 0.3 wt. % (Meyers, 1997). To minimize the effect of grain size in interpretation of C/N values, samples of the Ischichuca Fm with C_{org} < 0.5 wt. % were not used to interpret the source of the organic matter because they yielded inconsistent and geologically unreasonable C/N values (0.1-2.0%). These samples with low organic contents are clay-rich palustrine to paleosol deposits and are not considered in this paper. Only siltstone and coarser-grained deposits are used in this study.

C/N ratios of silt-sized and coarser-grained rocks of the Ischichuca Fm indicate significant quantities of terrestrial land plants accumulated in the lake because C/N values are high (>18), which is expected based on the grain size and diagenetic loss of aquatic organic matter. The range in C/N values (11.8-32.6) for lake marginal coal, littoral siliciclastic rocks, deltaic, and profundal rocks record fluctuations in the amount of land-

derived organic matter delivered to the lake sediments. Low C/N ratios (4-14) occur only in littoral-zone carbonates indicating algal production and lack of terrestrial input. The C/N ratio of samples from the Ischichuca Fm cannot be readily compared to similar-age deposits because very few studies have used C/N ratios to examine to source of the lacustrine plant material in Triassic-aged rocks. Meyers and Kowalski (1994) studied Late Triassic shallow marine rocks from northern Gondwanaland from Australia and the Himalayas. The organic matter from these marine sequences indicate the presence of land plant kerogen can be distinguished from marine algal matter (Meyers and Kowalski 1994). Inferred source for the organic matter in the Late Triassic sequences from northern Gondwanaland using C/N ratios is comparable to the interpretations made using Rock-Eval hydrogen index values (Meyers and Kowalski 1994). The C/N ratios of claystones and limestones range from 1.9 to 44.5 in the Late Triassic rocks (Meyers and Kowalski 1994) and are similar to the C/N ratios of the Middle Triassic Ischichuca Fm. The inferred source of the organic matter is consistent with data on hydrogen indices in the Ischichuca Fm from Milana (1998).

8.4 $\delta^{13}C_{org}$ Values of the Ischichuca Fm

Reconstruction of ancient lake and lake watershed conditions using $\delta^{13}C_{org}$ requires that the carbon isotopic composition of the organic matter has not been significantly altered after deposition. The $\delta^{13}C_{org}$ of modern lacustrine sediment often ranges from –8 to –41‰, which overlaps with the range observed for both land and aquatic plants (Deins, 1980; Meyers and Ischiwatari, 1993). The average $\delta^{13}C_{org}$ value of modern C3 plants is –26‰, but values range from –20 to –33 ‰ (O'Leary, 1981;

Bocherens et al., 1993). The two other photosynthetic pathways, C_4 and CAM, are not known to have existed during the Middle Triassic (Bocherens et al., 1993). Plants from the Paleozoic and most of the Mesozoic was characterized by a dominantly C3 photosynthetic pathway, indistinguishable from the C3 pathway of modern systems (Bocherens et al. 1993). Major shifts in the $\delta^{13}C$ of pedogenic carbonate from the Siwlak Fm indicate the spread of C4 grasses did not occur until the Miocene (Cerling, Wang, and Quade 1993). Using organic matter in lake sediments to reconstruct past climate can be problematic, depending on the extent of degradation that occurred between settling out from the water column to bioturbation and burial. In general, the $\delta^{13}C_{org}$ of coal and lacustrine rocks reflects the dominant source of the organic carbon with only relatively small shifts of the $\delta^{13}C_{org}$, between 1-2‰, as a result of diagenetic processes such as oxidation (Clayton and Swetland, 1978; Deins, 1980; Anderson and Arthur, 1983). Observed organic carbon isotopic shifts in thousand- to million-year old lacustrine sediments indicate a progressive loss of algal matter in the sediment and a relative gain in land-derived plant matter (Meyers and Ischiwatari, 1995). However, if land plants contribute more material to the lake than algae, then diagenetic alteration would be insignificant over any time scale.

In lacustrine environments, sulfate reduction and methane fermentation (carbonate reduction) can alter the original $\delta^{13}C_{org}$ composition of plant material (Kelts, 1988). Sulfate reduction is common in saline or volcanic lakes with a source of sulfate from bedrock gypsum or volcanic sulfuric gases (Kelts, 1988). Methanogensis is more common in fresh water to alkaline lakes (Kelts, 1988). Sulfate reduction leads to

markedly depleted $\delta^{13}C_{org}$ whereas methanogenesis to markedly enriched $\delta^{13}C_{org}$ values (Clark and Fritz, 1997).

Multiple lines of evidence suggest that diagenetic alteration of organic matter is insignificant in lacustrine rocks from the Ischichuca Fm. The C/N ratios indicate that land plant contribution to the lake is greater than algal matter. In addition, our $\delta^{13}C_{org}$ results argue against significant post-depositional microbial changes because the $\delta^{13}C_{org}$ values fall within the expected range of modern C_3 terrestrial plant carbon isotopic values. However, some of the variation in the $\delta^{13}C_{org}$ values may be the result of oxidation as lake levels dropped. The average $\delta^{13}C_{org}$ value for samples with high C/N values (>18) is -23.8 ‰ (n=30). Previous studies of Mesozoic and Cenozoic fossil plants from around the world indicate carbonized leaves and lignin of fossil leaves appear to retain their original isotopic compositions (Bocherens et al., 1993). Environmental factors likely have a greater control on the carbon isotope composition of terrestrial organic material. Such high values of $\delta^{13}C_{org}$ can be attributed to many factors: 1) low pCO_2 levels, 2) water stress or high salinity leading to closure of the stomata in leaves, or 3) increasing altitude (Bocherens et al., 1993; Arens et al., 2000).

Previous studies of the flora of the Ischichuca Fm by Stipanícic (1983), Bonaparte (1997), and Milana (1998) already identified a significant proportion of terrestrial land plants found in both fluvial-deltaic and lacustrine rocks. Lacustrine algae are not the dominant source of organic matter in the Ischichuca Fm based on atomic C/N values. However, when there was a significant algal component in the lake based on interpretations of the C/N ratios, the carbon isotopic composition ranged from –22.4 to

–23.6‰ (Figs. 4 and 5). Variability in the $\delta^{13}C_{org}$ values suggests lake productivity varied, likely due to water and nutrient input into the lake system. Carbonate formation typically occurs in regions where clastic input is low (Talbot and Allen, 1996). The low $\delta^{13}C_{org}$ values indicate high lake productivity and higher values indicate less productive time intervals (Meyers, 1997). In the carbonate intervals in lake episode #2 in both Cañon de la Peña and Rio Marco, the $\delta^{13}C_{org}$ values are higher, indicating lower productivity (Figs. 2 and 3). Highly productive lake waters may indicate high nutrient levels in the lake, which reflects significant weathering in the watershed. The $\delta^{13}C_{org}$ values of the organic matter in profundal rocks also do not reflect sources that underwent significant methanogenesis or sulfate reduction.

8.5 Paleosalinity of the Ischichuca Fm

The C_{org}/total S paleosalinity indicator can be used to determine whether the lake water was fresh or saline (Berner and Raiswell, 1984; Leventhal, 1995). C_{org} values of lacustrine sediments range from less than 1 to 9.1%, and in most samples, the total sulfur content is very low, < 0.07 (Fig. 4). This suggests that sediment and organic matter deposition in all three lacustrine phases occurred in freshwater conditions. In addition, there is no mineralogical (e.g. pyrite, gypsum) or paleontological evidence of anoxia or salinity. Additional support for freshwater conditions includes shell impressions of freshwater *Unioinidea* within massive siltstone beds of the littoral zone (Appendix A). The presence of fragmented charophyte stems observed in rippled carbonate sediments also suggests a freshwater lake (Appendix A).

9. Summary of the Climate Reconstruction in the Ischigualasto Basin

The lithologic and organic geochemical data from the Ischigualasto Basin suggest that a seasonal climate played an important role in sedimentation processes in the lake and on land during the Middle Triassic. The clastic-organic dominated couplets found in the lacustrine sequences indicate significant fluvial input of water, sediment, and plant material from the lake watershed (Appendix A). The thick (>1m) lake-margin coal and coaly shale deposits indicate significant accumulation of plant material. Thick accumulations of coal are often thought to represent a humid climate. However, peat and coal can accumulate in fluvial and lacustrine environments if the water table remains high if there is runoff from surrounding highlands (Gyllenhaal, 1991). A locally high water table can still be maintained in a seasonally wet climate if the area of the wetlands is small relative to the drainage basin and little evapotranspiration takes place (Gyllenhaal, 1991). Coeval vertisol and palustrine formation in the eastern region of the basin indicates that climate likely oscillated between wet and dry conditions in order to develop large rounded peds with clay cutans (Appendix A). The combination of these lithologic indicators of climate observed in the Ischigualasto Basin, vertisols and peats (now coals), and lack of pedogenic carbonate suggests the mean annual precipitation in the Ischigualasto Basin was between 120-250 cm based on comparison with a study using modern analogs by Gyllenhaal (1991), but was likely seasonal based on other sedimentologic evidence including mudchips in lacustrine and fluvial deposits, rhythmically laminated lacustrine rocks, and ped structures in paleosols (Appendix A). The organic geochemical evidence supports moderately wet climate interpretation based on the presence of a freshwater lake in the basin. The high $\delta^{13}C_{org}$ values of the terrestrial

organic matter are most likely the result of periodic water stress or low relative humidity, but could be the result of high altitudes or modest diagenesis of organic matter in soils surrounding the lake, or some combination of the above.

10. Paleoclimatic Reconstruction Across Pangea During the Middle Triassic

The Middle Triassic was characterized by semi-arid to arid climates between ~40°N and S latitude, and wetter climates north and south of ~40° latitude, based on geologic evidence (Fig. 5) (Tucker and Benton, 1982, Parrish, 1993; Fawcett et al., 1994; Francis, 1994). Previous studies suggest that the monsoonal maximum occurred during the early Late Triassic on the Colorado Plateau in the western United States and possibly later in Australia (Dubiel et al., 1991; Parrish et al., 1996). More recently, studies of loessite-paleosol sequences from the Colorado Plateau region indicating alternations between dry windy conditions and humid conditions in the western equatorial region of Pangea may indicate the monsoon maximum began during the Early to Middle Triassic (Chan, 1999).

Inferred climate conditions, with respect to moisture, during the Middle Triassic appear to be controlled by the distance from coasts (Fig. 5). The wettest climate is interpreted to be closest to the coastlines, especially along southern Pangea. Semi-arid conditions are favored in central, southern Pangea, eastern Pangea, and for the Ischigualasto Basin, Argentina. In the mid-latitudes of the interior of Pangea (Argentina, Brazil, and South Africa), coeval coal, lacustrine, and fluvial deposits are common, typical of semi-arid to wet climates (Tucker and Benton, 1982). On the eastern side of Pangea, in India and much of Europe, the presence of calcisols indicate a seasonal

climate (Tucker and Benton, 1982; Mader, 1990, 1992; Bandyopadhyay and Sengupta, 1999), and is interpreted to be more arid than in the Ischigualasto Basin based on the presence of pedogenic carbonate that is lacking in Argentina during this time interval. The presence of calcisols and fluvial and lacustrine deposits in the Lower Keuper Fm across Europe indicates a semi-arid climate likely persisted (Mader, 1990, 1992a,b). Stable carbon isotopic analyses of Middle Triassic fossil plants from the Lower Keuper Fm in Germany yield $\delta^{13}C_{org}$ values ranging from –26.0 to -26.8 ‰ (Bocherens et al., 1993). Fossil plants from mesic environments typically have $\delta^{13}C_{org}$ values that range from –26.7 to –24.1‰ (Bocherens et al., 1993).

In Australia, between 40° and 70°S latitude during the Middle Triassic, red beds, *Dicrodium*-dominated flora, paleosols, coal swamps, and lacustrine deposits are thought to represent a cool, semi-arid climate, possibly seasonally wet (Retallack, 1977; Fawcett et al., 1994; Parrish et al., 1996). The $\delta^{13}C_{org}$ values of coals from the Molteno Fm in South Africa range from –24.0 to -24.4 ‰ (Faure et al., 1995). The range of values for the Ischigualasto Basin is comparable to those from the Molteno Fm, probably because they come from similar depositional environments and latitudes. These $\delta^{13}C_{org}$ values probably reflect water-stressed environmental conditions. Both the $\delta^{13}C_{org}$ values and paleobotanical studies of the thin coal beds of the Molteno Fm suggest the climate was warm, temperate, but with seasonal rainfall (Tucker and Benton, 1982). At a more southerly latitude (70°S), Middle Triassic non-calcareous, clay- and organic-rich paleosols of the Lashly Fm from Antarctica indicate a humid, temperate climate with evidence of seasonal rainfall (Retallack and Alonso-Zarza, 1998), but with cooler

temperatures than observed in South Africa in the Molteno Fm (Tucker and Benton, 1982). Growth rings in fossil wood, broadleaf plants, cones from conifer trees, and abscission scars of leaves from the Lashly Fm support this climatic interpretation (Retallack and Alonso-Zarza, 1998). The flora of the Lashly Fm is similar to those observed in the Ischichuca Fm and other localities on southern Pangea. *Dicrodium* are typical Gondwana flora found in Middle Triassic coals across southern Pangea (Retallack et al., 1996). Although freezing temperatures may have occurred at 70°S, there is no geologic evidence for perennial ice caps at either of the two poles during the Triassic (Retallack and Alonso-Zarza, 1998).

The abundance of lacustrine deposits, coals, non-calcareous paleosols, plants, and vertebrate fauna in the Southern Hemisphere does not agree with extreme temperature variations predicted by GCM sensitivity experiments (Tucker and Benton, 1982; Kutzbach and Gallimore, 1989; Wilson et al, 1994) because the climate is expected to be drier than observed in the geologic record in the interior of Pangea during this time interval. The paleotopographic effects on seasonality of rainfall in the southern hemisphere should be explored further.

11. Conclusions

1) The carbon isotopic values of terrestrial organic matter from the Ischichuca Fm range from –22.1 to –24.9‰. These values are typical of plants that live under environmental stress, especially water stress. The sedimentological and geochemical evidence supports a seasonally wet climate.

2) The climate of the Ischigualasto Basin is inferred to have been semi-arid to semi-humid during the Middle Triassic. The combination vertisols, coals, and lack of pedogenic carbonate in the paleosols suggests the mean annual precipitation in the Ischigualasto Basin was between 120-250 cm.

3) Most lithologic, geochemical, and paleontological evidence across southern Pangea suggest a warm to cool seasonal temperate climate. Extreme aridity in continental interiors predicted by GCMs is difficult to reconcile with the geologic evidence of temperate, not arid conditions, in the southern hemisphere.

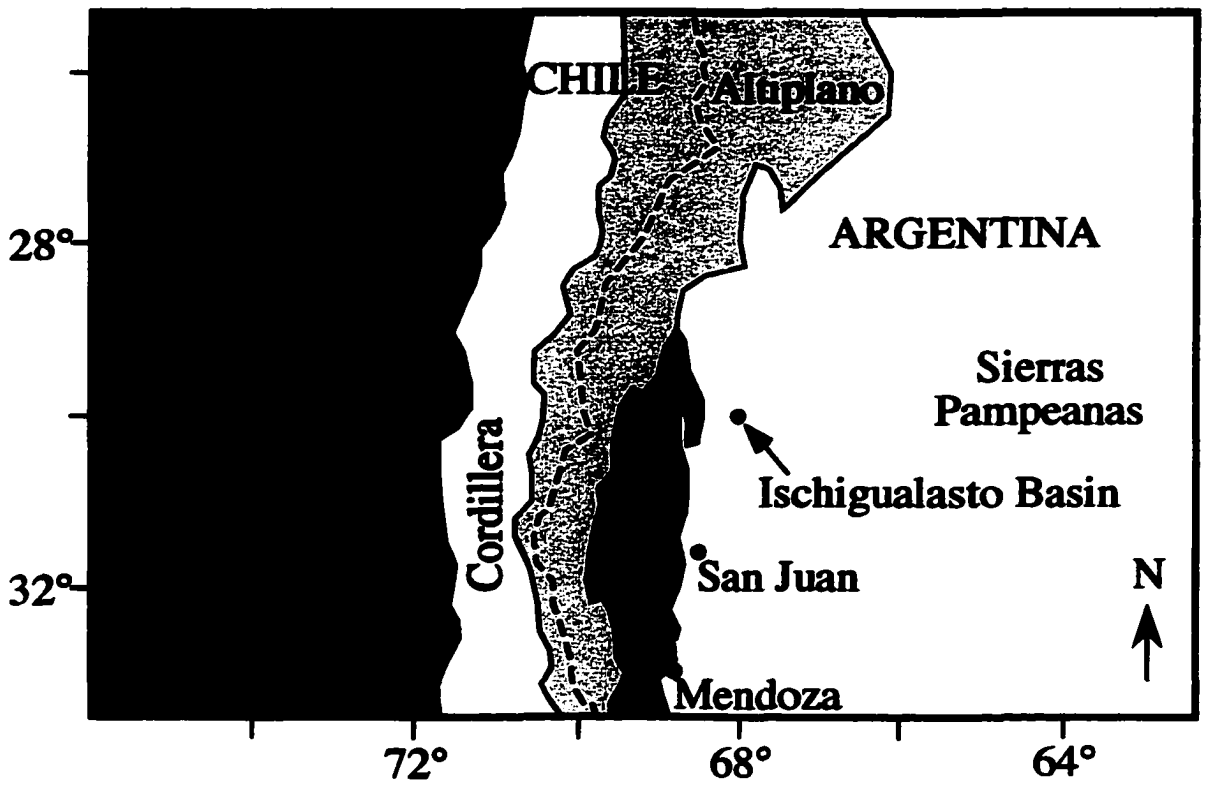

FIGURE C-1a. Tectonic provinces of South America between 26°and 33°S latitude and location of the Ischigualato Basin. The dashed line is the border between Chile and Argentina.

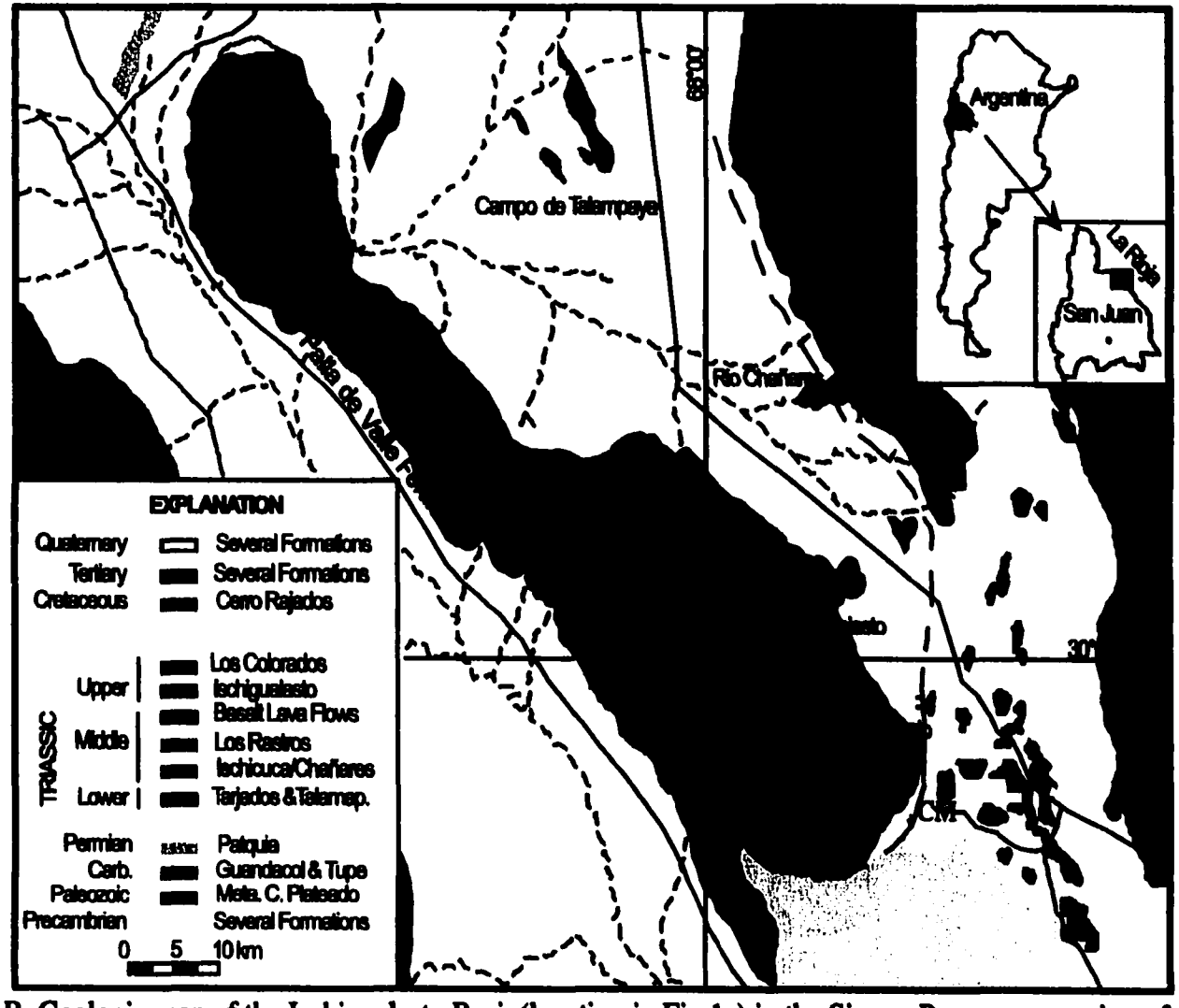

FIGURE C-1B. Geologic map of the Ischigualasto Basin(location in Fig 1a) in the Sierras Pampeanas region of NW Argentina (from Milana and Alcober, 1994). Measured sections are labeled on the map as follows: CP- Canon de la Pena, RM- Rio Marco, CM- Cerro Morado, and RG- Rio Gualo.

FIGURE C-3. Organic carbon concentrations, atomic C/N ratios, and organic $\delta^{13}C$ signatures of sediments from the Cañon de la Peña section. Decreased C/N ratios and $\delta^{13}C_{org}$ in Lake #2 may record a period of enhanced lake productivity in the lake. Lakes #1 and 2 have a higher proportion of terrestrial organic matter that washed into the lake system.

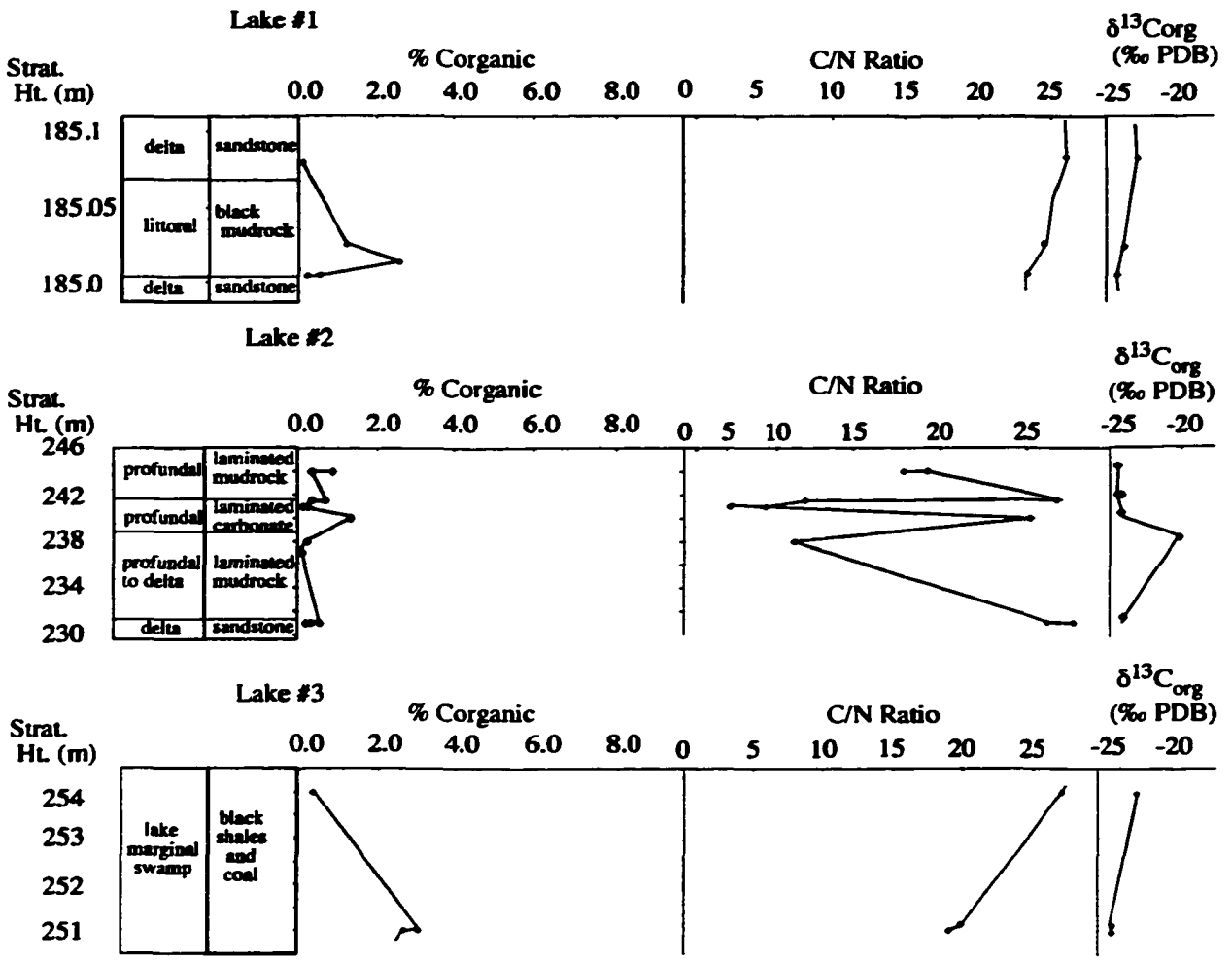

FIGURE C-3. Organic carbon concentrations, atomic C/N ratios, and organic $\delta^{13}C$ signatures of sediments from the Rio Marco section. A high proportion of terrestrial organic matter is found in the lacustrine sequences. Lake #2 has the highest proportion of organic matter because the sequence includes lake marginal swamps.

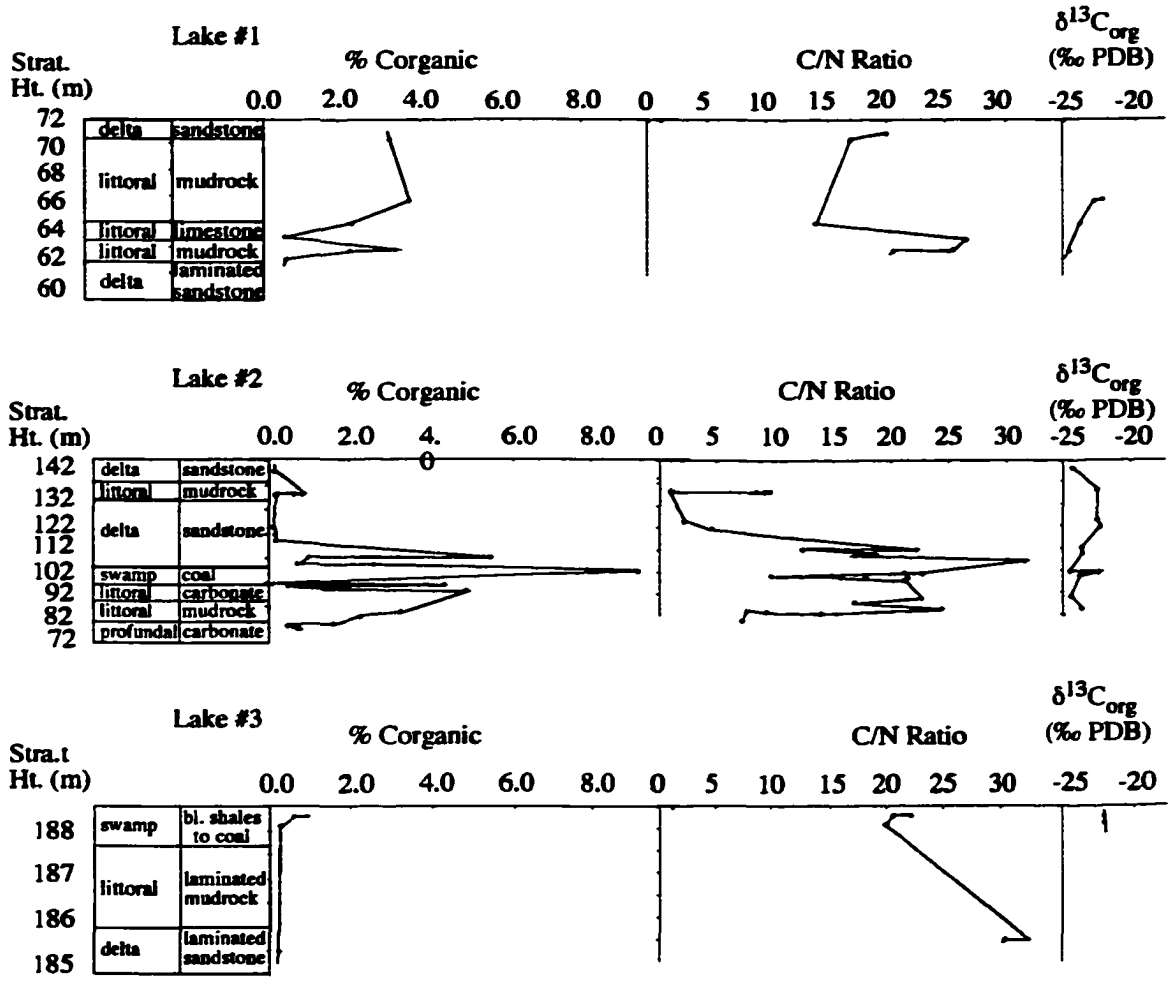

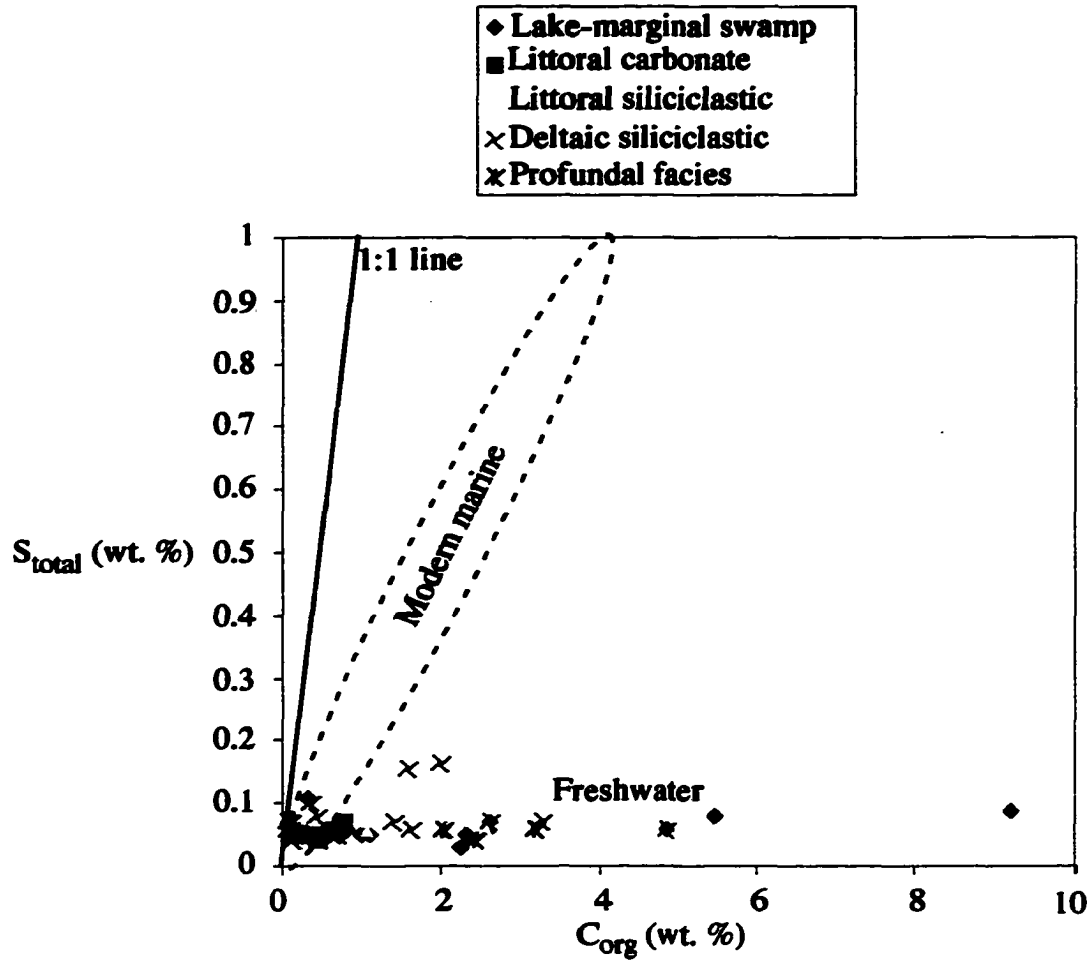

FIGURE C-4. Plot of weight percent organic carbon versus weight percent of total sulfur for Ischichuca Fm lacustrine rocks. The region enclosed by dashed lines indicates normal modern marine sediments after Berner and Raiswell (1984) and Leventhal (1995). Most non-marine environments have low sulfur content and variable amounts of organic carbon as indicated on the graph, but if anoxia is common in the lake, higher sulfur contents are expected. The two deltaic samples with higher S_{total} content reflect modern gypsum contaimination

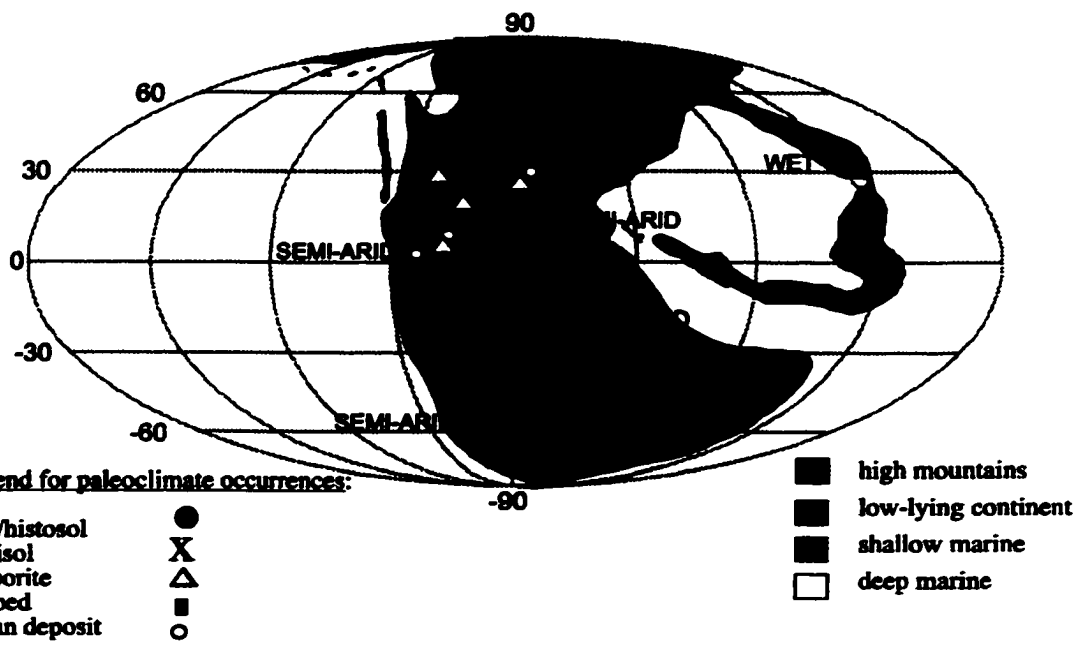

FIGURE C-5. Distribution of "raw" paleoclimate indicators during the Middle Triassic. Data is from Parrish and Peterson, 1988; Chan 1999; Golonka and Ford, 2000; Bandyopadhyay and Sengupta, 1999; Nyambe, 1999; Guerra-Sommer et al., 1999; Tucker and Benton, 1982; Gordon, 1975; Clemmensen, 1978; Mader 1992a, b; Francis, 1994; Fawcett, 1994; Parrish et al., 1996; Retallack 1977a,b; Retallack. and Alonso-Zarza, 1996; Veerers, 1994; Nalivkin, 1973; Clemmenson, 1979; Retallack et al., 1996; Taylor et al., 1989; Taylor and Taylor, 1993; Retallack and Ryburn, 1982; Retallack, 1980; Turner, 1999; Mader, 1990; and Stipanicic 1983; Base map created using PGIS /MAC (Scotese, 1997).

Works Cited

Anderson, T.F. and Arthur, M.A., 1983, Stable isotopes of oxygen and carbon and their application to sedimentologic and paleoenvironmental problems, *in* Stable Isotopes in Sedimentary Geology, SEPM Short Course No. 10, 1-151.

Arens, N.C., Jahren, A.H., and Amundson, R., 2000, Can C3 plants faithfully record the carbon isotopic composition of atmospheric carbon dioxide?, Paleobiology, 26, 1, 137-164.

Bandyopadhyay, S. and Sengupta, D.P., 1999, Middle Triassic vertebrates of India, Journal of African Earth Sciences, 29, 233-241.

Barron, E.J., 1990, Climate and lacustrine petroleum source prediction, *in* B.J. Katz (ed.), Lacustrine Basin Exploration: Case Studies and Modern Analogs, AAPG Memoir 50, 1-18.

Berner, R.A. and Raiswell, R., 1984, C/S method for distinguishing freshwater from marine sedimentary rocks, Geology, 12, 365-368.

Bocherens, H., Friis, E.M., Mariotti, and Pedersen, K.R., 1993, Carbon isotopic abundances in Mesozoic and Cenozoic fossil plants: palaeoecological implications, Lethaia 26, 347-358.

Bohacs, K.M., Carroll, A.R., Neal, J.E., and Mankiewicz, P.J., 2000, Lake-basin type, source potential, and hydrocarbon character: an integrated-sequence-stratigraphic framework, *in* E.H. Gierlowski-Kordesch and K.R. Kelts (eds.), Lake basins through space and time: AAPG Studies in Geology 46, 3-34.

Bonaparte, J.F., 1997, El Triasico de San Juan-La Rioja Argentina y sus Dinosaurios, Museo Argentino de Ciencias Naturales, Buenos Aires, Argentina, 196p.

Cerling, T.E., Wang, H., Quade, J., 1993, Expansion of C4 ecosystems as an indicator of global ecosystem change in the Miocene, Nature, 361, 344-346.

Cerling, T.E., 1994, Chemistry of closed basin lake waters: a comparison between African Rift Valley and some central North American rivers and lakes, *in* E. Gierlowski-Kordesch and K. Kelts, (eds.) Global geological record of lake basins,Volume 1, Cambridge University Press, Cambridge, United Kingdom., 29-30.

Chan, M.A., 1999, Triassic loessite of north-central Utah: stratigraphic, petrophysical character, and paleoclimatic implications, Journal of Sedimentary Research B, 69, 2, 477-485.

Clark, I. and Fritz, P., 1997, Environmental Isotopes in Hydrogeology, Lewis Publishers, New York, 327p.

Clayton, J. L. and Swetland, P. J., 1978, Subaerial weathering of sedimentary organic matter, Geochimica et Cosmochimica Acta, 42, 3, 305-315.

Clemmensen, L.B., 1978, Alternating aeolian, sabkha and shallow-lake deposits from the Middle Triassic Gipsdalen Formation, Scoresby Land, East Greeenland, Palaeogeography, Palaeoclimatology, Palaecology, 24, 111-135.

Crowley, T.J., 1994, Pangean climates, *in* Klein, GD (ed.) Pangea: Paleoclimate, Tectonics, and Sedimentation During Accretion, Zenith, and Breakup of a Supercontinent, GSA Special Paper 288, 25-39.

Deins, P., 1980, The isotopic composition of stable carbon isotopes *in* P. Fritz and J.C. Fontes, (eds.), Handbook of Environmental Isotope Geochemistry volume 1: The Terrestrial Environment, Elsevier, Amsterdam, 329-406.

Dubiel, R.F., Parrish, J.T., Parrish, J.M., and Good, S.C., 1991, The Pangean megamonsoon- Evidence from the Upper Triassic Chinle Foramtion, Colorado Plateau, Palaios, 6, 347-370.

Eugster, H.P., and Kelts, K., 1983, Lacustrine chemical sediments: *in*, Goudie, A.S., and Pye, K., (eds.), Chemical Sediments and Geomorphology: Precipitates and Residua in the Near-Surface Environment, Academic Press, New York, p. 321-368.

Faure, K. de Wit, M.J., and Willis, J.P., 1995, Late Permian global coal hiatus linked to ^{13}C-depleted CO_2 flux into the atmosphere during the final consolidation of Pangea, Geology, 23, 6, 507-510.

Fawcett, P.J., Barron, E.J., Robison, V.D., and Katz, B.J, 1994, The climatic evolution of India and Australia from the late Permain to mid-Jurassic: a comparison of climate model results with the geologic record, *in* G.D. Klein, (ed.), Pangea: Paleoclimate, Tectonics, and Sedimentation During Accretion, Zenith, and Breakup of a Supercontinent: Boulder, Colorado, Geological Society of America Special Paper 288, 139-157.

Francis, J.E., 1994, Palaeoclimates of Pangea – Geological Evidence, Pangea: Global Environments and Resources, Canadian Society of Petroleum Geologists, Memoir 17, 265-274.

Golonka, J., and Ford, D., 2000, Pangean (Late Carboniferous-Middle Jurassic) paleoenvironemnt and lithofacies, Palaeogeography, Palaeoclimatology, Palaecology, 161, 1-34.

Gordon, W.A., 1975, Distribution by latitude of Phanerozoic evaporite deposits, Journal of Geology, 83, 671-684.

Guerra-Sommer, M., Cazzulo-Klepzig, M., and Iannuzzi, R., 1999, The Triassic taphoflora of the Paraná Basin, southern Brazil: a biostratigraphical approach, Journal of African Earth Sciences, 29, 243-255.

Gyllenhaal, E.D., 1991, How accurately can paleoprecipitation and paleoclimate change be interpreted from subaerial disconformities? Ph.D. thesis. University of Chicago.

Hay, W.W, and Wold, C., 1998, The role of mountains and plateaus in a Triassic climate model, *in* T.J. Crowley and K.C. Burke (eds.), Tectonic Boundary Conditions for Climate Reconstructions, Oxford Monograph on Geology and Geophysics No 39, 116-146.

Huc, A.Y., 1988, Aspects of depositional processes of organic matter in sedimentary basins, Organic Geochemistry, 13, 263-272.

Jordan, T. E. and Allmendinger, R.W., 1986, The Sierras Pampeanas of Argentina; a modern analogue of Rocky Mountain foreland deformation, American Journal of Science, 286, 10, 737-764.

Katz, B.J., 1988, Clastic and carbonate lacustrine systems: an organic geochemical comparison (Green River Formation and East African lake sediments), *in* A.J. Fleet, K. Kelts, and M.R. Talbot (eds.), Lacustrine Petroleum Source Rocks, Geological Society of London Special Publication 40, 81-90.

Katz, B.J., 1990, Controls on the distribution of lacustrine source rocks through time and space, *in* B.J. Katz (ed.), Lacustrine Basin Exploration: Case Studies and Modern Analogs, AAPG Memoir 50, Tulsa Oklahoma, 61-76.

Kelts, K., 1988, Environments of deposition of lacustrine petroleum source rocks: an introduction, *in* A.J. Fleet, K. Kelts, and M.R. Talbot (eds.), Lacustrine Petroleum Source Rocks, Geological Society of London Special Publication 40, 3-26.

Krishnamurthy, R.V., Syrup, K, and Long, A., 1999, Is selective preservation of nitrogenous organic matter reflected in the $\delta^{13}C$ signal of lacustrine sediments? Chemical Geology, 158, 165-172.

Kutzbach, J.E., 1994, Idealized Pangean climates: sensitivity to orbital change, *in* Klein, G.D. (ed.), Pangea: Paleoclimate, Tectonics, and Sedimentation During Accretion, Zenith, and Breakup of a Supercontinent: Boulder, Colorado, Geological Society of America Special Paper 288, 41-55.

Kutzbach, J.E. and Gallimore, R.G., 1989, Pangean climates: Megamonsoons of the megacontinent: Journal of Geophysical Research, 94, 3341-3357.

Leventhal, J.S., 1995, Carbon-sulfur plots to show diagenetic and pigenetic sulfidization in sediments, Geochimica et Cosmochimica Acta, 59, 1207-1211.

López-Galamundi, O.R., Alvarrez, L., Andreis, R.R., Bossi, G.E., spejo, I., Seveso, F.F., Legarreta, L., Kokogian, D., Limarino, C.O., and Sessarego, H., 1989, Cuencas intermontanas, Cuencas Sedimentarias Argentinas 1989, p. 123-167.

McKenzie, J.A., 1985, Carbon isotopes and productivity in the lacustrine and marine environment: *in* W. Stumm, (ed.), Chemical Processes in Lakes, John Wiley & Sons. New York, NY, p. 99-118.

Mader, D., 1990, Palaeoecology of the flora in Buntsandstein and Keuper in the Triassic of Middle Europe; Volume 1, Buntsandstein, Gustav Fischer Verlag, Stuttgart, 936p.

Mader, D., 1992a, Evolution of Palaeocology and Palaeonvironment of Permian and Triassic Fluvial Basins in Europe, vol. 1 Western and Eastern Europe, Gustav Fischer Verlag, New York, 738p.

Mader, D., 1992b, Evolution of Palaeocology and Palaeonvironment of Permian and Triassic Fluvial Basins in Europe, vol. 2 Southeasterb Europe and Index, Gustav Fischer Verlag, New York, 602p.

Magaritz, M., Krishnamurthy, R.V., and Holser, W.T., 1992, Parallel trends in organic and inorganic carbon isotopes across the Permian/Triassic boundary, American Journal of Science, 292, 727-739.

May, C.L., 1998, Applying hierarchy theory to macroevolutionary questions: examples from the Ischigualasto-Villa Union Basin (Triassic; Northwest Argentina) Ph..D.Thesis. University of California, Berkeley.

Milana, J.P., 1993, Estratigrafía de eolianitas en la zona de Jáchal-Huaco, Precordillera de San Juan: Revista de la Asociación Argentina, 48, 283-298.

Milana, J.P., 1998, Anatomía de parasecuencias en un lago de rift y sus relación con la generación de hidrocarburos, Cuenca triásica de Ischigualasto, San Juan, Revista Asoción Geológica Argentina, 53, 3.

Meyers, P.A., 1994, Preservation of elemental and isotopic source identification of sedimentary organic matter, Chemical Geology, 144, 289-302.

Meyers, P.A., 1997, Organic geochemical proxies of paleoceanographic, paleeolimnologic, and paleoclimatic processes, Organic Geochemistry, 27, 213-250.

Meyers, P.A. and Eadie, B.J., 1993, Sources, degradation and recycling of organic matter associated with sinking particles in Lake Michigan. Organic Geochemistry. 20; 47-56.

Meyers, P.A. and Ischiwatari, R., 1993, Lacustrine organic geochemistry- an overview of indicators of organic matter sources and diagenesis in lake sediments, Organic Geochemistry, 20, 867-900.

Meyers, P.A. and Ischiwatari, R., 1995, Organic matter accumulation records in lake sediments, *in* A. Lerman, D. Imboden, and J. Gat, (eds.), Physics and Chemistry of Lakes, Springer, New York, 279-328.

Meyers, P.A. and Kowalski, E.A., 1994, Enhanced accumulation of continental organic matter in coastal sediments of northern Gondwana during the Late Triassic: evidence from the Wombat Plateau and the Carnarvon Basin, northwest Australia, and the Himalayas, Pangea: Global Environments and Resources, Canadian Society of Petroleum Geologists, Memoir 17, 439-448.

Nalivkin, D. V., Geology of the U.S.S.R, Edinburgh, 855 p.

Nyambe, I.A., 1999, Tectonic and climatic controls on sedimentation during deposition of the Sinakumbe Group and Karoo Supergroup, in the mid-Zambezi Valley Basin, southern Zambia, Journal of African Earth Sciences, 28, 443-463.

O'Leary, M.H., 1988, Carbon isotopes in photosynthesis. Bioscience 38, 328-336.

Parrish, J.T., 1993, Climate of the supercontinent Pangea, Journal of Geology, 101, 215-233.

Parrish, J.T., Bradshaw, M.T., Brakel, A.T., Mulholland, S.M., Totterdell, J.M, and Yeates, A.N., 1996, Paleoclimatology of Australia during the Pangean interval: Palaeoclimates- Data and Modelling, 1, 23-57.

Parrish, J.T., and Peterson, F., 1988, Wind directions predicted from global circulation models and wind directions determined from eolian sandstones of the western United States- a comparison, Sedimentary Geology, 56, 261-282.

Parrish, J.T., Ziegler, A.M., and Scotese, C.R., 1982, Rainfall patterns and the distributions of coals and evaporites in the Mesozoic and Cenozoic, Palaeogeography, Palaeoclimatology, Palaeoecology, 40, 67-101.

Reineck, H.E. and Singh, I.B., 1980, Depositional Sedimentary Environments, Springer-Verlag, New York, 549p.

Retallack, G.J., 1977a, Two new approaches for reconstructing fossil vegetation; with examples from the Triassic of eastern Australia. Journal of Paleontology. 51; 2, Suppl., Part III, 22.

Retallack, G.J., 1977b, Triassic palaeosols in the upper Narrabeen Group of New South Wales; Part II, Classification and reconstruction. Journal of the Geological Society of Australia. 24, Part 1; 19-36.

Retallack, G. J., 1980, Middle Triassic megafossil plants and trace fossils from Tank Gully, Canterbury, New Zealand, Journal of the Royal Society of New Zealand, 10, 1, 31-63.

Retallack, G.J., 1981, Middle Triassic megafossil plants form Long Gully, near Otematata, North Otago, New Zealand. Journal of the Royal Society of New Zealand. 11, 3, 167-200.

Retallack, G.J. and Alonso-Zarza, A.M., 1998, Middle Triassic paleosols and paleoclimate of Antarctica, Journal of Sedimentary Research, 68, 169-184.

Retallack, G. J. and Ryburn, R. J., 1982, Middle Triassic deltaic deposits in Long Gully, near Otematata, North Otago, New Zealand, Journal of the Royal Society of New Zealand, 12, 3, 207-227.

Robinson, P.L., 1973, Paleoclimatology and continental drift, in Tarling. D.H. and Runcorn, S.K. (eds.), Implications of Continental Drift to the Earth Sciences, 1 : London, Academic Press, 449-476.

Romer, A.S. and Jensen, J.A., 1966, The Chañares (Argentina), Triassic reptiles fauna XIX, Sketch of the geology of the Rio Chañares -Rio Gualo region, Breviora, 225, 1-20.

Stipanicic, P.N., 1983, The Triassic of Argentina and Chile, in Moullade, M. and A.E.M. Nairn (eds.), The Phanerozoic Geology of the World II, The Mesozoic, B, Elsevier: New York, 181-199.

Talbot, M.R., 1988, The origin of lacustrine oil source rocks: evidence from the lakes of tropical Africa, from Fleet, A.J., Kelts, K., and Talbot, M.R., (eds), Lacustrine Petroleum Source Rocks, Geological Society Special Publication No. 40, p. 29-43.

Talbot, M.R. and Allen, P.A., 1996, Lakes, *in* H.G. Reading, Sedimentary Environments: Processes, Facies and Stratigraphy, Blackwell Science, Oxford, p. 83-124.

Talbot, M.R. and Livingstone, D.A., 1989, Hydrogen indices and carbon isotopes of lacustrine organic matter as lake level indicators, Palaeogeography, Palaeoclimatology, Palaeocecology, 78, 185-193.

Taylor, G. H., Liu, S. Y., Diessel, and Claus, F. K., 1989, The cold-climate origin of inertinite-rich Gondwana coals, International Journal of Coal Geology, 11, 1, 1-22.

Tucker, M.E. and Benton, M.J., 1982, Triassic environments, climates and reptile evolution, Palaeogeography, Palaeoclimatology, Palaecology, 40, 361-179.

Uliana, M.A., Biddle, K.T., and Cerdan, J., 1989, Mesozoic extension and the formation of Argentine sedimentary basins, *in* A.J. Tankard and H.R. Balkwill, (eds.), Extensional Tectonics and Stratigraphy of the North Atlantic Margins, AAPG Memoir 46, 599-614.

Veerers, J.J., 1994, Pangea: evolution of a supercontinent and its consequence for Earth's paleoclimate and sedimentary environments, *in* Klein, G.D. (ed.), Pangea: Paleoclimate, Tectonics, and Sedimentation During Accretion, Zenith, and Breakup of a Supercontinent, Boulder, Colorado, Geological Society of America Special Paper 288, 13-23.

Webster, P.J., 1987, The elementary monsoon, *in* Fein J.S. and Stevens, P.L. Monsoons, John Wiley, New York, 3-32.

Wilson, K., Pollard, D., Hay, W.W., Thompson, S.L., and Wold, C.N., 1994, General circulation model simulations of Triassic climates: preliminary results, *in* Klein, G.D. (ed.), Pangea: Paleoclimate, Tectonics, and Sedimentation During Accretion, Zenith, and Breakup of a Supercontinent, Boulder, Colorado, Geological Society of America Special Paper 288, 91-116.

Zapata, T.R. and Allmendinger, R.W., 1996, Growth stratal records of instantaneous and progressive limb rotation in the Precordillera thrust belt and Bermejo basin, Argentina, Tectonics, 15, 5, 1065-1083.

APPENDIX D: SUPPLEMENTAL DATA

Table D-1. Bulk sample mineralogy in weight abundance from the southern region of the Ischigualasto Basin, NW Argentina. Stratigraphic height is measured from the base of each measured section. Standard deviation is ± 7%. Mineralogic abbreviations: Qtz = quartz; Clay = total amount of clay in sample; Plag = plagioclase feldspars; Kspar = potassium feldspars; Cte = calcite; Gyp = gypsum; Mica = muscovite and/or biotite; Clino = clinoptolite; Anal = analcime; Sid = siderite.

Cañon de la Peña

Sample	Lithology	Strat. Height (m)	Qtz	Clay	Plag	Kspar	Cte	Gyp	Mica	Clino	Anal	Sid
98-6-10A	mudrock	0	86	8	1	0	0	0	0	3	0	0
98-6-10C	silcrete layer	0	100	0	0	0	0	0	0	0	0	0
99-7-17C	silcrete layer	0	100	0	0	0	0	0	0	0	0	0
98-6-10D	sandy root matrix carbonate	1	11	0	1	0	88	0	0	0	0	0
98-6-12A	nodule	10.5	83	2	1	0	13	0	1			
98-6-12B	mudrock carbonate	10.75	76	20	3	0	0	0	1	0	0	0
98-6-12C	nodule shaley	10.8	40	3	1	0	56	0	0	0	0	0
98-6-12D	mudrock silicified	18	35	7	1	0	43	0	1	7	0	0
98-6-12E	claystone shaley	35	89	3	1	0	0	0	0	2	0	0
98-6-12F	mudrock silicified	35	88	9	1	0	0	0	0	0	0	0
99-7-17D	claystone shaley	38	96	2	2	0	0	0	0			
98-6-12G	mudrock	39.8	82	17	0	0	0	0	0	0	1	0

Sample	Lithology	Stratigraphic Height (m)	Quartz	Clay	Plag	Kspar	Calcite	Gypsum	Mica	Clino	Anal	Sid
	silicified									0	0	0
98-6-12H	claystone	54	84	10	2	0	0	0	1			
	shaley									0	0	0
98-6-12I	mudrock	58	87	10	2	0	0	0	1			
	shaley									0	0	0
98-6-12J	mudrock	65	769	17	3	0	0	0	1			
98-6-12K	sandstone	65.5	92	5	2	0	1	0	0	0	0	0
	silicified											
98-6-12L	claystone	69.5	58	4	1	1	33	0	0	3	0	0
	shaley											
99-7-17F	mudrock	70	85	8	1	0	6	0	0	0	0	0
99-7-17G	bentonite	70.5	9	3	0	0	87	0	0	0	0	0
99-7-17H	siltstone	71	86	5	4	0	5	0	0	0	0	0
99-7-18A	sandstone	80	93	0	3	0	3	0	0	0	0	0
99-7-18B	sandstone	101	92	0	2	0	6	0	0	0	0	0
99-7-18C	siltstone	102	95	0	4	0	1	0	0	0	0	0
99-7-18D	bentonite	113	69	26	2	2	0	1	0	0	0	0
99-7-18E	sandstone	123	95	0	0	0	0	0	5	0	0	0
99-7-18F	sandstone	135	98	0	2	0	0	0	0	0	0	0
98-6-13C	bentonite	141.5	90	9	0	1	0	0	0	0	0	0
	laminated									0	0	0
98-6-13D	claystone	141.6	85	14	0	1	0	0	0			
98-6-13E	bentonite	141.7	86	12	1	0	2	0	0	0	0	0
98-6-13F	sandstone	142	89	8	1	0	2	0	0	0	0	0
	laminated									0	0	0
99-7-19O	claystone	142	78	13	2	0	7	0	0			
99-7-19L	sandstone	165	94	0	2	0	4	0	0	0	0	0
99-7-19K	sandstone	170	96	0	3	0	1	0	0	0	0	0
99-7-18G	sandstone	172	58	0	2	0	40	0	0	0	0	0
98-6-14A	siltstone	185	82	11	3	0	2	0	1	0	0	0
99-7-18H	mudrock	185	86	13	1	0	0	0	0	0	0	0
99-7-19J	siltstone	185	70	28	1	0	0	0	1	0	0	0

Sample	Lithology	Stratigraphic Height (m)	Quartz	Clay	Plag	Kspar	Calcite	Gypsum	Mica	Clino	Anal	Sid
98-6-14B	sandstone	185.1	91	4	2	0	2	0	1	0	0	0
98-6-14C	siltstone	186	86	9	2	0	0	0	3	0	0	0
98-6-14D	sandstone	188	96	2	1	0	1	0	1	0	0	0
98-6-14E	siltstone	207.5	78	11	5	1	0	0	5	0	0	0
98-6-14F	sandstone	215	93	4	2	0	0	0	1	0	0	0
98-6-14G;	sandstone	215	49	45	6	9	0	0	0	0	0	0
098-6-14H	shale	215	71	26	2	1	0	0	0	0	0	0
98-6-14I	sandstone	215	92	3	2	0	0	0	3	0	0	0
98-6-14J	sandstone	216	88	4	4	0	0	0	4	0	0	0
98-6-14K	sandstone	221.5	91	3	3	1	0	0	3	0	0	0
98-6-14L	sandstone	229	84	11	1	0	4	0	0	0	0	0
99-7-19G	sandstone	231	85	0	3	0	12	0	0	0	0	0
99-7-19H	sandstone	231	96	0	0	0	4	0	0	0	0	0
99-7-19H1	shale	231	80	17	2	0	0	0	0	0	0	0
99-7-19I	mudstone	231	70	28	1	0	0	0	0	0	0	0
98-6-14M	shale	236	84	15	1	0	0	0	0	0	0	0
98-6-14N	shale	236.1	91	5	2	1	1	0	0	0	0	0
98-6-15A	shales laminated	237	93	6	1	0	0	0	0	0	0	0
98-6-15B	sandstone	237.1	88	11	1	0	0	0	0	0	0	0
98-6-15C	silty shale	238	73	10	3	0	14	0	0	0	0	0
98-6-15E	shale	240	91	8	1	0	0	0	0	0	0	0
99-7-19F	sandstone	240	98	0	2	0	0	0	0	0	0	0
99-7-19D	sandstone	241	84	3	1	0	13	0	0	0	0	0
99-7-19E	carbonate	241	21	2	0	0	76	0	0	0	0	0
98-6-15F	sandstone	241.5	87	4	3	1	5	0	0	0	0	0
99-7-19B	sandstone	244	92	3	3	0	2	0	0	0	0	0
99-7-19C	mudstone	244	91	7	3	0	0	0	0	0	0	0
98-6-15G	shale	245	92	6	2	0	0	0	0	0	0	0
99-7-19A	sandstone	245	79	1	3	0	17	0	0	0	0	0

Sample	Lithology	Stratigraphic Height (m)	Quartz	Clay	Plag	Kspar	Calcite	Gypsum	Mica	Clino	Anal	Sid
98-6-15H	sandstone	247	90	2	1	0	7	0	0	0	0	0
99-7-18K	bentonite	250.5	64	26	4	0	6	0	0	0	0	0
99-7-18K2	claystone	250.5	62	35	0	0	3	0	0	0	0	0
98-6-15I	shale	251	91	3	5	0	0	0	1	0	0	0
99-7-18J	bentonite	251	27	68	2	2	0	1	0	0	0	0
99-7-18L	shale	251	94	5	1	0	0	0	0	0	0	0
98-6-15J	shale	254	52	2	2	1	43	0	0	0	0	0

Rio Marco

Sample	Lithology	Stratigraphic Height (m)	Quartz	Clay	Plag	Kspar	Calcite	Gypsum	Mica	Clino	Anal	Sid
99-7-6A	silcrete	0	100	0	0	0	0	0	0	0	0	0
98-6-21A	silcrete silicified	0	100	0	0	0	0	0	0	0	0	0
98-6-21B	claystone	2	79	3	2	0	3	0	0	13	0	0
99-7-6B	mudrock	5	89	2	1	0	8	0	0	0	0	0
99-7-6C	bentonite	5.25	67	32	1	0	0	0	0	0	0	0
99-7-6D	bentonite silicified	5.5	98	2	0	0	0	0	0	0	0	0
99-7-6F	claystone	7.5	94	1	0	0	5	0	0	0	0	0
99-7-6G	bentonite	8	99	1	0	0	0	0	0	0	0	0
99-7-6H	sandstone	13	83	0	2	0	15	0	0	0	0	0
99-7-7A	siltstone	30.25	93	5	2	0	0	0	0	0	0	0
99-7-7B	sandstone	32	95	1	1	0	3	0	0	0	0	0
99-7-7D	sandstone	33.5	91	8	0	0	1	0	0	0	0	0
99-7-7E	sandstone	35	94	3	3	0	0	0	0	0	0	0
99-7-7F	sandstone	35.9	92	5	2	0	1	0	0	0	0	0
98-6-21C	sandstone	38	75	18	3	1	0	0	3	0	0	0
99-7-7G	sandstone	49.5	100	0	0	0	0	0	0	0	0	0

Sample	Lithology	Stratigraphic Height (m)	Quartz	Clay	Plag	Kspar	Calcite	Gypsum	Mica	Clino	Anal	Sid
99-7-7H	sandstone	49.5	98	0	1	0	1	0	0	0	0	0
99-7-7K	sandstone	61.25	89	6	4	0	0	0	1	0	0	0
99-7-7J	mudrock	61.9	69	28	3	0	0	0	0			
98-6-22B	mudrock	62	93	2	3	1	0	0	1	0	0	0
99-7-7I	limestone laminated	63	22	2	1	0	75	0	0	0	0	0
										0	0	0
98-6-22C	sandstone	63	91	2	3	3	0	0	1			
98-6-22D	sandstone faintly laminated	63.5	85	1	2	0	12	0	0	0	0	0
99-7-7L	mudstone laminated	64	69	29	2	0	0	0	0	0	0	0
99-7-7M	sandstone; laminated	64.8	92	4	3	0	1	0	0	0	0	0
99-7-7N	claystone oxidized	65.8	82	15	3	0	0	0	0	0	0	0
99-7-7O	claystone	65.9	82	14	4	0	0	0	0	0	0	0
99-7-7P	shale	70.5	90	9	1	0	0	0	0	0	0	0
99-7-7Q	bentonite laminated	70.6	5	55	0	1	13	26	0	0	0	0
98-6-22E	sandstone	72	74	8	1	0	17	0	0	0	0	0
99-7-8B	shale laminated	72.8	82	10	0	0	8	0	0	0	0	0
99-7-8A	carbonate	73	17	2	0	0	81	0	0	0	0	0
99-7-8C	shale laminated	73.8	84	10	0	0	6	0	0	0	0	0
99-7-8D	carbonate laminated	74.5	92	6	0	0	2	0	0	0	0	0
98-6-22F	sandstone laminated	75	91	3	1	0	5	0	0	0	0	0
98-6-23A	mudrock	79.8	51	3	2	1	43	0	0	0	0	0

Sample	Lithology	Stratigraphic Height (m)	Quartz	Clay	Plag	Kspar	Calcite	Gypsum	Mica	Clino	Anal	Sid
98-6-23C	laminated sandstone	80	69	30	1	0	0	0	0	0	0	0
98-6-23D	laminated mudrock	80.1	93	4	1	2	0	0	0	0	0	0
98-6-23E	laminated mudrock;	81	82	7	2	0	9	0	0	0	0	0
98-6-23F	laminated sandstone	83.2	95	2	2	0	0	0	1	0	0	0
98-6-23G	laminated sandstone	83.3	88	10	1	0	0	0	1	0	0	0
99-7-8E	laminated mudstone	88.5	85	12	3	0	0	0	0	0	0	0
98-6-23H	laminated sandy shale	88.6	87	10	1	1	0	0	1	0	0	0
98-6-23I	sandstone	89	75	2	2	0	21	0	0	0	0	0
99-7-8F	laminated sandstone	89.4	85	13	2	0	0	0	0	0	0	0
99-7-8G	laminated carbonate	90.3	36	4	0	0	60	0	0	0	0	0
99-7-8H	laminated carbonate	90.4	18	1	0	0	81	0	0		0	0
99-7-8I	sandstone	91.2	90	0	0	2	7	0	0	0	0	0
99-7-8J	peat	91.3	72	27	1	0	0	0	0	0	0	0
99-7-8K	sandstone	95.4	95	2	3	0	0	0	0	0	0	0
098-6-23J	sandstone	96	95	4	1	0	0	0	0	0	0	0
98-6-23K	shale	96.5	88	10	1	1	0	0	0	0	0	0
98-6-23L	sandstone	99.5	94	1	5	0	0	0	0	0	0	0
98-6-23M	silty shale	99.6	93	5	2	0	0	0	0	0	0	0
99-7-8L	sandstone	100	92	2	6	0	0	0	0	0	0	0
99-7-8M	peat	102.4	88	7	4	1	0	0	0	0	0	0
99-7-8N	sandstone	109.3	94	1	3	0	1	0	0	0	0	0

Sample	Lithology	Stratigraphic Height (m)	Quartz	Clay	Plag	Kspar	Calcite	Gypsum	Mica	Clino	Anal	Sid
99-7-8P	sandstone	115	94	2	4	0	1	0	0	0	0	0
98-6-23N	sandstone laminated	115	94	2	4	0	0	0	0	0	0	0
98-6-24C	sandstone faintly laminated	125	88	3	4	2	3	0	0	0	0	0
98-6-24B	siltstone laminated	127	82	12	5	0	0	0	1	0	0	0
99-7-8R	mudstone	128.5	84	13	3	0	0	0	0	0	0	0
99-7-8S	sandstone laminated	128.6	92	4	4	0	0	0	0	0	0	0
99-7-8V	mudstone	133	81	13	5	1	0	0	0	0	0	0
99-7-8U	sandstone laminated	138	91	6	3	0	0	0	0	0	0	0
99-7-9A	sandstone	142.5	88	5	6	1	0	0	0	0	0	0
99-7-9B	sandstone laminated	143.2	94	2	4	0	0	0	0	0	0	0
99-7-9C	sandstone laminated	143.5	86	11	3	0	0	0	0	0	0	0
99-7-9D	sandstone	147.5	93	5	2	0	0	0	0	0	0	0
99-7-9E	siltstone	147.6	76	21	3	0	0	0	0	0	0	0
099-7-9F	sandstone	148.2	85	1	3	1	10	0	0	0	0	0
99-7-9G	bentonite laminated	148.4	78	19	3	0	0	0	0	0	0	0
99-7-9H	sandstone laminated	155	49	2	2	0	47	0	0	0	0	0
99-7-9I	siltstone	155.1	81	15	3	1	0	0	0	0	0	0
99-7-9J	sandstone	162	88	9	3	0	0	0	0	0	0	0
99-7-9K	siltstone laminated	162.2	74	23	3	0	0	0	0	0	0	0
99-7-9L	sandstone	173.2	94	1	3	2	0	0	0	0	0	0
99-7-9N	mudstone	174.8	75	22	3	0	0	0	0	0	0	0

Sample	Lithology	Stratigraphic Height (m)	Quartz	Clay	Plag	Kspar	Calcite	Gypsum	Mica	Clino	Anal	Sid
99-7-9O	sandstone	178	92	0	0	3	4	0	0	0	0	0
99-7-9P	sandstone	179.5	82	1	2	0	15	0	0	0	0	0
98-6-24D	sandstone	180.2	90	1	4	0	5	0	0	0	0	0
98-6-24E	sandstone	182	96	1	3	0	0	0	0	0	0	0
98-6-24F	shale	182.4	95	4	1	0	0	0	0	0	0	0
99-7-4J	sandstone	185.5	92	3	3	2	0	0	0	0	0	0
99-7-10F	mudstone	185.5	82	13	4	1	0	0	0	0	0	0
99-7-4L	bentonite	187	12	84	0	2	3	0	1	0	0	0
99-7-10A	sandstone	187.8	94	1	3	2	0	0	0	0	0	0
99-7-10B	sandstone	187.8	94	1	4	1	0	0	0	0	0	0
99-7-10E	bentonite	187.9	1	13	0	0	86	0	0	0	0	0
99-7-4M	bentonite laminated	188	47	45	5	3	0	0	0	0	0	0
99-7-10G	mudstone	188.1	46	54	0	0	0	0	0	0	0	0
99-7-10H	sandstone	188.2	48	52	0	0	0	0	0	0	0	0
99-7-4K	mudstone laminated	188.3	78	20	1	1	0	0	0	0	0	0
98-6-22A	sandstone	189	81	0	1	0	18	0	0	0	0	0
98-6-24A	sandstone	190	77	15	4	4	0	0	0	0	0	0

Cerro Morado

Sample	Lithology	Stratigraphic Height (m)	Quartz	Clay	Plag	Kspar	Calcite	Gypsum	Mica	Clino	Anal
99-7-1A	silicified wood	0	100	0	0	0	0	0	0	0	0
99-7-1B	silicified wood	0	100	0	0	0	0	0	0	0	0
99-7-1C	sillicified roots	0	100	0	0	0	0	0	0	0	0
99-7-1E	silcrete	0	100	0	0	0	0	0	0	0	0
99-7-1F	silcrete	0	100	0	0	0	0	0	0	0	0
98-6-19A	silcrete	0	100	0	0	0	0	0	0	0	0

Sample	Lithology	Stratigraphic Height (m)	Quartz	Clay	Plag	Kspar	Calcite	Gypsum	Mica	Clino	Anal
99-7-2A	mudrock	3.9	72	11	3	0	14	0	0	0	0
98-6-19B	mudrock shaley	6	87	6	4	0	0	0	0	0	0
99-7-2B	mudrock	8.9	82	15	2	0	1	0	0	0	0
99-7-2C	mudrock	13.3	82	17	1	0	0	0	0	0	0
99-7-2D	mudrock	16.6	84	15	1	0	0	0	0	0	0
99-7-2E	mudrock	22	28	3	0	0	69	0	0	0	0
99-7-2F	mudrock	24.1	84	15	1	0	0	0	0	0	0
99-7-2G	mudrock	25.6	20	4	1	0	75	0	0	0	0
99-7-2H	mudrock;	27.8	17	2	0	0	81	0	0	0	0
98-6-19C	bentonite shaley	31	87	10	1	0	2	0	0	0	0
99-7-2I	mudrock	31.6	79	20	0	0	1	0	0	0	0
99-7-2L	bentonite	34.9	95	5	0	0	0	0	0	0	0
99-7-2M	bentonite	35.1	97	3	0	0	0	0	0	0	0
99-7-2K	mudrock	35.8	28	1	0	0	71	0	0	0	0
99-7-4A	bentonite	36.7	95	5	0	0	0	0	0	0	0
99-7-4C	bentonite	37.3	99	1	0	0	0	0	0	0	0
99-7-4D	bentonite	38.8	99	1	0	0	0	0	0	0	0
99-7-4F	siltstone	44.6	95	2	3	0	0	0	0	0	0
99-7-4G	sandstone	47.1	97	2	1	0	0	0	0	0	0

Rio Gualo

Sample	Lithology	Strat. Height (m)	Quartz	Clay	Plag	Kspar	Calcite	Gypsum	Mica	Clino	Anal
Sample 1	silcrete	0	100	0	0	0	0	0	0	0	0
Sample 2	mudrock	4.5	21	2	0	0	77	0	0	0	0
Sample 3	mudrock	5.25	83	14	1	0	2	0	0	0	0
Sample 4	concretion	5.5	19	3	0	0	78	0	0	0	0
Sample 5	mudrock	9	86	14	0	0	0	0	0	0	0
Top Bentonite	bentonite	16.5	91	1	0	0	8	0	0	0	0
Sample 6	mudrock	17	86	13	1	0	0	0	0	0	0
Sample 7	mudrock	18.4	86	12	0	0	1	0	0	0	0

Table D-2. Size-fractionated (< 0.5μm) clay mineralogy from the southern region of the Ischigualasto Basin, NW Argentina based on NEWMOD © and PLOTMOD© modeling of ethylene gylcolated samples. Standard deviations are <5%. Stratigraphic height is measured from the base of each measured section. Mont = montmorillonite; Kaol = kaolinite; Chl = chlorite; C/S= mixed-layered chlorite-smectite, 60% chlorite and Reichweite (R) is 1; Ill = illite; I/S = mixed-layered illite-smectite. Right-hand column indicates the R and the percent illite in I/S.

Cañon de la Peña

Sample	Lithology	Strat. Ht.	Mont	Kaol	Chl	Ill	C/S 60%,R1	I/S	70%Il/S R1	80%Il/S R1
98-6-10A	mudrock	0	0	0	5	95	0	0		
98-6-12B	mudrock	10.75	0	3	0	97	0	0		
98-6-12D	mudrock	18	0	0	0	100	0	0		
98-6-12E	claystone	35	0	3	1	26	0	70		X
98-6-12F	mudrock	35	0	0	0	0	0	100		X
99-7-17D	claystone	38	0	2	0	98	0	0		
98-6-12G	mudrock	39.8	0	0	0	40	0	60	X	
99-7-17E	claystone	40	100	0	0	0	0	0		
9-06-12H	claystone	54	0	0	0	80	20	0		
98-6-12I	mudrock	58	0	0	5	55	0	40	X	
98-6-12J	mudrock	65	0	2	0	60	0	40	X	
98-6-12K	sandstone	65.5	0	0	10	90	0	0		
99-7-17F	mudrock	70	100	0	0	0	0	0		
99-7-17H	siltstone	71	0	10	0	90	0	0		
99-7-18C	siltstone	102	0	0	0	0	12	88	X	
99-7-18D	bentonite	113	0	0	0	0	30	70	X	
98-6-13C	bentonite	141.5	0	0	0	0	0	100		X
98-6-13D	claystone	141.6	0	0	0	0	0	100		X
98-6-13E	bentonite	141.7	0	0	2	0	0	98	X	
99-7-19O	claystone	142	0	0	0	0	0	100		X
99-7-19P	bentonite	142	0	0	0	0	0	100		X

Cañon de la Peña (cont'd)

Sample	Lithology	Strat. Ht.	Mont	Kaol	Chl	Ill	C/S 60%,R1	I/S	70%Il/S R1	80%Il/S R1
98-6-14A	siltstone	185	0	10	5	65	0	0		
99-7-18H	mudrock	185	0	10	0	55	5	30	X	
99-7-18I	sandstone	185	0	10	0	55	5	30	X	
99-7-19J	siltstone	185	0	10	0	90	0	0		
98-6-14B	sandstone	185.1	70	10	0	20	0	0		
98-6-14C	siltstone	186	0	2	3	80	0	15		
98-6-14E	siltstone	207.5	0	5	0	60	5	30	X	
98-6-14F	sandstone	215	0	2	0	95	3	0		
98-6-14G	sandstone	215	0	50	0	0	0	50	X	
98-6-14H	sandstone	215	0	20	0	0	10	70	X	
98-6-14I	sandstone	215	0	35	0	20	5	40	X	
98-6-14J	sandstone	216	0	15	0	20	5	60	X	
98-6-14K	sandstone	221.5	0	10	5	75	0	60	X	
98-6-14L	sandstone	229	0	10	0	0	5	85	X	
99-7-19H	sandstone	231	0	40	0	60	0	0		
99-7-19H1	shale	231	0	0	0	0	0	100	X	
99-7-19I	mudrock	231	0	0	0	0	0	100	X	
98-6-15B	sandstone	237.1	0	10	0	0	5	85	X	
98-6-15C	silty shale	238	0	2	0	0	3	95	X	
98-6-15E	shale	240	0	10	5	80	5	0		
99-7-19D	sandstone	241	0	10	0	10	0	80	X	
99-7-19E	carbonate	241	0	0	0	0	0	100	X	
98-6-15F	sandstone	241.5	0	10	5	40	5	40	X	
99-7-19B	sandstone	244	0	20	0	80	0	0		
99-7-19C	mudrock	244	0	15	0	35	10	40	X	
98-6-15G	shale	245	0	25	0	10	5	60	X	

Cañon de la Peña (cont'd)

Sample	Lithology	Strat. Ht.	Mont	Kaol	Chl	Ill	C/S 60%,R1	I/S	70%II/S R1	80%II/S R1
98-6-15H	sandstone	247	0	65	0	20	5	10	X	
99-7-18K	bentonite	250.5	0	0	0	0	0	100	X	
99-7-18K2	claystone	250.5	0	0	0	0	0	100	X	
98-6-15I	shale	251	0	25	0	70	5	0		
99-7-18L	shale	251	0	10	0	25	10	55	X	
98-6-15J	shale	254	0	35	0	60	5	0		

Roadcut

Sample	Lithology	Strat. Ht.	Mont	Kaol	Chl	Ill	C/S 60%,R1	I/S	70%II/S R1	80%II/S R1
99-07-13A	NA	bentonite	0	2	0	0	0	98	X	
99-07-13B	NA	shale	0	4	0	96	0	0		

Rio Marco

Sample	Lithology	Strat. Ht.	Mont	Kaol	Chl	Ill	C/S 60%,R1	I/S	70%II/S R1	80%II/S R1
98-6-21B	claystone	2	100	0	0	0	0	0		
99-7-7A	siltstone	30.25	0	20	0	50	0	30	X	
99-7-7D	sandstone	33.5	0	40	0	60	0	0		

Rio Marco (cont'd)

Sample	Lithology	Strat. Ht.	Mont	Kaol	Chl	Ill	C/S 60%,R1	I/S	70%II/S R1	80%II/S R1
98-6-21C	sandstone	38	0	20	0	45	5	30	X	
99-7-7H	sandstone	49.5	0	90	0	10	0	0		
99-7-7K	sandstone	61.25	0	20	0	0	0	80	X	
99-7-7J	mudrock	61.9	0	3	0	0	0	97	X	
98-6-22B	mudrock	62	0	9	0	90	1	0		
99-7-7I	limestone	63	0	40	0	0	30	30	X	
98-6-22C	sandstone	63	0	40	0	5	5	50	X	
98-6-22D	sandstone	63.5	0	60	0	30	10	0		
99-7-7L	mudrock	64	0	20	0	0	0	80	X	
99-7-7M	sandstone	64.8	0	80	0	20	0	0		
99-7-7N	claystone	65.8	0	80	0	20	0	0		
99-7-7P	shale	70.5	0	5	0	0	0	95	X	
98-6-22E	sandstone	72	0	0	0	0	10	90	X	
99-7-8B	shale	72.8	0	0	0	0	20	80	X	
99-7-8A	carbonate	73	0	0	0	0	0	100	X	
99-7-8C	shale	73.8	0	0	0	0	0	100	X	
99-7-8D	carbonate	74.5	0	0	0	0	10	90	X	
98-6-23B	mudrock	79.9	0	30	0	60	10	0		
98-6-23C	sandstone	80	0	35	0	30	5	30	X	
98-6-23D	mudrock	80.1	0	30	0	30	5	35	X	
98-6-23E	mudrock	81	0	0	35	35	0	35	X	
98-6-23F	sandstone	83.2	0	0	30	40	0	30	X	
98-6-23G	sandstone	83.3	0	50	0	20	10	20	X	
99-7-8E	mudstone	88.5	0	30	0	8	2	60	X	
98-6-23H	sandstone	88.6	0	80	0	20	0	0		
98-6-23I	sandstone	89	0	55	0	10	5	30	X	

Rio Marco (cont'd)

Sample	Lithology	Strat. Ht.	Mont	Kaol	Chl	Ill	C/S 60%,R1	I/S	70%Ill/S R1	80%Ill/S R1
99-7-8F	sandstone	89.4	0	30	0	0	10	60	X	
99-7-8G	carbonate	90.3	0	5	0	0	5	90	X	
99-7-8H	carbonate	90.4	0	0	0	0	5	95	X	
99-7-8I	sandstone	91.2	0	100	0	0	0	0		
99-7-8J	coal	91.3	0	40	0	0	0	60	X	
98-6-23J	sandstone	96	0	55	0	10	5	30	X	
98-6-23L	sandstone	99.5	0	55	0	10	5	30	X	
98-6-23M	silty shale	99.6	0	20	0	80	0	0		
99-7-8M	coal	102.4	0	0	0	0	5	95	X	
99-7-8P	sandstone	115	0	40	0	0	0	60	X	
98-6-23N	sandstone	115	0	30	0	30	5	35	X	
98-6-24C	sandstone	125	0	50	0	20	5	25	X	
99-7-8R	mudrock	128.5	0	40	0	0	0	60	X	
99-7-8S	sandstone	128.6	0	40	0	0	0	60	X	
99-7-8T	sandstone	128.6	0	50	0	0	0	50	X	
99-7-8V	mudrock	133	0	15	0	0	1	84	X	
99-7-8U	sandstone	138	0	20	0	0	0	80	X	
99-7-9F	sandstone	148.2	0	60	0	0	0	40	X	
98-6-24D	sandstone	180.2	0	65	0	0	5	10	X	
98-6-24E	sandstone	182	0	35	0	63	2	0		
99-7-10F	mudrock	185.5	0	20	0	0	0	80	X	
99-7-10G	mudstone	188.1	0	0	0	0	0	100	X	
99-7-10H	sandstone	188.2	0	0	0	0	0	100	X	
99-7-4K	mudstone	188.3	0	4	0	0	0	96	X	

Cerro Morado

Sample	Lithology	Strat. Ht.	Mont	Kaol	Chl	Ill	C/S 60%,R1	I/S	70%II/S R1	80%II/S R1
99-07-02A	3.9	mudrock	100	0	0	0	0	0		
98-06-19B	6	mudrock	100	0	0	0	0	0		
99-07-02B	8.9	mudrock	100	0	0	0	0	0		
99-07-02C	13.3	mudrock	100	0	0	0	0	0		
99-07-02D	16.6	mudrock	100	0	0	0	0	0		
99-07-02E	22	mudrock	100	0	0	0	0	0		
99-07-02F	24.1	mudrock	100	0	0	0	0	0		
99-07-02G	25.6	mudrock	100	0	0	0	0	0		
99-07-02H	27.8	mudrock	100	0	0	0	0	0		
98-06-19C	31	bentonite	95	3	0	0	2	0		
99-07-02I	31.6	mudrock	100	0	0	0	0	0		
99-07-02J	35.5	mudrock	100	0	0	0	0	0		
99-07-02K	35.8	mudrock	90	0	10	0	0	0		
99-07-02L	34.9	bentonite	90	0	10	0	0	0		
99-07-02M	35.1	bentonite	95	5	0	0	0	0		
99-07-04A	36.7	bentonite	55	45	0	0	0	0		
99-07-04B	37.1	bentonite	55	45	0	0	0	0		
99-07-04C	37.3	bentonite	55	45	0	0	0	0		
99-07-04D	38.8	bentonite	55	45	0	0	0	0		
99-07-04E	39.2	bentonite	55	45	0	0	0	0		
99-07-04G	47.1	siltstone	98	2	0	0	0	0		

Rio Gualo

Sample	Lithology	Strat. Ht.	Mont	Kaol	Chl	Ill	C/S 60%,R1	I/S	70%Ill/S R1	80%Ill/S R1
Sample 2	4.5	mudrock	98	2	0	0	0	0		
Sample 3	5.25	mudrock	100	0	0	0	0	0		
Sample 4	5.5	concretion	100	0	0	0	0	0		
Sample 5	9	mudrock	100	0	0	0	0	0		
Lowermost Bentonite	10.75	bentonite	0	5	0	15	80	0		
Bottom Bentonite	15.25	bentonite	98	2	0	0	0	0		
Middle Bentonite	15.8	bentonite	97	3	0	0	0	0		
Top Bentonite	16.5	bentonite	96	4	0	0	0	0		
T	17	mudrock	98	2	0	0	0	0		
BAP	18	mudrock	100	0	0	0	0	0		

Table D-3. Organic geochemical analyses of lacustrine samples from the southern region of the Ischigualasto Basin, NW Arge TC= total carbon in wt. percent; TOC= total organic carbon in wt. percent; TS= total sulfur in wt. percent.

Sample	Lithology	Strat Sect	Strat Ht (m)	Facies	TC	TOC	TS	%Corg	C/N	d13Corg
99-07-02A WR	mudrock	C Morado	3.9	paleosol	0.42	0.07	0.05	0.02	0.51	
99-07-02I WR	mudrock	C Morado	31.6	paleosol	0.03	0.12	0.04	0.03	0.78	
99-07-18C WR	green silstone	C Pena	102	fluvial	0.15	0.09	0.05	0.03	10.10	-17.73
98-06-14A WR	black mudstone	C Pena	185	lake	2.50	2.53	0.06	2.62	22.66	-23.31
99-07-18H WR	black mudstone	C Pena	185	lake	0.10	0.19	0.05	0.10	1.23	-24.74
99-07-19J WR	black mudstone	C Pena	185	lake	0.15	0.17	0.05	0.17	1.29	
98-06-14B WR	ss	C Pena	185.1	prodelta	0.15	0.17	0.05	0.17	1.29	-23.90
98-06-14F WR	siltstone	C Pena	215	prodelta	0.15	0.17	0.05	0.17	1.29	-23.30
99-07-19H WR	sandstone	C Pena	231	fluvial	0.15	0.05	0.05			
99-07-19H WR	sandstone	C Pena	231	lake	0.12	0.05	0.05			
99-07-19H1 WR	black shale	C Pena	231	lake	0.31	0.41	0.05	0.34	4.61	
99-07-19I WR	black mudstone	C Pena	231	lake	0.14	0.20	0.06	0.18	1.27	-23.03
98-06-15A WR	laminated mudrock	C Pena	237	lake	0.15	0.18	0.05			
98-06-15C WR	laminated carbonate	C Pena	238	lake	4.27	0.33	0.07	0.32	6.40	-18.50
98-06-15E WR	claystone	C Pena	240	lake	2.17	2.04	0.06	1.45	20.20	-24.27
99-07-19D	laminated claystone	C Pena	241	lake	0.67	0.34	0.05	0.20	4.76	
99-07-19E WR	laminated carbonate	C Pena	241	lake	4.44	0.20	0.07	0.17	1.91	
98-06-15F dark	sandstone	C Pena	241.5	prodelta	1.00	0.72	0.05	0.25	21.88	-24.13
98-06-15F light	laminated sandstone	C Pena	241.5	prodelta	0.79	0.35	0.1	0.31	7.07	-24.00
99-07-19B	sandstone	C Pena	244	prodelta	0.46	0.42	0.08	0.44	11.60	-23.25
99-07-19C WR	black mudstone	C Pena	244	lake	1.04	1.11	0.05	1.00	12.72	
98-06-15I WR	laminated claystone	C Pena	251	lake	2.53	2.44	0.04	2.66	19.97	
99-07-18L WR	black shale	C Pena	251	lake	2.64	2.62	0.06	2.81	18.80	-24.35
98-06-15J	black mudstone	C Pena	254	lake	1.78	0.32	0.11	5.51	25.90	-23.49
Sample 3	mudrock	R Gualo	5.25	marginal	0.12	0.10	0.05	0.04	0.66	-24.07
9m	mudrock	R Gualo	9	marginal	0.07	0.06	0.06	0.01	0.32	
T WR	mudrock	R Gualo	18.4	marginal	0.07	0.09	0.07	0.03	0.85	-22.12
99-07-07D WR	green f. gr. Ss	Rio Marco	33.5	fluvial	0.07	0.09	0.04	0.08	2.85	

Sample	Lithology	Strat Sect	Strat Ht (m)	Facies	TC	TOC	TS	%Corg	C/N	d13Corg
99-07-07E WR	green sandstone	Rio Marco	35	fluvial	0.05	0.14	0.05	0.05	4.06	
99-07-07K WR	green sandstone	Rio Marco	61.25	lake	0.46	0.45	0.05			
99-07-07J WR	black mudstone	Rio Marco	61.9	lake	1.99	2.03	0.04	2.19		-24.31
98-06-22B WR	black mudstone	Rio Marco	62	lake	3.07	2.93	0.05	3.32	24.72	
99-07-07I WR	limestone	Rio Marco	63	lake	11.19	0.29	0.05			
99-07-07L WR	mudstone	Rio Marco	64	lake	2.02	2.04	0.05	1.95	14.22	-24.08
99-07-07N WR	laminated claystone	Rio Marco	65.8	lake	3.09	3.19	0.06			-23.70
99-07-07O WR	laminated claystone	Rio Marco	65.9	lake	3.09	3.19	0.06			-22.86
99-07-07P WR	shale	Rio Marco	70.5	lake	2.02	2.31	0.05	2.03	16.93	
99-07-17H WR	red siltstone	Rio Marco	71	fluvial	0.10	0.05	0.06	0.01	0.59	
99-07-08B WR	shale	Rio Marco	72.8	lake	0.78	0.82	0.06	0.04	0.81	
99-07-08A WR	laminated carbonate	Rio Marco	73	lake	3.10	0.47	0.04	0.72	14.03	
99-07-08C WR	laminated carbonate	Rio Marco	73.8	lakae	0.93	0.65	0.06	0.46	9.46	
99-07-08D WR	carbonate	Rio Marco	74.5	lake	0.46	0.41	0.05	0.29	7.73	-23.62
98-06-22F WR	laminated sandstone	Rio Marco	75	prodelta	1.75	1.62	0.06	1.81	24.51	
99-07-07P WR	shale	Rio Marco	78.5	lake	2.05	2.25	0.03	2.03	16.93	
98-06-23C WR	laminated sandstone	Rio Marco	80	prodelta	3.25	3.27	0.07	3.38	22.69	-24.39
98-06-23H WR	shale	Rio Marco	88.6	prodelta	4.98	4.87	0.06	4.46	21.27	
99-07-08F lower	fine gr. lam. sandstone	Rio Marco	89.4	prodelta	1.34	1.41	0.07	1.52	15.66	-23.73
99-07-08F middle	fine gr. lam. sandstone	Rio Marco	89.4	prodelta	2.33	2.00	0.43	2.32	21.53	
99-07-08F top	fine gr. lam. sandstone	Rio Marco	89.4	prodelta	1.90	1.61	0.31	1.19	17.90	
99-07-08G WR	laminated carbonate	Rio Marco	90.3	lake	6.28	0.80	0.07	1.18	14.95	
99-07-08H WR	laminated carbonate	Rio Marco	90.4	lake	7.33	0.50	0.05	0.86	9.87	
99-07-08I WR	sandstone	Rio Marco	91.2	prodelta	0.55	0.06	0.06	0.03	22.78	-22.39
99-07-08J WR	lam. gray mudstone	Rio Marco	91.3	prodelta	4.35	4.35	0.08	3.52	21.16	-24.43
98-06-23K WR	peaty	Rio Marco	96.5	prodelta	9.97	9.20	0.09	23.23	31.60	
98-06-23M WR	shale	Rio Marco	99.6	prodelta	2.71	2.61	0.07	2.87	16.95	
99-07-08L WR	sandstone	Rio Marco	100	prodelta	0.71	0.72	0.06	0.58	18.84	-23.58
99-07-08M	peaty	Rio Marco	102.4	prodelta	5.39	5.48	0.08	3.12	22.25	
99-07-08M	peaty	Rio Marco	102.4	prodelta	0.95	1.00	0.05	0.86	12.50	-23.60
99-07-08N WR	green sandstone	Rio Marco	109.3	prodelta	0.20	0.13	0.05			

Sample	Lithology	Strat Sect	Strat Ht (m)	Facies	TC	TOC	TS	%Corg	C/N	d13Corg
99-07-08O WR	lam. green siltstone	Rio Marco	111.9	prodelta	0.08	0.14	0.04	0.10	4.70	-22.22
99-07-08P WR	fine-grained sandstone	Rio Marco	115	prodelta	0.25	0.07	0.07	0.07	2.28	-10.47
99-07-08Q WR	fine-grained sandstone	Rio Marco	128.4	lake	0.22	0.12	0.06	0.03	1.20	-22.54
99-07-08Q WR	fine-grained sandstone	Rio Marco	128.4	prodelta	0.21	0.12	0.07	0.05	0.98	
99-07-08R bottom	laminated mudstone	Rio Marco	128.5	lake	0.99	0.24	0.05	0.56	9.26	
99-07-08R WR		Rio Marco	128.5	lake	0.79	0.84	0.05	0.80	9.80	
99-07-08S WR	sandstone	Rio Marco	128.6	prodelta	0.70	0.64	0.05	0.56	8.58	
99-07-08U WR	fine-grained sandstone	Rio Marco	138	prodelta	0.25	0.10	0.05			-24.32
99-07-10F top		Rio Marco	185.5					2.21	11.77	
99-07-10F bot.	black mudstone	Rio Marco	185.5	lake	4.30	1.09	0.06	0.37	32.55	
99-07-10G WR	laminated mudstone	Rio Marco	188.1	lake	0.29	0.38	0.05	0.36	2.13	
99-07-04K bot.	black mudstone	Rio Marco	188.3	lake	2.04	2.10	0.06	1.30	10.32	
99-07-04K top	black mudstone	Rio Marco	188.3	lake	2.49	2.58	0.06	0.61	11.90	-22.08